The response of Tropical Dry Forests to meteorological drought and El Niño Southern Oscillation

by

Lidong Zou

A thesis submitted in partial fulfillment of the requirements for the degree of

Doctor of Philosophy

Department of Earth and Atmospheric Sciences
University of Alberta

Abstract

As a result of economic pressures from agricultural development, timber extraction, tourism and the expansion of cattle ranching, Tropical Dry Forests (TDFs) are considered one of the most threatened and least protected ecosystems in the neotropics. Interacting with these human-induced effects, natural disturbances resulting from climate change are also affecting their capacity to provide key ecosystem services. One of the most recurrent effects associated to climate change is the increase in the frequency, and intensity of meteorological droughts driven by the El Niño-Southern Oscillation (ENSO). The former in turn leads to changes in the structure and function of these tropical ecosystems. Despite the importance that drought plays on the provision of ecosystem services, the response of TDFs to meteorological droughts is not fully understood. In this context, the utility of remote-sensing drought indices in the context of the ENSO was evaluated in this doctoral dissertation via four chapters. *Chapter 1* conducts a review of droughts in the context of the ENSO. *Chapter 2* evaluates the utility of three remote-sensing drought indices: the Vegetation Condition Index (VCI), the Temperature Condition Index (TCI), and the Vegetation Health Index (VHI), in a TDF located at the Santa Rosa National Park Environmental Monitoring Super site (SRNP-EMSS), Guanacaste, Costa Rica. This evaluation was done at multiple temporal scales (year, month and season). *Chapter 2* findings suggests that the TCI performed best over the VCI and the VHI. *Chapter 3* assesses the response of Gross Primary Productivity of the SRNP-EMSS to meteorological droughts. The former is done using a temporal correlation analysis of the Normalized Difference Vegetation Index (NDVI), Land Surface Temperature (LST), and the Standard Precipitation Index (SPI) at monthly and seasonal scales. Results indicate that the NDVI and LST are largely influenced by seasonality as well as the magnitude, duration, and timing of precipitation. The responses of the NDVI and the LST to meteorological droughts mainly reflect how greenness and evapotranspiration at the SRNP-

EMSS TDFs respond to precipitation. *Chapter 4* assesses the response of TDFs to Sea Surface Temperature (SST) anomalies in Niño 3.4 (a proxy for ENSO) across multiple TDFs sites in the Americas. This analysis was conducted from both, a long-term (18-years) and a short-term (1-year) perspective. Selected sites were chosen at the Chamela-Cuixmala Biosphere Reserve (CC-BR; Jalisco, Mexico); the Parque Estadual da Mata Seca (PEMS; Minas Gerais, Brazil); the Tucabaca Valley Municipal Wildlife Reserve (TV-MWR; Santa Cruz, Bolivia); and SRNP-EMSS (Guanacaste, Costa Rica). Results indicate that the Gross Primary Productivity at the SRNP-EMSS and the PEMS are negatively impacted by the long-term SST anomaly, while there is no long-term impact at the CC-BR and the TV-MWR. The long-term effect of the SST anomaly is more significant during the dry season at the SRNP-EMSS and the PEMS. Findings from a short-term perspective, suggest that the SRNP-EMSS and the CC-BR are sensitive to the ENSO warm phase, but not the other two sites. Finally, Chapter 5 addresse's general conclusions and provides ideas for future research.

Preface

Results generated from this research are original work by Lidong Zou.

Chapter 2 of this Dissertation has been published as Zou, L., Cao, S. and Sanchez-Azofeifa, A., Evaluating the utility of various drought indices to monitor meteorological drought in Tropical Dry Forests. International Journal of Biometeorology, 2019，pp.1-11.

Chapter 3 of this Dissertation, “Assessing the temporal response of Tropical Dry Forests to meteorological drought”, will be submitted to *Science of The Total Environment*.

Chapter 4 of this Dissertation, “Assessment of the response of Tropical Dry Forests to El Niño Southern Oscillation”, will be submitted to *Journal of climate*.

Acknowledgments

First and foremost, I would like to especially thank my supervisor, Dr. Arturo Sanchez-Azofeifa, for the years of guidance and support during my PhD period at the University of Alberta that lead to the successful completion of this dissertation. I am extremely grateful for your help, especially in my tough periods. I will not know the rewards of perseverance without your patience and support. Besides my supervisor, I would like to thank my committee members, Dr. Benoit Rivard and Dr. Keith Tierney, for their support, insightful comments and scientific advices. I also thank Dr. Janice Cooke for her guidance regarding the plant physiology. I thank Dr. Michael Lipsett for his comments and suggestions regarding the modeling. I thank Dr. Ralf Ludwig for providing me an excellent opportunity to study and visit at Ludwig Maximilian University of Munich.

I thank M.Sc. Mei Mei Chong and Dr. Michael Hesketh from the Centre for Earth Observation Sciences (CEOS) Laboratory for their help during my PH.D period. I thank my fellow graduate students and lab mates for their patience, help, and suppor during my graduate studies, especially Felipe Alencastro, Sofía Calvo, Branko Hilje Rodriquez, Dominica Harrison, Brad Danielson, Sen Cao, Saulo Castro, Sandra Durán, Jing Chen, Virginia Garcia-Millán, Kayla Stan, Leila Taheriazad, Antonio Guzmán, Carlos Campos, Wei Li, Iain Sharp, Marissa Castro, Ericka James, Rebeca Campos, Challan Sun, Xu Yuan, Yaqian Long, Tao Han, Genping Zhao, Yao Shi, and Hamed Sabzchi at the Centre for Earth Observation Sciences (CEOS), University of Alberta.

I thank the China Scholarship Council (CSC) for providing fellowship scholarship during my graduate studies, which allowed me to focus on the research.

Finally, I would like to thank my parents who have always loved me, supported me, and trust me unconditionally.

Table of Contents

List of Tables

List of Figures

List of acronyms

ENSO: El Niño - Southern Oscillation

LST: Land Surface Temperature

MODIS: Moderate Resolution Imaging Spectroradiometer

MWCA: Moving Window Correlation Analysis NDVI Normalized Difference Vegetation Index

NVSWI: Normalized Vegetation Supply Water Index

PSDI: Palmer Drought Severity Index

SPI: Standardized Precipitation Index

SPEI: Standardized Precipitation Evapotranspiration Index

SOI: Southern Oscillation Index

SRNP: Santa Rosa National Park

SST: Sea Surface Temperature

TCI: Temperature Condition Index

TVDI: Temperature Vegetation Dryness Index

VCI: Vegetation Condition Index

VHI: Vegetation Health Index

Chapter 1

Introduction

1.1 Background

Tropical Dry Forests (TDFs) are ecosystems dominated by deciduous trees, with a mean annual precipitation of 700-2000 mm per year, an annual average temperature of at least 25°C, and a dry season (precipitation less than 100 mm) for three or more months (Sanchez-Azofeifa et al. 2005). TDFs have a strong connection to the social and economic development in Latin America (Maass et al., 2005). TDFs supply agricultural and urban areas with various ecosystem services, such as food, timber, biofuels, regulation of soil fertility and water purification (Balvanera et al., 2011; Calvo-Rodriguez et al., 2017; Maass et al., 2005).

TDFs cover approximately 42% of all tropical forests worldwide (Murphy & Lugo, 1986) and support a large diversity of plant and animal species, many of them endemic (Mooney et al., 1995, Trejo & Dirzo 2002; Du et al., 2013). TDFs are currently considered the most heavily threatened and least protected ecosystem in the Neotropics, due to anthropogenic activities such as agricultural development, timber extraction, tourism and expansion of cattle ranching (Janzen, 1988; Sanchez-Azofeifa et al. 2005; Calvo-Alvarado et al. 2009). In Latin America, roughly 60% of all TDFs have been converted to other land uses (Portillo & Sanchez-Azofeifa, 2010). With TDFs suffering from extensive human and natural disturbances (Rodriguez et al., 2017), there is concern these disturbances are impacting the provision of ecosystem services (Kalacska et al., 2004). Droughts are one of the most significant natural disturbances impacting these services (Zhang et al., 2013). Global climate models predict an overall reduction in precipitation amount and an extension of dry intervals in the tropical region (Chadwick et al., 2016), increasing TDF susceptability to drought.

Droughts are classified into four categories: (1) meteorological droughts, (2) hydrological droughts, (3) vegetation droughts , and (4) economic droughts. Meteorological droughts are recurring climate phenomena, which occur when rainfall is significantly lower than average for a sustained period (Olukayode Oladipo, 1985). High temperatures and associated increases in potential evapotranspiration are also factors which induce a meteorological drought (Williams et

al., 2013). Meteorological droughts can lead to hydrological droughts (defined as lower stream-flows or reductions in reservoir storage below average), vegetation droughts (defined as a lack of soil moisture in the root zone), and economic droughts (defined as shortage of water supply for economic goods) (Olukayode Oladipo, 1985; Patel et al., 2007). Meteorological drought monitoring, therefore, is crucial for developing strategies which allow the preservation of ecosystem services and biodiversity.

Meteorological drought indices were developed by integrating in-situ variables, including precipitation, evapotranspiration, and temperature, into one single value (Patel et al., 2007). The Standardized Precipitation Index (SPI; McKee et al., 1993), the Standardized Precipitation Evapotranspiration Index (SPEI; Vicente-Serrano et al., 2010), and the Palmer Drought Severity Index (PDSI; Palmer, 1965) are the most commonly used meteorological drought indices. SPI is a precipitation-based drought index which considers the essential character of droughts as a deficiency of usable water, including soil moisture, rivers/streams, groundwater, and reservoirs. SPI is calculated by fitting precipitation totals over different time scales to a gamma distribution and, subsequently, transforming the gamma distribution into a standard normal distribution (McKee et al., 1993). The SPI is particularly useful when rainfall variability is much higher than the other climate variables, or when other climate variables are constant (Vicente-Serrano et al., 2010). SPEI is an extension of the SPI; however, SPEI uses the difference between precipitation and potential evapotranspiration (PET) as an input, instead of just precipitation. One of the main shortcomings of SPEI is the amount of data needed for calculation, as PET requires many variables including relative humidity, temperature, wind speed, and solar radiation (Vicente-Serrano et al., 2010). The PDSI is a drought index calculated based on previous precipitation, soil moisture supply, runoff, and evaporation demand; however, PDSI can only be calculated at a fixed time scale of between 9 and 12 month, reducing its utilization for identifying droughts lasting shorter time periods (Guttman, 1999).

Uncertainties associated with the in-situ indices largely depend on the density and distribution of the meteorological stations (Brown et al., 2008), which restrict their widespread application. Many remote sensing-based drought indices have been proposed as substitutes to in-situ drought indices due to higher temporal and spatial resolutions (Kogan, 1995; Ji & Peters, 2003; Quiring & Ganesh, 2010; Rhee et al., 2010; Zhang et al., 2013; Nichol et al., 2015; Zhang et al.,

2017). These remote-sensing indices use image-based parameters to indirectly reflect a meteorological drought. The Vegetation Condition Index (VCI) represents the greenness and vigor of vegetation, while the Temperature Condition Index (TCI) indicates the evapotranspiration on the canopy surface and the Vegetation Health Index (VHI) reflects the health condition of vegetation (Kogan, 1995; Kogan, 1997). The effectiveness of remote-sensing drought indices vary with climate zone, ecosystem, and land cover (Zhang et al. 2017). To date, there are no published studies which assess remote-sensing drought indices in TDFs.

Increases in the frequency, interval, and severity of meteorological droughts contribute to changes in the structure, function, and composition of tropical ecosystems (Allen, Breshears, & McDowell, 2015; Choat et al., 2012). The primary response of tropical forests to meteorological drought is to reduce primary production and water use (Dale et al., 2001). Under severe droughts, forest mortality increases due to carbon starvation and carbon failure (McDowell et al., 2008), ecosystems are susceptible to insects and disease (Rouault et al., 2006), and there are increases in the frequency and intensity of wildfires (Dale et al., 2001).

Several studies report the response of tropical forests to a meteorological drought during that drought year or drought event (Asner et al ., 2004; Anderson et al., 2010; Castro et al., 2018)). Asner et al. (2004) found canopy water content, light-use efficiency, and Net Primary Productivity (NPP) were sensitive to the meteorological drought in Amazon forests. Anderson et al. (2010) found that the Gross Primary Productivity (GPP) was associated with radiation income, regardless of precipitation amount during the 2005 drought. Castro et al. (2018) found the gross primary productivity (GPP) in TDFs in the Santa Rosa National Park (SRNP), Costa Rica declined by 13% and 42% during the meteorological drought that took place in 2014 and 2015. To my knowledge, there have been no studies aimed to quantify how TDF respond to meteorological droughts over a long-term (decadal) perspective.

The El Niño Southern Oscillation (ENSO) is one of the drivers of regional and local drought (Fuller & Murphy, 2006) in the tropics. ENSO is a coupled oscillation of ocean surface temperature and air surface pressure in the central Pacific Ocean that affects the global climate and weather in the world (Propastin et al., 2010). This phenomenon is defined by the National Oceanic and Atmospheric Administration (NOAA) when, over five consecutive three-month periods, mean Sea Surface Temperature (SST)anomalies are at or above +0.5°C in the Niño 3.4 region (warm

phase). When the anomaly is below -0.5°C, a cold phase is present (La Niña). In general, ENSO can lead to the redistribution of precipitation and temperature patterns for certain regions (IPCC, 2007) with significant impacts in the tropical ecosystems.

SST anomalies associated with the coupled ocean-atmosphere system have been found to be a key indicator of climate variability at regional scales which, in turn, influence the vegetation state (Kassas, 1998; Propastin et al., 2010). Several studies reported the response of vegetation to El Niño events based on the relationship between SST anomalies and drought indices around the world (Kogan et al., 2000; Mennis, 2001; Anyamba et al.,2002; Erasmi et al., 2009; Propastin et al.,2010). Kogan (2000) reported that in central Argentina, northern Brazil and southern Africa vegetation was sensitive to El Niño events during the boreal winter (1997 to 1998). Anyamba et al. (2002) found that NDVI variations had a positive correlation with SST anomalies during the El Niño in 1997 and 1998, and a negative correlation during the La Niña event in 1999 and 2000 in eastern Africa, a reversal of the southern Africa response. Erasmi et al. (2009) illustrated that only 1982-1983 and 1997-1998 El Niño events significantly influenced the vegetation drought condition for the period 1982-2006, which is also echoed by Propastin et al. (2010) in Africa.

The response of vegetation to El Niño events varied by climate zone, ecosystem, and land cover (Zhang et al., 2017). Research associated with the response of TDFs to El Niño is limited. Campos (2018) conducted a correlation between SST anomaly and precipitation in the Santa Rosa National Park (SRNP), Costa Rica where massive TDFs inhabit. They found the driest and wettest periods on record happened in connection with strong El Niño and cold La Niña, respectively. Castro et al. (2018) explored the impact of drought on the productivity of TDFs in Santa Rosa National Park, Costa Rica, and found that gross primary productivity declined during drought seasons; however, a direct and quantitative analysis of the response of TDFs to El Niño is not reported.

Despite the importance of drought in TDFs, there are limited studies associated with effective drought indices, and the response of TDFs to meteorological droughts and its drivers. To fill these knowledge gaps, Chapter 2 evaluates the utility of popular remote-sensing indices to monitor meteorological drought in TDFs, Chapter 3 assesses the response of TDFs to meteorological drought, Chapter 4 assesses the response of TDFs to SST anomalies (a ENSO

proxy) at multiple sites across Americas, and Chapter 5 reports the main conclusions, the limitations, and future work.

1.2 Thesis overview

The overall objective of this dissertation is to assess various remote-sensing drought indices and the response of TDFs to meteorological drought and its drivers. To this end, I evaluated the utility of various remote-sensing drought indices to monitor the meteorological drought in TDFs at the Santa Rosa National Park Environmental Monitoring Super Site (SRNP-EMSS), Guanacaste, Costa Rica. This analysis was conducted over multiple temporal scales. In addition, the temporal response of TDFs to the meteorological drought at the SRNP-EMSS was assessed.The response of TDFs to Sea Surface Temperature (SST) anomalies in Niño 3.4 across multiple TDFs sites in the Americas was also explored. As such, the dissertation is divided into:

Chapter 2. Evaluating the utility of various drought indices to monitor meteorological drought in Tropical Dry Forests.

While existing remote sensing-based drought indices are widely used in many different types of ecosystem, their utility in TDFs has not been assessed. The aim of this chapter, therefore, is to evaluate the performance of three remote sensing-based drought indices, the Vegetation Condition Index (VCI), the Temperature Condition Index (TCI), and the Vegetation Health Index(VHI), for meteorological drought monitoring in TDFs using the Moderate-resolution Imaging Spectroradiometer (MODIS) NDVI (MOD13Q1, collection v006) and LST (MOD11A12, collection v006) product.The correlation between VCI, TCI and VHI and multiple time scales of Standardized Precipitation Indexes (SPIs) (1-, 3-, 6-, 9-, 12-, 15-, 18-, 21-, 24-months) for each month (January to December) and each season (dry season, dry-to-wet season, wet season, and wet-to-dry season) was conducted using a Pearson correlation analysis . I also correlated year-to-year changes of satellite-based drought indices with the changes on in-situ annual SPI (A_SPI) which can be considered a proxy of annual mean meteorological drought conditions.

Chapter 3. Assessing the temporal response of Tropical Dry Forests to the meteorological drought.

Due to excessive human disturbances such as deforestation, as well as predicted changes in precipitation regimes, TDFs are susceptible to meteorological droughts. The purpose of this chapter is to assess the response of a TDFs to a meteorological drought by conducting temporal correlations between the MODIS-derived Normalize Difference Vegetation Index (NDVI) and Land Surface Temperature (LST) to a Standarized Precipitation Index (SPI) between March 2000 and March 2017 at the SRNP-EMSS. This analysis is conducted at montlhy and seasonal scales. The NDVI-LST correlation was conducted to analyze the dominant factor for growth in different seasons. Additionally, the primary response of TDFs to meteorological drought was estimated indirectly based on the results of the temporal correlations.

Chapter 4. Assessing the response of Tropical Dry Forests across the Americas to El Niño Southern Oscillation.

As an indicator of ENSO, SST anomalies in the tropical Pacific Ocean have been found to be a key indicator of climate variability in the tropical region (Kassas, 1998). As a result, they can affect vegetation state of tropical ecosystems. The objective of this chapter is to assess the response of TDFs across multiple sites in Meso- and South America to SST anomalies in Pacific Ocean Niño 3.4 from both short- and long-term perspectives. For the short-term perspective, I conducted a Window Moving Correlation Analysis (WMCA) during the five El Niño events between March 2000 and March 2017. For the long-term pespective, I conducted a temporal correlation between MODIS-derived VCI and TCI across multiple TDFs sites (CCBR, Mexico; PEMS, Brazil; TVMWR, Bolivia; and SRNP-EMSS, Costa Rica) and SST anomalies for dry and wet season.

1.3 References

Allen, C. D., Breshears, D. D., & McDowell, N. G. (2015). On underestimation of global vulnerability to tree mortality and forest die-off from hotter drought in the Anthropocene. *Ecosphere, 6*(8), 129.

Allen, C. D., Macalady, A. K., Chenchouni, H., Bachelet, D., McDowell, N., Vennetier, M.,Hogg, E. T. (2010). A global overview of drought and heat-induced tree mortality reveals emerging climate change risks for forests. *Forest Ecology and Management, 259*(4), 660-684.

Anderson, L. O., Malhi, Y., Aragão, L. E., Ladle, R., Arai, E., Barbier, N., & Phillips, O. (2010). Remote sensing detection of droughts in Amazonian forest canopies. *New Phytologist, 187*(3), 733-750.

Anyamba, A., Tucker, C. J., & Mahoney, R. (2002). From El Niño to La Niña: Vegetation response patterns over east and southern Africa during the 1997–2000 period. *Journal of Climate, 15*(21), 3096-3103.

Asner, G. P., Nepstad, D., Cardinot, G., & Ray, D. (2004). Drought stress and carbon uptake in an amazon forest measured with Spaceborne imaging spectroscopy. *Proceedings of the National Academy of Sciences, 101*(16), 6039-6044.

Balvanera, P., Castillo, A., & Martínez-Harms, M. J. (2011). Ecosystem services in seasonally dry tropical forests. *Seasonally dry tropical forests.* 259-277.

Brown, J. F., Wardlow, B. D., Tadesse, T., Hayes, M. J., & Reed, B. C. (2008). The vegetation drought response index (VegDRI): A new integrated approach for monitoring drought stress in vegetation. *GIScience & Remote Sensing, 45*(1), 16-46.

Calvo-Alvarado, J., McLennan, B., Sánchez-Azofeifa, A., & Garvin, T. (2009). *Deforestation and forest restoration in Guanacaste, Costa Rica: Putting conservation policies in context, 258(6),* 931-940

Calvo-Rodriguez, S., Sanchez-Azofeifa, A. G., Duran, S. M., & Espirito-Santo, M. M. (2017). Assessing ecosystem services in Neotropical dry forests: A systematic review. *Environmental Conservation, 44*(1), 34-43.

Campos, F. A. (2018). A synthesis of long-term environmental change in Santa Rosa, Costa Rica. *Primate life histories, sex roles, and adaptability*, 331-358

Castro, S. M., Sanchez-Azofeifa, G. A., & Sato, H. (2018). Effect of drought on productivity in a Costa Rican tropical dry forest. *Environmental Research Letters, 13*(4), 045001.

Chadwick, W. W., Paduan, J. B., Clague, D. A., Dreyer, B. M., Merle, S. G., Bobbitt, A. M., Nooner, S. L. (2016). Voluminous eruption from a zoned magma body after an increase in supply rate at axial seamount. *Geophysical Research Letters, 43*(23), 1206-12070.

Choat, B., Jansen, S., Brodribb, T. J., Cochard, H., Delzon, S., Bhaskar, R., Hacke, U. G. (2012). Global convergence in the vulnerability of forests to drought. *Nature, 491*(7426), 752.

Dale, V. H., Joyce, L. A., McNulty, S., Neilson, R. P., Ayres, M. P., Flannigan, M. D., Peterson, C. J. (2001). Climate change and forest disturbances: Climate change can affect forests by altering the frequency, intensity, duration, and timing of fire, drought, introduced species, insect and pathogen outbreaks, hurricanes, windstorms, ice storms, or landslides. *Bioscience, 51*(9), 723-734.

Du, L., Tian, Q., Yu, T., Meng, Q., Jancso, T., Udvardy, P., & Huang, Y. (2013). A comprehensive drought monitoring method integrating MODIS and TRMM data. *International Journal of Applied Earth Observation and Geoinformation, 23*, 245-253.

Erasmi, S., Propastin, P., Kappas, M., & Panferov, O. (2009). Spatial patterns of NDVI variation over Indonesia and their relationship to ENSO warm events during the period 1982–2006. *Journal of Climate, 22*(24), 6612-6623.

Guttman, N. B. (1999). Accepting the standardized precipitation index: A calculation algorithm. Journal of the American Water Resources Association, *35(2),* 311-322.

Janzen, D. H. (1988). Management of habitat fragments in a tropical dry forest: Growth. Annals of the Missouri Botanical Garden, 105-116.

Ji, L., & Peters, A. J. (2003). Assessing vegetation response to drought in the northern Great Plains using vegetation and drought indices. *Remote Sensing of Environment, 87*(1), 85-98.

Kalacska, M., Sanchez-Azofeifa, G. A., Calvo-Alvarado, J. C., Quesada, M., Rivard, B., & Janzen, D. H. (2004). Species composition, similarity and diversity in three successional stages of a seasonally dry tropical forest. *Forest Ecology and Management, 200*(1-3), 227-247.

Kassas, M. (1998). Currents of change: El Niño‘s impact on climate and society. *The Environmentalist, 19*(2), 177-178.

Kogan, F. N. (1995). Application of vegetation index and brightness temperature for drought detection. *Advances in Space Research, 15*(11), 91-100.

Kogan, F. N. (1997). Global drought watch from space. *Bulletin of the American Meteorological Society, 78*(4), 621-636.

Maass, J. M., Balvanera, P., Castillo, A., Daily, G. C., Mooney, H. A., Ehrlich, P., García-Oliva, F. (2005). Ecosystem services of tropical dry forests: Insights from longterm ecological and social research on the pacific coast of mexico. *Ecology and Society: A Journal of Integrative Science for Resilience and Sustainability, 10*(1), 1-23.

McDowell, N., Pockman, W. T., Allen, C. D., Breshears, D. D., Cobb, N., Kolb, T., Yepez, E. A. (2008). Mechanisms of plant survival and mortality during drought: Why do some plants survive while others succumb to drought? *New Phytologist, 178*(4), 719-739.

McKee, T. B., Doeskin, N. J., & Kleist, J. (1993). The relationship of drought frequency and duration to time scales. *Eighth Conference on Applied Climatology, Anaheim, California*, 179–184.

Mennis, J. (2001). Exploring relationships between ENSO and vegetation vigour in the south-east USA using AVHRR data. *International Journal of Remote Sensing, 22*(16), 3077-3092.

Murphy, K. (2006). The ENSO-fire dynamic in insular Southeast Asia. *Climatic Change, 74*(4), 435-455.

Murphy, P. G., & Lugo, A. E. (1986). Ecology of tropical dry forest. *Annual Review of Ecology and Systematics, 17*(1), 67-88.

Nichol, J. E., & Abbas, S. (2015). Integration of remote sensing datasets for local scale assessment and prediction of drought. *Science of the Total Environment, 505*, 503-507.

Olukayode Oladipo, E. (1985). A comparative performance analysis of three meteorological drought indices. *International Journal of Climatology, 5*(6), 655-664.

Palmer, W. C. (1965). Meteorological drought, US Department of Commerce, *Research Paper 45*, 58.

Parry, M. L., Canziani, O. F., Palutikof, J. P., Van Der Linden, Paul J, & Hanson, C. E. (2007). IPCC, 2007: Climate change 2007: Impacts, adaptation and vulnerability. *Cambridge University Press, Cambridge, UK.*

Patel, N. R., Chopra, P., & Dadhwal, V. K. (2007). Analyzing spatial patterns of meteorological drought using standardized precipitation index. *Meteorological Applications, 14*(4), 329-336.

Portillo-Quintero, C. A., & Sanchez-Azofeifa, G. A. (2010). Extent and conservation of tropical dry forests in the Americas. *Biological Conservation, 143*(1), 144-155.

Propastin, P., Fotso, L., & Kappas, M. (2010). Assessment of vegetation vulnerability to ENSO warm events over Africa. *International Journal of Applied Earth Observation and Geoinformation, 12*, S83-S89.

Quiring, S. M., & Ganesh, S. (2010). Evaluating the utility of the vegetation condition index (VCI) for monitoring meteorological drought in Texas. *Agricultural and Forest Meteorology, 150*(3), 330-339.

Rhee, J., Im, J., & Carbone, G. J. (2010). Monitoring agricultural drought for arid and humid regions using multi-sensor remote sensing data. *Remote Sensing of Environment, 114*(12), 2875-2887.

Rodriguez, S. C., Alvarado, J. C. C., Santo, M. M. E., & Nunes, Y. R. (2017). Changes in forest structure and composition in a successional tropical dry forest. *Revista Forestal Mesoamericana Kurú, 14*(35), 12-23.

Rouault, G., Candau, J., Lieutier, F., Nageleisen, L., Martin, J., & Warzée, N. (2006). Effects of drought and heat on forest insect populations in relation to the 2003 drought in Western Europe. *Annals of Forest Science, 63*(6), 613-624.

Sanchez-Azofeifa, G. A., Quesada, M., Rodríguez, J. P., Nassar, J. M., Stoner, K. E., Castillo, A., Cuevas-Reyes, P. (2005). Research priorities for Neotropical dry forests. *Biotropica, 37*(4), 477-485.

Trejo, I., & Dirzo, R. (2002). Floristic diversity of Mexican seasonally dry tropical forests. *Biodiversity & Conservation, 11*(11), 2063-2084.

Vicente-Serrano, S., Beguería, S., & López-Moreno, J. I. (2010). A multiscalar drought index sensitive to global warming: The standardized precipitation evapotranspiration index. *Journal of Climate, 23*(7), 1696-1718.

Williams, A. P., Allen, C. D., Macalady, A. K., Griffin, D., Woodhouse, C. A., Meko, D. M., Grissino-Mayer, H. D. (2013). Temperature as a potent driver of regional forest drought stress and tree mortality. *Nature Climate Change, 3*(3), 292-297.

Xiao, X., Zhang, Q., Braswell, B., Urbanski, S., Boles, S., Wofsy, S., Ojima, D. (2004). Modeling gross primary production of temperate deciduous broadleaf forest using satellite images and climate data. *Remote Sensing of Environment, 91*(2), 256-270.

Zhang, L., Jiao, W., Zhang, H., Huang, C., & Tong, Q. (2017). Studying drought phenomena in the continental United States in 2011 and 2012 using various drought indices. *Remote Sensing of Environment, 190*, 96-106.

Zhang, Y., Peng, C., Li, W., Fang, X., Zhang, T., Zhu, Q., Zhao, P. (2013). Monitoring and estimating drought-induced impacts on forest structure, growth, function, and ecosystem services using remote-sensing data: Recent progress and future challenges. *Environmental Reviews, 21*(2), 103-115.

Chapter 2

Evaluating the utility of various drought indices to monitor meteorological drought in Tropical Dry Forests

2.1 Introduction

Tropical Dry Forests (TDFs), are defined as a vegetation type where more than half of its species are drought deciduous, there are four to six months with low or no precipitation (<100 mm per month), a mean annual temperature of 25°C, and total annual precipitation between 700 and 2000 mm (Sanchez-Azofeifa et al., 2005). TDFs comprise about 42% of all tropical forests worldwide (Murphy & Lugo, 1986). TDFs are habitats with abundant plant and animal species, many of them endemic (Du et al., 2013). In Latin America, 60% of all TDFs have been replaced by other land cover types such as agriculture and pasture for cattle ranching (Portillo-Quintero & Sanchez-Azofeifa, 2010). This ecosystem is estimated to store close to 22 Pg of carbon (Du et al., 2013).

As TDFs undergo tremendous human disturbances (Rodriguez et al., 2017), ongoing climate change is affecting the provision of ecosystem services (Kalacska et al., 2004). Much of these changes are via droughts (Zhang et al., 2013). In general, drought is defined as a precipitation deficit that occurs over a period of time and that impacts both water resources and ecosystem services (Du et al., 2013). Droughts can introduce great damage to tropical forests in terms of their biophysical properties and ecosystem services (Portillo-Quintero et al., 2015).

Increases in the frequency, duration, and severity of droughts can change the structure, composition, and function of tropical forests, which in turn contribute to declines in forest productivity (Choat et al., 2012; Engelbrecht et al., 2007; Zhang et al., 2013). Droughts can also lead to an increase in tree mortality rates of tropical forests, and an impact on the hydrological dynamics in the neotropics (Allen et al., 2010; Phillips et al., 2009; 2010; Portillo-Quintero et al., 2015). Allen et al. (2010) reviewed the potential of droughts to amplify tree mortality around the world, and found any forest type and any climate zone is vulnerable to climate change in terms of tree mortality. Phillips et al (2009) found the Amazon forests were vulnerable to growing moisture deficit, with the potential for losing large amounts of carbon (1.2 to 1.6 petagrams) in response to drought. Phillips et al. (2010) indicated that mortality rates of tropical forests tended to increase

disproportionately when the moisture stress is at higher levels, and trees in Borneo are more vulnerable than those in the Amazon. Portillo-Quintero et al. (2015) indicated droughts are potential threatens to water resources in the neotropics where a large fraction of population (approximate 90 million) lived.

Meteorological drought occurs mainly when rainfall is significantly lower than the average precipitation for a sustained period of time (Olukayode Oladipo, 1985). High temperatures and associated increases on potential evapotranspiration are important drivers associated to meteorological droughts (Williams et al., 2013). Many drought indices have been developed to characterize meteorological drought in terms of its severity, magnitude, duration, and spatial extent. Popular drought indices, such as the Palmer Drought Severity Index (PDSI, Palmer, 1965) and the Standardized Precipitation Index (SPI, McKee et al., 1993), are derived from data coming from in-situ weather stations. The PDSI considers prior precipitation, soil moisture, runoff and evaporation demand; however, its fixed time scale (between 9 and 12 months) precludes its use for identifying drought lasting shorter time periods (e.g., less than 9 months). The PDSI has been widely applied to determine the areal extent and severity of the drought in the northeastern United States over the years (Alley, 1984; Palmer, 1965). The SPI is a precipitation-based drought index, which considers the essential character of the drought as the deficiency of usable water, including the soil moisture, rivers and streams, groundwater and reservoirs (McKee et al., 1993). The SPI can be calculated for flexible scales depending on the purpose of the study. Its applications have encompassed a wide range of ecosystems at varying scales (Guttman, 1999; McKee et al., 1993; Patel et al., 2007).

Uncertainties associated with the in-situ meteorological indices depend on the density and distribution of the meteorological stations (Brown et al., 2008). In a remote area where the meteorological stations are limited, the use of the in-situ indices for drought monitoring faces a great risk of low accuracy (Rhee et al., 2010). Remote sensing, which can characterize meteorological and terrestrial biophysical attributes from a regional to global coverage, has gained much attention over the past several decades in drought monitoring. Many remote sensing-based drought indices have been proposed as substitutes to in-situ drought indices (Kogan, 1995; Ji & Peters, 2003; Quiring & Ganesh, 2010; Rhee et al., 2010; Zhang et al., 2013; Nichol et al., 2015;

Zhang et al., 2017). Their abilities vary with climate zone, ecosystem, and land cover (Zhang et al. 2017).

Among remote sensing vegetation indices, the Normalized Difference Vegetation Index (NDVI) and the Vegetation Condition Index (VCI, scaled inter-annual NDVI), have been extensively used for drought monitoring (Kogan, 1995; 1997; Quiring & Ganesh, 2010). Bhuiyan et al. (2006) carried out a detail analysis of spatial and temporal drought dynamics during monsoon and non-monsoon seasons for the years 1984 to 2003 in Rajasthan (India), and found the correlation between the VCI and SPI increased in the monsoon season because the growth of vegetation was largely dependent on rainfall, while it was partly controlled by irrigation in the non-monsoon season.. Dutta et al. (2008) conducted the correlation analysis of NDVI and VCI derived from NOAA-AVHRR data and precipitation in the northwest of Iran between 1997 and 2001, and correlations were obtained between average NDVI and VCI and average three-month precipitation, indicating NOAA-AVHRR derived NDVI can reflect the precipitation fluctuation in the study area. Quiring and Ganesh (2010) examined the relationship between the VCI, and meteorological drought indices during Texas' growing seasons. Results suggested that the VCI responded to relative prolonged moisture stress instead of short-term precipitation deficiency. The authors also reported that the correlations between the VCI and meteorological indices varied significantly across the state; being the correlation between the SPI and PSDI weaker in east Texas than west Texas due to higher permeable soils in the east.

The Temperature Condition Index (TCI, scaled inter-annual LST) is another index that has been proposed for drought monitoring due to its potential ability to quantify evapotranspiration (Kogan, 1995). Seiler et al. (1998) used the TCI and VCI to assess drought conditions in Argentina, and found a close relationship with precipitation patterns. Karnieli et al. (2006) compared satellite-based drought indices, such as the TCI and VCI, with the PDSI across the desert regions of Mongolia, and concluded that there was little agreement among those indices. The vegetation Heath index (VHI), a combination of the VCI and TCI (Kogan; 2002), was an early warning tool for drought. Rhee et al. (2010) tested various remote sensing-based drought indices in the arid regions of Arizona and New Mexico and humid regions of North Carolina and South Carolina, and found that the VHI performed better than the VCI and TCI in both arid and humid regions when tested against in-situ meteorological drought indices. Shamsipour et al. (2011) conducted

correlation analysis of various remote-sensing indices and meteorological drought indices in semi-arid central plains of Iran confined to the spring season from 1998 to 2004 and found that VCI better correlated to meteorological drought indices than TCI, and VHI is not a reliable measure of drought condition in this region. Amalo1 & Hidayat. (2017) compared the remote-sensing-based drought indices in East Java, and found TCI was sensitive to drought in dry season or months; VCI is proved to detect drought more sensitive in wet season than TCI and VHI; VHI provided better comprehension about drought occurrence.Zhang et al. (2017) compared various satellite-based drought indices to monitor drought events in the Continental United States. They found that VHI performed better than the VCI and TCI in most climate regions.

Despite the fact that there is a considerable amount of scientific literature associated to the development, testing, and evaluation of drought indexes across many different types of ecosystems, little has been done in tropical dry forests ecosystems. As such, the objective of this study is to evaluate the performance of three remote sensing-based drought indices to monitoring meteorological drought conditions in a TDF at the local scale. We focus this study on the monthly, seasonal and yearly correlations between remote sensing-based drought indices and SPIs. This evaluation uses the MODIS NDVI and LST products from 2000 to 2017, as well as local precipitation data from 1979 to 2017. Figure 2.7 shows the flowchart for this study.

2.2 Methods

2.2.1 Study area

This study was conducted at the Santa Rosa National Park Environmental Monitoring Super Site (SRNP-EMSS), Northwest Costa Rica (Figure 2.1). The total study area covers 109 km^2 with an average slope of 7%. For over 200 years, the region was part of a cattle ranch until it became a National Park in the early 1970s (Castillo et al., 2012; Janzen, 2000; Cao & Sanchez-Azofeifa, 2016). Currently, the SNRP-EMSS is a mosaic of diverse vegetation types dominated by secondary tropical dry forests with three stages of ecological succession: early, intermediate and late (Kalacska et al., 2004; Cao & Sanchez-Azofeifa, 2016; Li et al., 2017). The early stage of regeneration is composed of shrubs, small trees with grasses and bare soil in open areas. The intermediate stage is composed of fast growing deciduous species, Lianas, and shade tolerant

species. The late succession is consisted of dominant evergreen species and regeneration of tolerant shade species (Kalacska et al., 2004).

This area receives between 915 mm and 2558 mm of annual precipitation, and mean annual temperature is stable at 26.6 °C (Sanchez-Azofeifa et al., 2005). The SNRP-EMSS experiences a three-month dry season (January to March) when the precipitation is extremely scarce (Figure 2. 2), and the majority of the deciduous vegetation loses its leaves (Figure 2.3). April and May are considered as a transition from dry to wet season (dry-to-wet season) because precipitation starts to grow in April and sharply increases in May. The wet season is usually from June to October. Then SNRP-EMSS goes through a transitional season from November to December (wet-to-dry season) when the rainfall decreases significantly. The dominant factor that affects the phenology of secondary TDFs with various successions at this TDF site is water availability (Sanchez-Azofeifa et al., 2005).

2.2.2 Data preprocessing

This study employed a set of Terra Moderate Resolution Imaging Spectroradiometer (MODIS) products between March 2000 and March 2017. Specifically, the 16-day MODIS NDVI product at 250 m resolution (MOD13Q1, collection v006) and the 8-day MODIS LST product at 1000 m resolution (MOD11A12, collection v006) were obtained at the "Reverb Echo" portal (http://reverb.echo.nasa.gov/reverb/). Both products were re-projected to WGS 1984 UTM Zone 16 North. The Land Surface Temperature (LST) product was then resampled to 250 m so that it had the same resolution with the NDVI product. We converted the 16-day NDVI and 8-day LST products to monthly data by considering the number of days belonging to each month for each phase of image products (Rhee et al., 2010). Quality flags in both products were used to extract the ideal quality pixels for reliable analysis. Specifically, the pixels where the values in the quality flags layer of MODIS products equal to zero, were selected as ideal quality pixels.

We also collected daily precipitation data between June 1979 and March 2017 in a meteorological station (10°50.408' N, 85°37.055' W) within the SNRP-EMSS. The daily precipitation data were also aggregated to monthly data.

2.2.3 Remote sensing drought indices

The Normalized Difference Vegetation Index (NDVI) is a good indicator of the chlorophyll content and vegetative cover, and indicates the capacity of the photosynthesis of the canopy

(Karnieli et al., 2010); in addition, the LST is a proxy for assessing the evapotranspiration of vegetation canopy and soil moisture (Karnieli et al., 2010). The VCI and the TCI, calculated on monthly NDVI and LST data using the equation (1) and (2), reflect relative greenness and temperature of plants (Kogan, 1995; Kogan, 1997). Specifically, VCI and TCI as the normalizations of NDVI and LST, emphasize the relative changes in the local NDVI and LST through time while reducing the influences of local climate conditions and ecosystems. The VHI, indicating vegetation health, is an additional combination of the VCI and TCI with the same weight assuming an even contribution from two elements (equation (3)), indicating the health condition of the vegetation.

$$VCI_{ij} = (NDVI_{ij} - NDVI_{j\,min})/(NDVI_{j\,max} - NDVI_{j\,min}) * 100 \quad (1)$$

$$TCI_{ij} = (LST_{j\,max} - LST_{j})/(LST_{j\,max} - LST_{j\,min}) * 100 \quad (2)$$

$$VHI_{ij} = 0.5 * (VCI_{ij} + TCI_{ij}) \quad (3)$$

Where *i* describes the *i*th year; and *j* represents the *j*th month.

These indices could indirectly reflect the meteorological drought conditions based on vegetation stress related to leaf vigor, evapotranspiration in the leaf or surface temperature in the leaf. The values of these drought indices range from 0 to 100, the low values (close to 0) show the stressed vegetation condition, middle values show fair conditions (close to 50), and high values (close to 100) indicate the optimal conditions (Kogan, 1995; Kogan, 1997). Specifically, the drought grades based on three drought indices can be defined as following (Table 2. 1).

2.2.4 In situ meteorological drought index (SPI)

The Standardized Precipitation Index (SPI) is a ground station-based meteorological drought index (McKee et al., 1993). As a standardized index, the SPI is comparable both temporally and spatially. Higher values of the SPI indicate humid conditions, and lower SPI values represent drought. McKee et al. (1993) proposed a classification for the SPI as follows: extremely wet (SPI>2.0), very wet (1.5<SPI<1.99), moderately wet (1.0<SPI<1.49), near normal (-0.99<SPI<0.99), moderately dry (-1.49<SPI<-1.0), severely dry (-1.99<SPI<-1.5), and extremely dry (SPI<-2.0). Because the SPI is strongly affected by the record length and longer records provide more consistent and accurate SPI values (Quiring 2009), the calculation of an SPI requires long-term historical precipitation data. As such, this study used information from the local meteorological station from June 1979 to March 2017. In calculation of the SPI, we assumed that

the precipitation records followed a Gamma distribution (Patel et al., 2007) as such the data will be transformed, using studentized residual normalization techniques, to a normal distribution, with a mean value of 0 and a variance value of 1. The z-scores for each record is therefore calculated as the SPI.

This study calculated SPIs of different time scales from short- and medium-term to long-term (1-, 3-, 6-, 9-, 12-, 15-, 18-, 21-, and 24-month) (McKee et al., 1993). One- and three-month SPIs reflect short-term drought conditions, indicating soil moisture and vegetation stress; six- and nine-month SPIs reflect medium-term precipitation trends, showing the precipitation over distinct seasons; twelve-month or more SPIs indicate long-term precipitation trends, which are tied to streamflow and groundwater level (Zargar et al., 2011).

2.2.5 The correlation and regression analysis

To evaluate the performance of the remote sensing-based indices in monitoring meteorological droughts in TDFs, we built relationships between the VCI, TCI and VHI and the multiple-scale SPIs using the Pearson correlation analysis (Quiring & Ganesh, 2010; Rhee & Carbone, 2010). Since the relationships could vary with season timing and time scales (Quiring & Ganesh, 2010), the Pearson correlation analysis was conducted at multiple time scales (1-, 3-, 6-, 9-, 12-, 15-, 18-, 21-, 24-months) for each month (January to December) and each season (dry season, dry-to-wet season, wet season, and wet-to-dry season), respectively. We also correlated year-to-year changes of satellite-based drought indices with the changes of in situ annual SPI (A_SPI) which was calculated as 12- month SPI ending in December of each year. The A_SPI is considered as the annual mean meteorological drought condition. Correlation coefficients (r) and p values were obtained to determine whether and how meteorological drought conditions affect vegetation conditions in different phases of the phenology cycle.

2.3 Result

2.3.1 The precipitation distribution at SRNP-EMSS

Figure 2. 2 shows monthly and seasonal precipitation distributions at the SRNP-EMSS based on historical records from 1979 to 2017. The precipitation in the dry season is extremely low with a median amount of 2.9 mm and average amount of 7.9 mm. The precipitation increases

sharply in the dry-to-wet season (median rainfall: 188.2 mm; average rainfall: 236.6 mm). In the wet season, the precipitation is generally abundant (median rainfall: 1152.9 mm; average rainfall: 1389 mm) even though July is a relatively dry month (median rainfall: 117.2 mm; average rainfall: 144.5 mm). The SNRP-EMSS experiences a sharp decline in the wet-to-dry season (median rainfall: 115.8 mm; average rainfall: 157.4 mm).

2.3.2 Seasonal correlations between remote sensing-based drought indices and multiple-scale SPIs

Figure 2.4 shows the correlation coefficients between satellite-based drought indices and multiple-scale SPIs over the SRNP-EMSS in four seasons. The correlations varied with season timing. The TCI had an overall better performance than the VCI and VHI in terms of seasonal scale.

In the dry season, three remote sensing-based drought indices had very similar correlations with SPIs: they had moderate correlations with the short- (3-month) and long-term (18-, 21-, and 24-month) SPIs ($r \approx 0.5$); and they had high correlations with the medium- to long-term (6-, 9-, 12- and 15-month) SPIs ($r \approx 0.70$). The maximum correlated values for VCI, TCI and VHI (dry season) and SPI (12-, 12-, and 12-month) are 0.69, 0.64, and 0.72 respectively. The VCI, TCI, and VHI also presented similar correlations with the SPIs in the wet season: for all time scales except for the 24-month SPI with which VCI was not significantly correlated, they were moderately correlated ($r \approx 0.40$) with SPIs. The maximum correlated values for VCI, TCI and VHI (wet season) and SPI (9-, 12-, and 12-month) are 0.38, 0.47, and 0.43 respectively. In the dry-to-wet season, three drought indices had poor performances: none of them could reflect meteorological drought conditions for any given scales. The performance of three drought indices differed in the wet-to-dry season: the VCI did not correlate with SPIs at all the time scales; the TCI had significant correlations with SPIs at all time scales, especially for 6-, 9-, 12-month SPIs; and the VHI had moderate correlations with SPIs from 1-month to the 12-month time scale. The maximum correlated values for TCI and VHI (wet-to-dry season) and SPI (12-, and 12-month) are 0.62 and 0.38 respectively.

2.3.3 Monthly correlations between remote sensing-based drought indices and multiple-scale SPIs

Figure 2. 5 describes monthly correlations of the VCI-SPIs, TCI-SPIs, and VHI-SPIs at the SRNP-EMSS. Three drought indices had a similar performance in February, June, and July: they responded to the short-, medium-, and long-term SPIs in February (1- to 15-month) and July (1- to 24-month) and the medium- and long-term SPIs in June (9- to 24-month). The VCI and VHI performed better than the TCI in February. The TCI and VHI performed better than the VCI in June. The VHI performed best in July.

Three drought indices had different performances in January, March, April, August, and December. In January, the VCI moderately responded to the middle-term SPIs; meanwhile, the TCI and VHI can respond to the short-, medium-, and long-term SPIs. In March and April, the VCI was more sensitive to shorter-term SPIs than TCI and VHI while TCI and VHI could also well monitor the medium- and long-term SPIs. In August, the VCI and VHI responded to short- and medium-term SPIs; and the TCI only responded to 24-month SPI. In December, there were no correlations between the VCI and SPIs, the TCI was able to respond to SPIs of all-time scales and, the VHI was significantly correlated the SPIs of 1 to 12 months. All of the three-remote sensing-based drought indices failed to correlate to SPIs in May, September, October, and November.

2.3.4 Yearly correlations between remote sensing-based drought indices and A_SPI

Figure 2. 6 shows the correlations between the annual mean values of satellite-based drought indices, the VCI, TCI and VHI, and the A_SPI. The TCI presented a significantly strong correlation (r^2=0.63, $p<0.01$, and $RMSE=0.81$) with the A_SPI, the VHI presented a moderate correlation ($r^2=0.39$, $p<0.01$, and $RMSE=1.03$) and the VCI did no significantly respond to the A_SPI ($r^2 \approx 0$, $p=0.92$, and $RMSE=1.03$)

2.4 Discussion

The performance of the remote sensing-based drought indices in monitoring droughts is phenologically and seasonally dependent at the SRNP-EMSS. In the dry season, the correlation between the remote sensing indices and the SPIs became significant when the time scale was larger than 3-months (i.e., 3-, 6-, 9-, 12-, 15-, 18-, 21-, and 24-month). This means that the remote sensing indices can better reflect the rainfall deficiency in previous (≥3) months rather than the current

month during the dry season. The fact that the remote sensing indices performed badly in the dry-to-wet season may be due to an insignificant correlation with the SPIs in May when the leaves of TDFs develop quickly fast (Figure 2.3). The remote-sensing indices moderately reflected meteorological condition in the wet season, probably associated with the water content in the root regions. In the early stage of wet season (June, July, and August), significant correlations between remote sensing-based indices, the VCI, TCI and VHI, and the SPIs were found when the soil moisture was not much high; when the water content in the root regions was much abundant (September and October), the remote sensing indices could no longer reflect the meteorological condition probably because TDFs, with sufficient water content in the root regions, were resistant to meteorological drought. Ji & Peters (2003) found similar patterns in areas of the northern Great Plain where high correlations between the NDVI and the SPIs occurred in the middle (June, July and August) of the growing season and low correlations occurred at the start (May) and end (September and October) of the same season.

Observed significant differences for the VCI, TCI and VHI reflected meteorological drought in the wet-to-dry season. We found that remote-sensing indices could not reflect the meteorological drought condition at the early stage of the wet to dry season (November), because the water content in the root regions was still saturated though its leaves started falling. But in the late stage of the wet-to-dry period (December) when falling leaves dramatically and water content being not saturated, the TCI reflected all the time-scale meteorological drought conditions. Moreover, the VHI described the precipitation deficiency within one year, and the VCI did not respond to the rainfall.

The varying performances of the VCI, TCI, and VHI reflect the seasonal and monthly dynamics of TDFs in different biochemical or biophysical manners. The VCI detected the canopy greenness, leaf vigor, and the deciduousness during the growing season (Kogan, 1995; 1997). The TCI is more sensitive to the soil moisture when the leaf falls during the dry season and is more sensitive to the water content in the canopy when the leaf is saturated during the wet season (Karnieli, 2010). The VHI, which indicates the vegetation health condition, inherits characteristics of the VCI and TCI. These indices performed similarly to reflect meteorological drought conditions except for the wet-to-dry season in terms of seasonal scales. The variation of precipitation regime triggered the changes in the canopy greenness and leaf vigor, in the evapotranspiration of the canopy and soil, and in the health conditions of TDFs. Thus, the VCI,

TCI, and VHI have the potential to detect meteorological drought indirectly. The biophysical and biochemical parameters responding to the VCI, TCI, and VHI in the dry seasons were associated with the rainfall in previous (≥3) months because the precipitation in the current dry season was pretty low. In the dry-to-wet season, the variabilities of the biophysical and biochemical parameters were related to the rapid growth of TDFs in May (Figure 2. 3) which was driven by the precipitation regime in previous months rather than in the current month, although the rainfall in May was pretty much (Figure 2. 2).

In the wet season, meteorological droughts can lower VCI by altering the leaf reflectance at both the red and near-infrared wavelength (Carter et al., 1996). In detail, when a leaf is in the water-stressed condition, the chlorophyll concentration would decrease and results in higher reflectance in the red band; meanwhile spaces within the spongy mesophyll would be enlarged and lead to an increase of the scattering effect for near-infrared photons at the cell wall-air interface and eventually increase the near-infrared reflectance (Carter et al., 1996; Asner, 1998). The sensitivity of red reflectance to decreased water content in the leaf was much more than near-infrared reflectance, resulting in lower values of the VCI while suffering from meteorological droughts. At the same time, meteorological droughts can trigger the closure of the leaf stomata leading to an increase in the surface temperature at the canopy (Carter et al., 1996). As such, the TCI also decreased under water stress. As a linear combination of VCI and TCI, VHI declined with VCI and TCI when suffering from drought. During the wet-to-dry period, the role of precipitation was no longer to sustain the canopy greenness (because phenologically falling leaves) but to promote evapotranspiration of plants and soil (Karnieli et al., 2010). As a result, the VCI did not reflect the precipitation deficiency (SPIs) in December while TCI was able to depict the evapotranspiration process in TDFs and thus well responded to variations in precipitation and soil moisture (Cao et al., 2017).

The remote sensing-based drought indices performed significantly different to reflect annual meteorological drought condition. The annual mean TCI and VHI explained 63% and 39% variability of the A_SPI respectively, and annual mean VCI was a poor indicator to account for the change in the A_SPI. This was because the evapotranspiration of TDFs was more sensitive than canopy greenness to the inter-annual precipitation deficiency.

The performance of a specific remote sensing-based drought index for the early, intermediate, and late stage of TDFs should be similar. This is because time-series of leaves

intensity for intermediate and late are very close during the whole period, and three stages of TDFs have similar leaves intensity during May and November. The changes in leaf intensity for early, intermediate and late stages of TDFs, driven by the effect of phenology, are simultaneous (no time lag) and have the same direction (Lopezaraiza-Mikel et al., 2013). The remote-sensing drought indices (e.g. VCI and TCI) emphasize the relative changes in the biophysical parameters (NDVI and LST) through time. As a result, the values of a specific remote sensing-based drought index for three stages of TDFs should be similar in each month, under the assumption that the difference in leaf intensity between early and intermediate/late stage in a certain month (from December to April) does not vary with a given year. Furthermore, the element of vegetation heterogeneity is buffered by the available MODIS satellite information (250 m and 1 Km), which prevents to fully consider differences between the different levels of successional stages present in our study area.

2.5 Conclusion

In this study, we evaluated the use of three popular remote sensing-based vegetation indices, i.e., the Vegetation Condition Index (VCI), Temperature Condition Index (TCI) and Vegetation Health Index (VHI), calculated on MODIS the NDVI and LST products, towards the monitoring of the meteorological drought in a TDF at SRNP-EMSS. Multiscale Standard Precipitation Index (SPIs) calculated on precipitation data from a meteorological station was used to evaluate satellite-based indices. Pearson correlation analysis was performed between remote-sensing indices and SPIs. We concluded that the ability of these remote sensing-based drought indices to monitor meteorological drought varied with timing, and TCI outperformed VCI and VHI in terms of seasonal and annual scale. They performed similarly in the dry, dry-to-wet and wet season while TCI performed best to monitor meteorological drought in the wet-to-dry period, followed by VHI, and VCI did worst. These remote-sensing indices performed well in monitoring meteorological drought in the dry season, poorly in the dry-to-wet season, and moderately reflected rainfall deficiency in the wet season. However, these remote-sensing indices were not suitable to reflect meteorological drought in the dry-to-wet season.

The utility of remote-sensing indices was also assessed in terms of the monthly scale. The varying performance of remote sensing indices can be mostly explained by their nature in describing the biophysical and biochemical properties in TDFs. All of them failed to well monitor the drought in May when the leaf flushed sharply and in September, October and November when

the water content in the root region was abundant. Besides, the inter-annual analysis showed that the evapotranspiration of TDF was more sensitive than canopy greenness to precipitation deficiency. Our study effectively increased the ability to provide real-time drought monitoring and early warning of drought in the TDF.

2.6 References

Allen, C. D., Macalady, A. K., Chenchouni, H., Bachelet, D., McDowell, N., Vennetier, M., & Hogg, E. T. (2010). A global overview of drought and heat-induced tree mortality reveals emerging climate change risks for forests. *Forest Ecology and Management, 259*(4), 660-684.

Amalo, L. F., & Hidayat, R. (2017). Comparison between remote-sensing-based drought indices in east Java. *Earth and Environmental Science*, *54(1)*, 012009.

Asner, G. P. (1998). Biophysical and biochemical sources of variability in canopy reflectance. *Remote Sensing of Environment, 64(3)*, 234-253.

Bayarjargal, Y., Karnieli, A., Bayasgalan, M., Khudulmur, S., Gandush, C., & Tucker, C. J. (2006). A comparative study of NOAA–AVHRR derived drought indices using change vector analysis. *Remote Sensing of Environment, 105*(1), 9-22

Bhuiyan, C., Singh, R. P., & Kogan, F. N. (2006). Monitoring drought dynamics in the Aravalli region (India) using different indices based on ground and remote sensing data. *International Journal of Applied Earth Observation and Geoinformation, 8(4),* 289-302.

Brown, J. F., Wardlow, B. D., Tadesse, T., Hayes, M. J., & Reed, B. C. (2008). The vegetation drought response index (VegDRI): A new integrated approach for monitoring drought stress in vegetation. *GIScience & Remote Sensing, 45(1)*, 16-46.

Cao, S., Sanchez-Azofeifa, G. A., Duran, S. M., & Calvo-Rodriguez, S. (2016). Estimation of aboveground net primary productivity in secondary tropical dry forests using the Carnegie–Ames–Stanford approach (CASA) model. *Environmental Research Letters, 11(7)*, 075004.

Cao, S., & Sanchez-Azofeifa, A. (2017). Modeling seasonal surface temperature variations in secondary tropical dry forests. *International Journal of Applied Earth Observation and Geoinformation, 62, 122-134.*

Carter, G. A. (1991). Primary and secondary effects of water content on the spectral reflectance of leaves. *American Journal of Botany,* 916-924.

Carter, G. A., Cibula, W. G., & Miller, R. L. (1996). Narrow-band reflectance imagery compared with thermal imagery for early detection of plant stress. *Journal of Plant Physiology, 148(5),* 515-522.

Castillo, M., Rivard, B., Snchez-Azofeifa, A., Calvo-Alvarado, J., & Dubayah, R. (2012). LIDAR remote sensing for secondary tropical dry forest identification. *Remote Sensing of Environment, 121*, 132-143.

Choat, B., Jansen, S., Brodribb, T. J., Cochard, H., Delzon, S., Bhaskar, R., Hacke, U. G. (2012). Global convergence in the vulnerability of forests to drought. *Nature, 491*(7426), 752.

Dabrowska-Zielinska, K., Kogan, F., Ciolkosz, A., Gruszczynska, M., & Kowalik, W. (2002). Modelling of crop growth conditions and crop yield in poland using AVHRR-based indices. *International Journal of Remote Sensing, 23*(6), 1109-1123.

Du, L., Tian, Q., Yu, T., Meng, Q., Jancso, T., Udvardy, P., & Huang, Y. (2013). A comprehensive drought monitoring method integrating MODIS and TRMM data. *International Journal of Applied Earth Observation and Geoinformation, 23*, 245-253.

Dutta, D., Kundu, A., Patel, N. R., Saha, S. K., & Siddiqui, A. R. (2015). Assessment of agricultural drought in Rajasthan (India) using remote sensing derived vegetation condition index (VCI) and standardized precipitation index (SPI). *The Egyptian Journal of Remote Sensing and Space Science*, *18(1),* 53-63.

Engelbrecht, B. M., Comita, L. S., Condit, R., Kursar, T. A., Tyree, M. T., Turner, B. L., & Hubbell, S. P. (2007). Drought sensitivity shapes species distribution patterns in tropical forests. *Nature, 447*(7140), 80.

Guttman, N. B. (1999). Accepting the standardized precipitation index: A calculation algorithm. Journal of the American Water Resources Association, *35(2),* 311-322.

Janzen, D. H. (1988). Management of habitat fragments in a tropical dry forest: Growth. Annals of the Missouri Botanical Garden, 105-116.

Janzen, D. H. (2000). Costa Rica's area de Conservacion Guanacaste: A long march to survival through non-damaging biodevelopment. *Biodiversity, 1*(2), 7-20.

Kalacska, M., Sanchez-Azofeifa, G. A., Calvo-Alvarado, J. C., Quesada, M., Rivard, B., & Janzen, D. H. (2004). Species composition, similarity and diversity in three successional stages of a seasonally dry tropical forest. *Forest Ecology and Management, 200(1-3)*, 227-247.

Karnieli, A., Bayasgalan, M., Bayarjargal, Y., Agam, N., Khudulmur, S., & Tucker, C. J. (2006). Comments on the use of the vegetation health index over Mongolia. *International Journal of Remote Sensing, 27(10)*, 2017-2024.

Karnieli, A., Agam, N., Pinker, R. T., Anderson, M., Imhoff, M. L., Gutman, G. G., Goldberg, A. (2010). Use of NDVI and land surface temperature for drought assessment: Merits and limitations. *Journal of Climate, 23(3)*, 618-633.

Kogan, F. N. (1995). Application of vegetation index and brightness temperature for drought detection. *Advances in Space Research, 15*(11), 91-100.

Kogan, F. N. (1997). Global drought watch from space. *Bulletin of the American Meteorological Society, 78*(4), 621-636.

Kogan, F. (2002). World droughts in the new millennium from AVHRR-based vegetation health indices. *Eos, Transactions American Geophysical Union, 83(48)*, 557-563.

Li, W., Cao, S., Campos-Vargas, C., & Sanchez-Azofeifa, A. (2017). Identifying tropical dry forests extent and succession via the use of machine learning techniques. *International Journal of Applied Earth Observation and Geoinformation, 63*, 196-205.

Lopezaraiza-Mikel, M., Quesada, M., Álvarez-Añorve, M., Ávila-Cabadilla, L., Martén-Rodríguez, S., Calvo-Alvarado, J. (2013). Phenological patterns of tropical dry forests along latitudinal and successional gradients in the Neotropics. *Tropical dry forests in the Americas*, 119-146

McKee, T. B., Doeskin, N. J., & Kleist, J. (1993). The relationship of drought frequency and duration to time scales. *Eighth Conference on Applied Climatology, Anaheim, California*, 179–184.

Murphy, P. G., & Lugo, A. E. (1986). Ecology of tropical dry forest. *Annual Review of Ecology and Systematics, 17*(1), 67-88.

Olukayode Oladipo, E. (1985). A comparative performance analysis of three meteorological drought indices. *International Journal of Climatology, 5*(6), 655-664.

Palmer, W. C. (1965). Meteorological drought, US Department of Commerce, *Research Paper 45*, 58.

Patel, N. R., Chopra, P., & Dadhwal, V. K. (2007). Analyzing spatial patterns of meteorological drought using standardized precipitation index. *Meteorological Applications, 14*(4), 329-336.

Phillips, O. L., Aragão, L. E., Lewis, S. L., Fisher, J. B., Lloyd, J., López-González, G., Quesada, C. A. (2009). Drought sensitivity of the amazon rainforest. *Science*, 323(5919), 1344-1347.

Phillips, O. L., Van Der Heijden, G., Lewis, S. L., López-González, G., Aragão, L. E., Lloyd, J., Dávila, E. A. (2010). Drought–mortality relationships for tropical forests. *New Phytologist, 187*(3), 631-646.

Portillo-Quintero, C. A., & Sanchez-Azofeifa, G. A. (2010). Extent and conservation of tropical dry forests in the Americas. *Biological Conservation, 143*(1), 144-155.

Portillo-Quintero, C., Sanchez-Azofeifa, A., Calvo-Alvarado, J., Quesada, M., & do Espirito Santo, Mario Marcos. (2015). The role of tropical dry forests for biodiversity, carbon and water conservation in the Neotropics: Lessons learned and opportunities for its sustainable management. *Regional Environmental Change, 15*(6), 1039-1049.

Quiring, S. M., & Ganesh, S. (2010). Evaluating the utility of the vegetation condition index (VCI) for monitoring meteorological drought in Texas. *Agricultural and Forest meteorology, 150*, 330-339.

Rhee, J., Im, J., & Carbone, G. J. (2010). Monitoring agricultural drought for arid and humid regions using multi-sensor remote sensing data. *Remote Sensing of Environment, 114*(12), 2875-2887.

Rodriguez, S. C., Alvarado, J. C. C., Santo, M. M. E., & Nunes, Y. R. (2017). Changes in forest structure and composition in a successional tropical dry forest. *Revista Forestal Mesoamericana Kurú, 14(35)*, 12-23.

Sanchez-Azofeifa, G. A., Quesada, M., Rodríguez, J. P., Nassar, J. M., Stoner, K. E., Castillo, A., Cuevas-Reyes, P. (2005). Research priorities for Neotropical dry forests. *Biotropica, 37*(4), 477-485.

Shamsipour, A. A., Zawar-Reza, P., Alavi Panah, S. K., & Azizi, G. (2011). Analysis of drought events for the semi-arid central plains of Iran with satellite and meteorological based indicators. *International Journal of Remote Sensing, 32(24)*, 9559-9569.

Singh, R. P., Roy, S., & Kogan, F. (2003). Vegetation and temperature condition indices from NOAA AVHRR data for drought monitoring over India. *International Journal of Remote Sensing, 24*(*22*), 4393-4402.

Williams, A. P., Allen, C. D., Macalady, A. K., Griffin, D., Woodhouse, C. A., Meko, D. M., Grissino-Mayer, H. D. (2013). Temperature as a potent driver of regional forest drought stress and tree mortality. *Nature Climate Change, 3*(3), 292-297.

Zargar, A., Sadiq, R., Naser, B., & Khan, F. I. (2011). A review of drought indices. *Environmental Reviews, 19*, 333-349.

Zhang, L., Jiao, W., Zhang, H., Huang, C., & Tong, Q. (2017). Studying drought phenomena in the continental United States in 2011 and 2012 using various drought indices. *Remote Sensing of Environment, 190*, 96-106.

Zhang, Y., Peng, C., Li, W., Fang, X., Zhang, T., Zhu, Q., Zhao, P. (2013). Monitoring and estimating drought-induced impacts on forest structure, growth, function, and ecosystem services using remote-sensing data: Recent progress and future challenges. *Environmental Reviews, 21*(2), 103-115.

2.7 Tables and Figures

Table 2. 1 Classification of remote sensing-based drought indices VCI, TCI, and VHI.

Name of class	VCI	TCI	VHI
Extreme drought	0-10	0-10	0-10
Severe drought	10-20	10-20	10-20
Moderate drought	20-30	20-30	20-30
Mild drought	30-40	30-40	30-40
Abnormally dry	40-50	40-50	
No drought	50-100	50-100	40-100

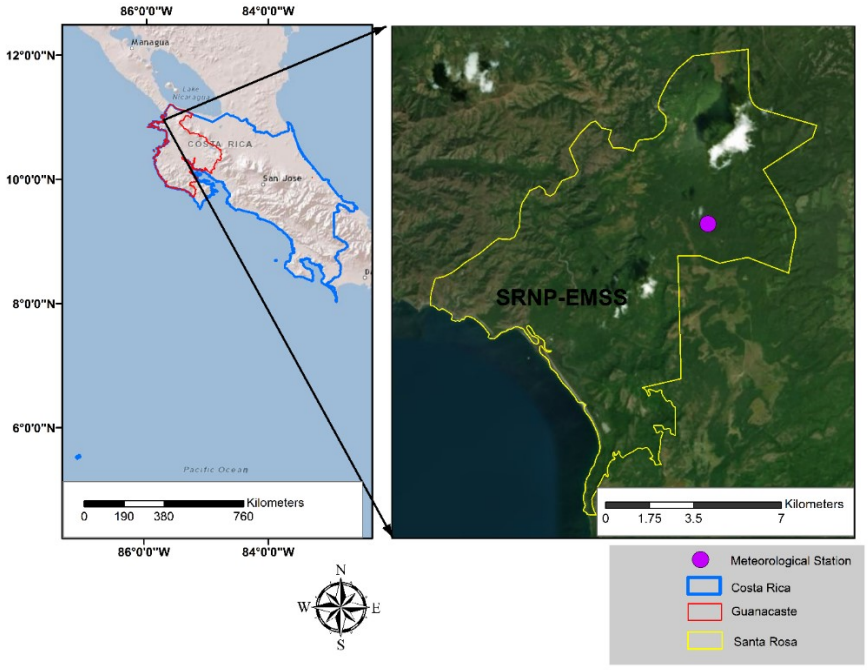

Figure 2. 1 Study area: Santa Rosa National Park Environmental Monitoring Super Site (SRNP-EMSS), and the location of the source of meteorological information used in this study.

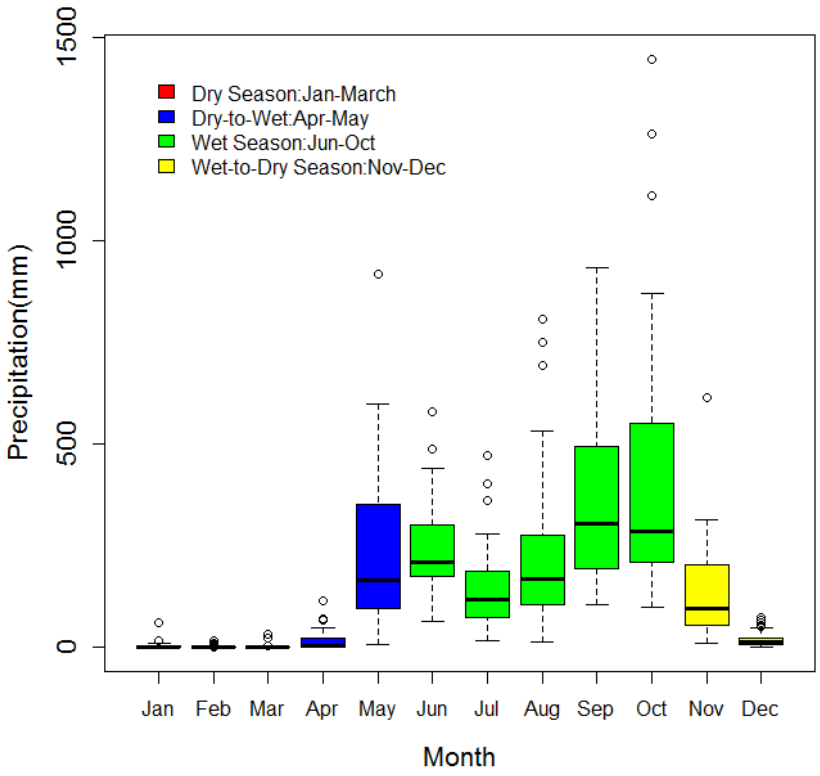

Figure 2. 2 Monthly precipitation distribution at the SRNP-EMSS in the dry, dry-to-wet, wet, and wet-to-dry seasons from June 1976 to March 2017. The dry season include January to March (Red); the dry-to-wet transitional season include April and May (Blue); the wet season include June to October (Green); the wet-to-dry transitional season include November and December (Yellow).

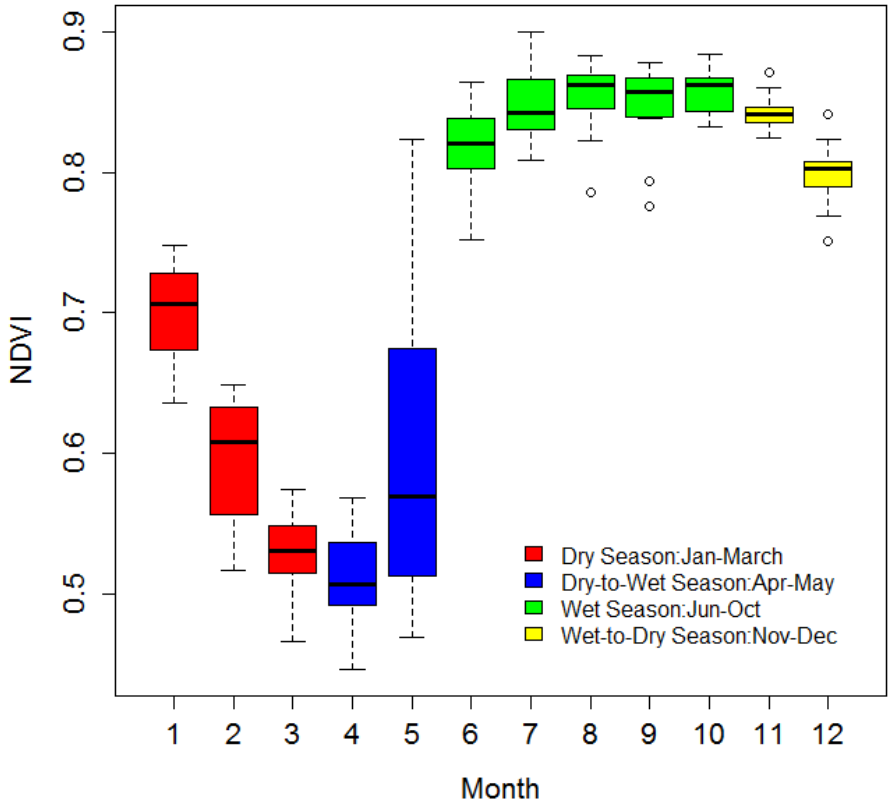

Figure 2. 3 The Monthly NDVI distribution at the SRNP-EMSS in the dry, dry-wet, wet, and wet-dry seasons from March 2000 to March 2017. The dry season includes January-March (Red); the dry-wet transitional season includes April-May (Blue); the wet season includes June-October (Green); the wet-dry transitional season includes November-December (Yellow). The monthly NDVI distributions were extracted from MODIS products (MOD13Q1, collection v006).

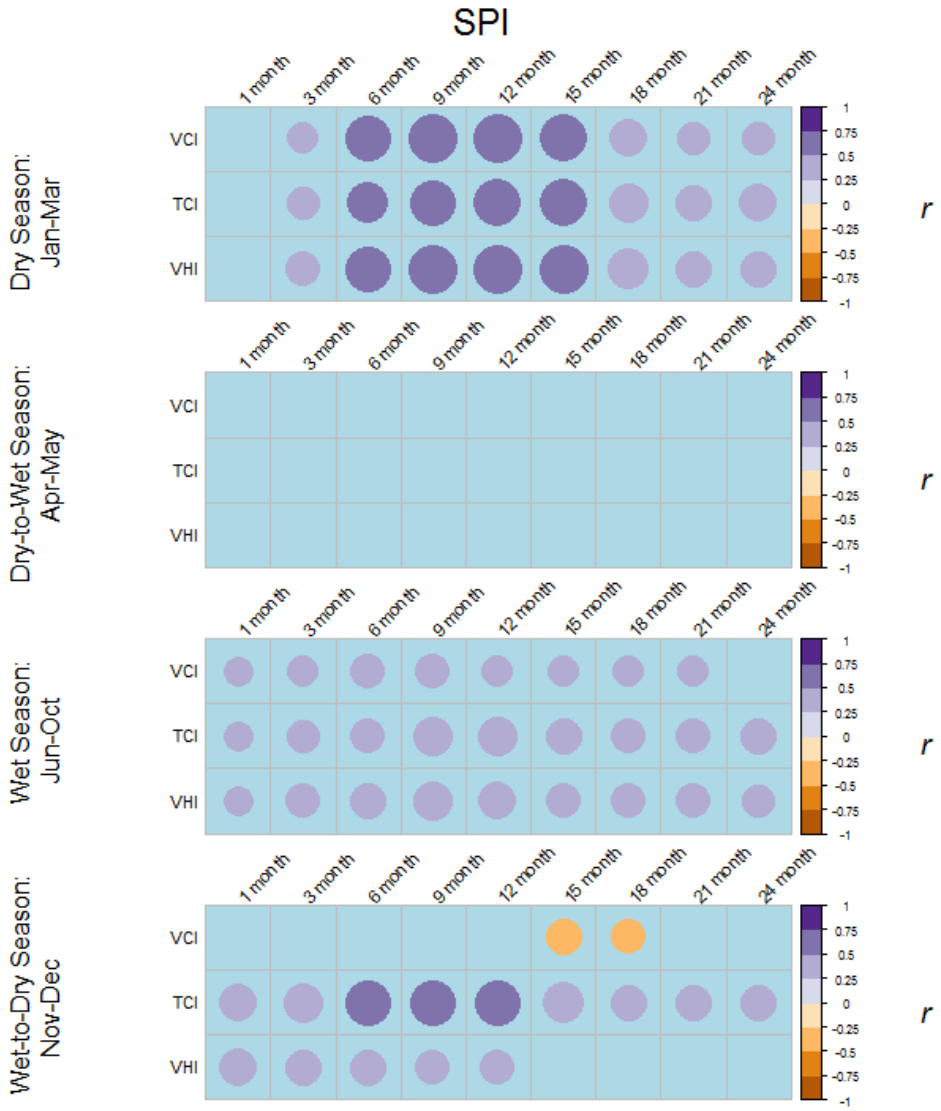

Figure 2. 4 The correlation coefficients (r) between remote sensing-based drought indices (the VCI, TCI, and VHI) and multiple-scale SPIs in four seasons at the SRNP-EMSS. Blank places represent p-values that are not significant (significance level=*0.05*). Purple circles indicate significantly positive relationships and yellow circles indicate significantly negative relationships. The darker and bigger circles stand for higher absolute *r* values.

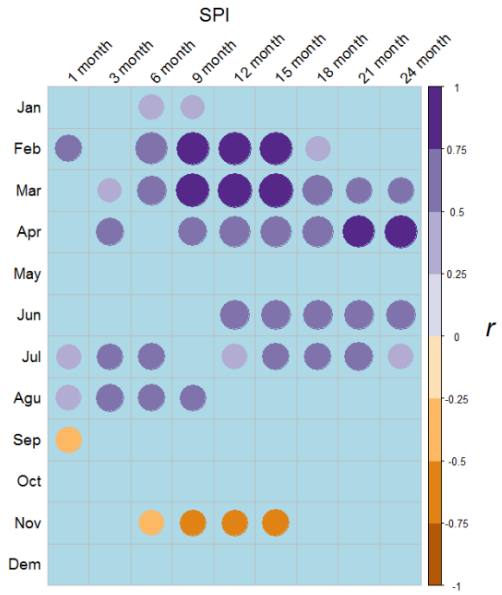

(a). the VCI-SPIs correlation

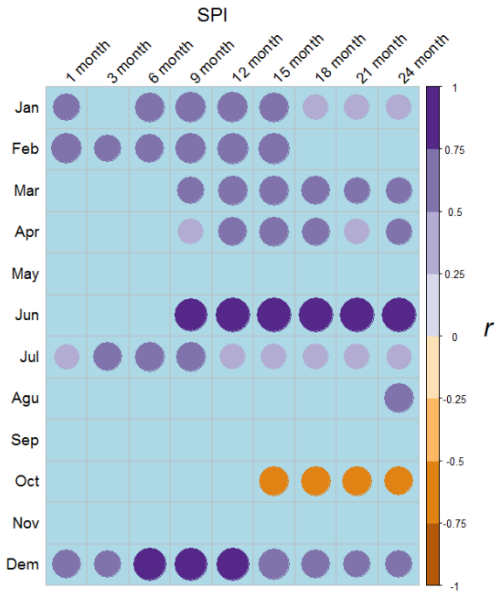

(b). the TCI-SPIs correlation

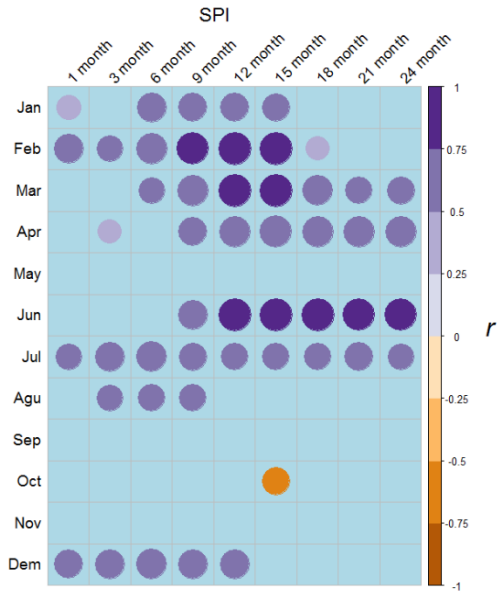

(c). the VHI-SPIs correlation

Figure 2. 5 The correlation coefficients (r) between the remote sensing-based drought indices (the VCI, TCI, and VHI) and the multiple-scale SPIs for each month at the SRNP-EMSS. Blank places represent p-values that are not significant (significance level=*0.05*). Purple circles indicate significantly positive relationships and yellow circles indicate significantly negative relationships. The darker and bigger circles stand for higher absolute r values.

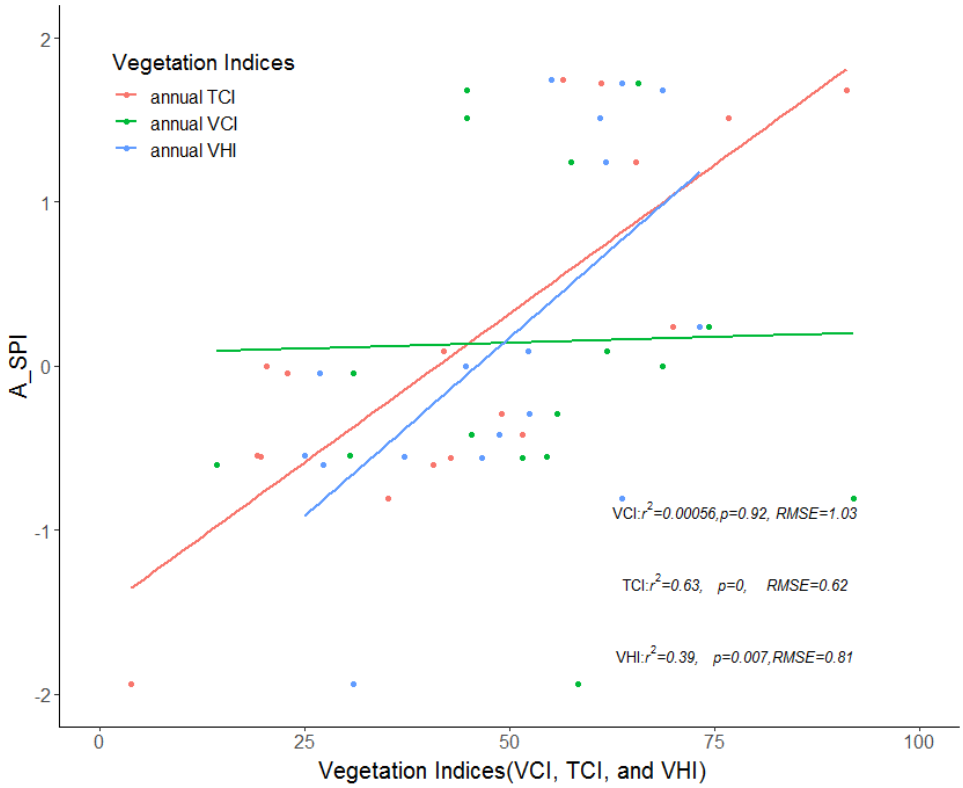

Figure 2. 6 The correlation coefficients between the annual satellite-based drought indices (the VCI, TCI, and VHI) and the A_SPI which indicates annual mean meteorological drought condition.

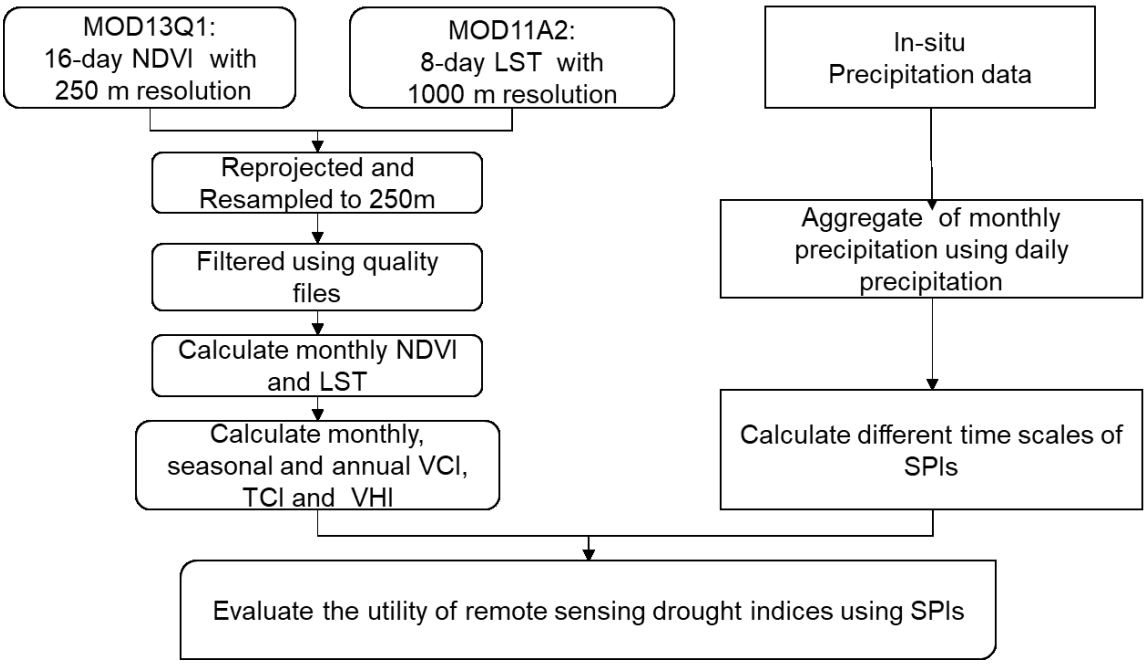

Figure 2. 7 Flowchart for evaluating the utility of remote sensing drought indices

Chapter 3

Assessing the temporal response of Tropical Dry Forests to meteorological drought

3.1 Introduction

Tropical Dry Forests (TDFs) are defined as a vegetation type of which at least 50% of the trees are drought deciduous, with a dry season of three or more months (precipitation < 100 mm/month), a mean temperature of 25°C or higher, and a total annual precipitation of 700–2000 mm (Sanchez-Azofeifa et al., 2005). TDFs are considered the first frontier for economic and social development in Latin America (Calvo-Rodriguez et al., 2017) and account for roughly 42% of all tropical forests worldwide (Murphy & Lugo, 1986; Quesada et al., 2009). They provide diverse ecosystem benefits, such as food, timber, non-timber forest products, biofuels, soil erosion control, soil fertility regulation, water quality improvements, carbon storage, and they help control carbon emissions (Maass et al., 2005; Balvanera et al.,2011; Calvo-Rodriguez et al., 2017). TDFs have greatly benefitted human development and are considered the most excessively utilized and least protected forest ecosystems of the Americas (Janzen, 1988; Sanchez-Azofeifa et al., 2005; Calvo-Alvarado et al., 2009; Portillo-Quintero & Sanchez-Azofeifa, 2010). More than 60% of TDFs have been destroyed in Latin America, and approximately half of all TDFs in the world have been converted to other land use types (Hoekstra et al.,2005; Portillo-Quintero & Sanchez-Azofeifa, 2010).

As TDFs undergo excessive human disturbances, ongoing climate change is interfering with the provision of ecosystem services (Kalacska et al., 2004). Global climate models have predicted an increase in the frequency, intervals, and severity of meteorological droughts in tropical regions (Chadwick et al., 2016). TDFs are particularly sensitive to meteorological droughts because water dynamics determine the alternating seasonality between wet and dry seasons (Castro et al., 2018).

Meteorological droughts are recurring climate phenomena that mainly occur when rainfall is significantly less than the normal level for a sustained period (Olukayode Oladipo, 1985; Thenkabail & Gamage, 2004). They can also be related to high temperature and high potential evapotranspiration (Williams et al., 2013). Meteorological droughts can cause other types of

droughts, such as agricultural (lack of soil moisture in the root zone), hydrological (lower than normal stream-flow or reservoir storage), and economic droughts (shortage of water supply for economic goods) (Olukayode Oladipo, 1985; Patel et al.,2007).

To quantify a meteorological drought, including its severity, magnitude, duration and spatial extent, many drought indices have been developed by integrating ground-station variables, including precipitation, evapotranspiration, and temperature, into one single variable (Patel et al., 2007). Popular meteorological indices include the Standardized Precipitation Index (SPI; McKee, et al.,1993), the Standardized Precipitation Evapotranspiration Index (SPEI; Vicente-Serrano et al., , 2010), and the Palmer Drought Severity Index (PDSI; Palmer, 1965). The calculation of the PDSI is based on prior precipitation, moisture supply, runoff and evaporation demand. It was designed for long-time scales (between 9 and 12 months) and is not able to identify droughts of shorter periods. Both the SPI and SPEI are multiscale meteorological drought indices. The SPI is a precipitation-based drought index that considers the essential character of a drought as the deficiency of usable water, including water from soil moisture, rivers, streams, groundwater and reservoir storages. The SPI is calculated by fitting precipitation totals to a gamma distribution in different time scales and then transforming the gamma distribution to the standard normal distribution. The SPEI is an extension of the SPI, which considers both precipitation and temperature as factors that can to trigger drought. The calculation of the SPEI requires multiple data sources as input, including relative humidity, temperature, wind speed and solar radiation (Vicente-Serrano et al., 2010). The high data requirement for the SPEI restricts its wide application, and the SPI is considered the most widely used and valid meteorological drought index (Zargar et al., 2011).

Increases in the frequency, intervals, and severity of meteorological droughts have led to changes in the structure, function, and composition of tropical ecosystems (Allen et al.,2015; Choat et al., 2012). The primary response of forests to drought is to reduce the net primary production (NPP) and water use as a result of reduced soil moisture and stomatal conductance (Dale et al., 2001). Secondary effects occur under severe meteorological drought conditions with an extreme decline in NPP. In this case, forest mortality is increased due to carbon starvation and hydraulic failure (McDowell et al., 2008), and susceptibility to insects and disease increases due to

physiological changes experienced by host trees (Rouault et al., 2006), and the frequency or intensity of wildfires increases due to a reduction in decomposition processing (Dale et al., 2001).

Some studies have focused on the primary effects of meteorological droughts on forest ecosystems during drought years or the years following a drought. Asner et al. (2004) analyzed the monthly meteorological precipitation and biophysical parameters of Amazon forest using spaceborne hyperspectral metrics from January 2001 to January 2002 and found that canopy water content, light-use efficiency, and NPP were highly sensitive to drought. Anderson et al. (2010) analyzed the impacts of a 2005 drought on the gross primary productivity (GPP), expressed as the Enhanced Vegetation Index (EVI), of Amazonia and concluded that EVI was associated with radiation income rather than the precipitation amount. Castro et al. (2018) found that GPP in TDFs in Santa Rosa National Park (SRNP), Costa Rica declined by 13% and 42% during drought seasons of 2014 and 2015, respectively. Other studies assessed the primary impacts of droughts on the forest ecosystem from a long-term perspective. Phillips et al. (2009) found that relative to pre-2005 conditions (1980–2004), Amazon forest subjected to a 100-mm increase in water deficit lost 5.3 mg of aboveground biomass of carbon per hectare. Brando et al. (2010) concluded that GPP declined with Vapor Pressure Deficit (VPD) and decreased precipitation and Plant Available Water (PAW) in sparse forested areas in the Amazon from 2000 to 2008. In densely forested areas, EVI was associated with leaf flushing rather than Leaf Area Index (LAI) or any climate variables. Williams et al. (2013) found that the Forest Drought Stress Index (FDSI), which is associated with tree productivity, was approximately equally influenced by warm-season temperature and cold-season precipitation for the forest ecosystem in the southwestern United States from 1896 to 2007.

There were only a few studies on the primary effects of meteorological droughts on TDFs from a long-term perspective. This study employed remote sensing-based indices, i.e., the Normalized Difference Vegetation Index (NDVI) and Land Surface Temperature (LST) as proxies for forest productivity (Liu et al., 2011). The NDVI reflected canopy greenness (Ji & Peters, 2003), and the LST reflected the evapotranspiration of plants (Cao & Sanchez-Azofeifa, 2017).

Relationships between remote-sensing drought indices (NDVI and LST) and meteorological drought indices have been explored in different regions. Ji & Peters (2003) quantified the relationship of monthly NDVI with multiscale SPIs in the growing season across the north and central U.S. Great Plains from 1989 to 2000. They found that NDVI-SPI correlations

varied significantly by month, and the best correlations occurred in the middle of the growing season. Wang et al. (2003) tested the temporal response of the satellite-derived NDVI to precipitation in Kansas, U.S. from 1989 to 1997. They concluded that the average NDVI values during the growing season had a high correlation with the cumulated precipitation of the current growing season plus the preceding seven months (15-month duration). Nichol & Abbas (2015) related the Normalised Vegetation Supply Water Index (NVSWI), (calculated using the NDVI and LST) to the Precipitation Condition Index (PCI) in Yunnan province of China from 2008 to 2011. They found that the NVSWI correlated best with 64 days of earlier rainfall in terms of the cropland and shrubland, while evergreen forest was sensitive to precipitation 90 days earlier.

The correlation between the NDVI and LST was also explored around the world (Prihodko & Goward, 1997; Goward et al. 2002). This is because the correlation can reflect the limiting factor for vegetation growth, which is a key component for drought monitoring Specifically, when the NDVI-LST correlation is significantly negative, resulting from the cooling effect of canopy transpiration, water is a limiting factor for vegetation growth; when the NDVI-LST correlation is significantly positive, attributable to warming inducing an increase in plant biomass, cover, and net primary productivity, energy is a limiting factor (Karnieli et al., 2006). In TDFs, the limiting factor for plant growth is water (Cao et al., 2016; Castro et al., 2018). However, the importance of water for TDFs growth in different seasons (i.e., dry, wet, and transitional seasons) is not discussed in detail.

In this context, the objective of this study is to explore how TDFs temporally respond to meteorological drought at monthly and seasonal scales from a long-term perspective and how water is important to the growth of TDFs in different seasons (dry, dry-to-wet transitional, wet, and wet-to-dry transitional seasons). Specifically, we try to answer the following questions: (1) How do the NDVI and LST temporally respond to SPIs in TDFs? And (2) what is the relationship between the NDVI and LST in different seasons in TDFs? This study will contribute to a deeper understanding of the primary response of TDFs to meteorological drought triggered by climate change and the importance of water to the growth of TDFs. Figure 3.6 shows the flowchart for this chapter.

3.2 Methods

3.2.1 Study area

The study was conducted at the Santa Rosa National Park Environmental Monitoring Super Site (SRNP-EMSS; Figure 3.1) in Guanacaste province of Costa Rica. The SRNR-EMSS is part of the regional conservation area known as the Area de Conservacion Guanacaste (ACG) in the northwest of Costa Rica. The SRNP-EMSS ranges from 85°31'W–85°39'W and 10°48'N–10° 56'N, covering approximately 109 km^2 with a mean slope of 7%. The SRNP-EMSS had been a part of a cattle ranch hacienda for almost 200 years until 1971. After that, the SRNP-EMSS was developed into a mosaic of diverse vegetation cover dominated by secondary forests in various stages of regeneration (Cao & Sanchez-Azofeifa, 2017; Janzen, 2000; Kalacska et al., 2004). The SRNP-EMSS receives a mean annual rainfall of 1391 mm with high variability (915–2558 mm per year) and has a stable mean annual temperature of 26°C (Cao & Sanchez-Azofeifa, 2017; Kalacska et al., 2004). The SRNP-EMSS is characterized by a three-month dry season from January to March when there is almost no rainfall, and the majority of deciduous vegetation loses its leaves (Figure 3. 2). After the dry season, the rainfall starts to increase in April and sharply rises in May. As such, April and May are considered the dry-to-wet transitional season. The wet season is between June and October, when the precipitation stays at a high level. A short dry period can occur in late July or August caused by a short intensification of trade wind activity (Campos, 2018). November and December are considered a wet-to-dry transitional season, when the precipitation declines sharply.

3.2.2 The NDVI and LST as response variables to drought

As a widely used vegetation index, the Normalized Difference Vegetation Index (NDVI) is calculated based on reflectance at the red and near-infrared wavelengths. It can be used to reflect the vegetation vigor and greenness (Karnieli et al., 2010). The Land Surface Temperature (LST) derived from the thermal band is related to vegetation water stress, soil moisture, and evapotranspiration (Karnieli et al., 2010). The NDVI and LST are widely used in the drought monitoring of terrestrial ecosystem dynamics on remote sensing (Ji & Peters, 2003) because temporal variations in the NDVI and LST can represent the primary response, the reduction in productivity, to meteorological drought. Sixteen-day and eight-day Terra Moderate Resolution

Imaging Spectroradiometer (MODIS) products with 250-m (MOD13Q1, collection v006) and 1000-m resolutions (MOD11A2, collection v006), respectively, from March 2000 to March 2017 were downloaded from NASA's website (http://reverb.echo.nasa.gov/reverb/). We first resampled the LST images to 250 m and then converted the NDVI and LST images to a Universal Transverse Mercator projection with central zone 16 N° and WGS84 using the nearest interpolation algorithm. Then, monthly NDVI and LST products were aggregated by considering the weight of the number of days belonging to each month after removing the missing data (Rhee et al., 2010).

3.2.3 Temporal correlations between the NDVI and LST and SPIs

We used the SPI as the meteorological drought index due to its lower requirement of data and its multiscale character (Vicente-Serrano et al., 2010). The responses of the NDVI and LST to meteorological drought were conducted using temporal correlation analysis of the NDVI and LST and multiple SPIs. Time duration and time lag are integrated into the temporal correlation analysis (Ji & Peters, 2003). Time duration refers to the time scales of SPIs (McKee, Doeskin, & Kleist, 1993). In this case, time lag refers to the interval between the occurrence of precipitation and the change in remote-sensing parameters (Ji & Peters, 2003).

In each month, from January to December, the correlations between the monthly NDVI and LST and the corresponding SPIs were calculated, with SPIs in twelve different time durations (1–12 months) and six different time lags (0–5-month lags). As a result, there were 72 correlation coefficients for each month as shown in Table 3.1. We can assess the temporal patterns (duration and lag) of SPIs that most significantly affected the current NDVI and LST in each month using the maximum SPI-NDVI and the minimum SPI-LST coefficients, respectively, based on the assumption that a meteorological drought can lead to lower NDVI and higher LST.

We also calculated the correlation coefficients between the average NDVI and LST in the dry, dry-to-wet, wet, and wet-to-dry season for various years and the corresponding temporal patterns of the SPIs. In Santa Rosa, the four seasons experienced 3 months, 2 months, 5 months, and 2 months respectively. Thus, the time duration of the SPIs for the four seasons ranged from 3 months (the current dry season), 2 months (the current dry-to-wet season), 5 months (the current wet season), and 2 months (the current wet-to-dry season) to 2 years ago (24 months ago). The SPI that most significantly affected the seasonal average NDVI and LST was obtained as the maximum SPI-NDVI and the minimum SPI-LST coefficients respectively.

3.2.4 The seasonal correlation between the average NDVI and LST

The NDVI-LST correlations vary spatially and temporally. To evaluate the predominant factors for the growth of TDFs in four seasons, Pearson Correlation Analysis was conducted between the average NDVI and the average LST in the dry, dry-to-wet, wet and wet-to-dry season, respectively.

3.3 Result

3.3.1 The monthly distribution of the NDVI and LST in SRNP-EMSS

Figure 3.3 shows the monthly distribution of NDVI and LST in each month. Overall, the median NDVI in the dry and the dry-to-wet seasons was lower than in the wet and wet-to-dry seasons, while the LST shows completely opposite trends. As is shown in Figure 3.3 (a), the median value of the NDVI decreased from 0.71 to 0.52 in the dry season from January to March. In the dry-to-wet season, it reached the lowest level at around 0.50 in April and increased to 0.55 in May. In the wet season, the median NDVI dramatically increased to 0.81 in June and stayed at a high level (around 0.85) through the wet season. In the wet-to-dry season, the NDVI stayed at a high level (around 0.8) with a slight decline.

The median LST increased from 302.3 K to 308 K in the dry season (Figure 3.3 b). During the dry-to-wet season, it increased to 309 K in April and decreased to 308.2 K in May. It sharply declined to around 302 K in June and kept relatively stable (between 301 K and 302 K) during the wet season. In the wet-to-dry season, the median LST slightly declined to 301 K in November and increased to 302 K in December. The NDVI and LST variations in the dry season were much higher than in the wet season. Both the NDVI and LST experienced the largest variations in May.

3.3.2 The temporal response of the NDVI and LST to meteorological drought

Table 3.2 shows the maximum SPI-NDVI correlation and the minimum SPI-LST correlation among 72 temporal relationships (time durations (1–12 months) and time lags (0–5-month lags)) in each month. The NDVI and LST can be well explained by the SPIs for most months. Low maximum SPI-NDVI correlations were seen in August, October, November and December, and high minimum SPI-LST correlations were seen in November. The maximum SPI-

NDVI and the minimum SPI-LST correlation varied with the combination of the time duration, time lag and month. The maximum SPI-NDVI and the minimum SPI-LST correlations were obtained at the same combination of the time durations and time lags in January, February, and March (the dry season). They also had the same time lags in April and May (the dry-to-wet season). The combinations for each month during June and December (the wet season and wet-to-dry season) were different, except for September. The time lags for the significant minimum SPI-LST correlations were no longer than the corresponding maximum SPI-NDVI during June and December.

Table 3.3 shows the maximum SPI-NDVI correlation and the minimum SPI-LST correlation in each season. The seasonal temporal correlations varied with the time duration, time lag and season. The maximum SPI-NDVI correlations are significant ($p<0.05$) except in the wet-to-dry season, and the minimum SPI-LST correlations are significant ($p<0.05$) for all the seasons. In addition, the absolute values of the minimum SPI-LST correlations in the dry, wet, and wet-to-dry seasons (0.83, 0.69, and 0.82, respectively) are higher than the maximum SPI-NDVI correlations (0.78, 0.78 and 0.27, respectively). In the dry-to-wet season, the maximum SPI-NDVI correlation (0.78) was higher than the absolute minimum SPI-LST correlation (0.55). In addition, the time durations for the maximum SPI-NDVI correlations (9 , 2, 6, and 3 months) were shorter than the corresponding absolute minimum SPI-LST correlations (11, 3, 13, and 3 months) in each season. The time lag for the maximum SPI-NDVI correlation in the wet season (4 months) was longer than the minimum SPI-LST correlation (1 month). They had the same time lags in the dry, dry-to-wet, and wet-to-dry season (0, 1, and 0 months, respectively).

Figure 3.4 shows the SPIs-NDVI and SPIs-LST correlations as a function of time duration, with 1-month increments given the fixed time lags in each season. The time lags were selected based on the maximum SPI-NDVI and the minimum SPI-LST correlations in each season (Table 3. 3). In the dry season, with the same 0-month time lag, the SPIs-NDVI correlations reached a very high level (r-values>0.75) at durations between 8 and 17 months, and the SPIs-LST correlations were at a very low level (r-values<-0.8) at durations between *11* and *16* months. In the dry-to-wet season, given the same *1*-month time lag, the SPIs-NDVI correlation reached a very high level (r-values>0.75) at 2- and 3-month durations, and the SPIs-LST correlation reached a moderately low level (r-values<-0.5) at the *2*-month duration. In the wet season, the SPIs-NDVI

correlation reached a high level (*r*-values>*0.65*) at durations between 5 months and 7 months given a time lag of 4 months. The SPIs-LST correlations reached a low level at durations between 5 months and 10 months given a time lag of 1 month. In the wet-to-dry season, the SPIs-LST correlations reached (*r*-values<-*0.8*) a very low level at durations between 8 and 13 months. The SPIs-LST correlations were not significant for the entire duration.

3.3.3 The correlation between the seasonal average NDVI and LST

Figure 3.5 shows the correlations between the average NDVI and the average LST in each season. In the dry and dry-to-wet season, they were strongly negatively correlated (*r-value=-0.85 and -0.88, p-value<0.001 and 0.001*). In the wet season, they had a medium negative correlation (*r-value=-0.52, p-value=0.029*). In the wet-to-dry season, the average NDVI and the average LST had a low negative (*r*-value=-*0.11, p-value=0.672*) correlation.

3.4 Discussion

3.4.1 Phenologically dependent responses of NDVI and LST to meteorological drought

The patterns of the NDVI and LST in response to meteorological drought strongly depend on the seasonality in the SRNP-EMSS. NDVI was highly sensitive to precipitation in the dry and dry-to-wet season (*r-value =0.78* and *0.78*) and highly sensitive in the wet season (*r-value =0.66*), and was not sensitive in the wet-to-dry season (*r-value =0.27*). LST was strongly affected by rainfall in the dry and wet-to-dry season (*r-value =-0.83* and *-0.82*), highly affected in the wet season (*r-value =-0.69*), and moderately impacted in the dry-to-wet season (*r-value =-0.55*).

This is due to the NDVI and LST reflecting different biophysical processes in TDFs. The NDVI describes the vegetation greenness and deciduousness of TDFs and LST describes the temperature and evapotranspiration on the surface. In the dry season, the deciduousness and evapotranspiration in the TDFs were highly sensitive to precipitation due to less water storage in the roots of TDFs. In the dry-to-wet season, the NDVI grew sharply due to leaf flush in May, which was driven by precipitation. The evapotranspiration in TDFs was impacted by not only the precipitation but also the amount of new leaves. In the wet season, although precipitation can affect the greenness and evapotranspiration in TDFs, they were resistant to meteorological drought due to the abundant water storage in the roots, especially in October, during the late stage of the wet

season. The response of LST was a deceasing trend, as expected. The response of the NDVI was weak (*r-value =0.41*) in August but very strong (*r-value =0.81*) in September. This resulted from TDFs experiencing a short-term rainfall deficiency at the end of July (Figure 3.2). This result indicates the greenness is more resistant to a short-term rainfall deficiency than evapotranspiration in TDFs, but the greenness is more sensitive to precipitation after a period of water deficiency. In the dry-to-wet season, the defoliation of TDFs, especially in December, is due to the phenological timing instead of precipitation; however, rainfall can still have a strong impact on the evapotranspiration on the canopy surface.

3.4.2 Water availability, duration, and timing as key factors controlling the NDVI and LST

The temporal responses of the NDVI and LST to water deficiency (magnitude of meteorological drought) largely depend on its duration (the period for precipitation accumulation) and the timing (the onset for precipitation) of precipitation.

In the dry season, the strongest correlations between NDVI and LST and SPIs (*r-value=0.78* and *-0.83*) were found when the precipitation was integrated over 9 and 11 months, which included the entire current dry season (3 months) plus the 6 and 8 preceding months, respectively. The average NDVI was affected by the precipitation of not only the current dry season, but also the precipitation of the wet and wet-to-dry season of the preceding year, and the average LST was influenced by the precipitation of the current dry season as well as the previous dry-to-wet, wet, and wet-to-dry seasons. This indicates that the greenness and evapotranspiration of TDFs in the dry season were strongly influenced by a relatively long period of precipitation. This is because much of the precipitation is stored in the root zone when the rainfall is abundant in the previous year, which can mitigate defoliation and provide water for evapotranspiration in TDFs in the dry season.

In the dry-to-wet season, the SPI-NDVI correlation peaked at the duration of 2 months and the lag of 1 month. This means the average NDVI was strongly affected (*r-value=0.78*) by the accumulated precipitation in March and April of the current year. The SPI-LST reached the bottom (*r-value=-0.55*) at the duration of 3 months and the lag of 1 month, showing that the average LST was moderately influenced by the total rainfall received during February to April of the current

year. This is because the leaf flush in the dry-to-wet season, especially in May, was strongly controlled by the sporadic rainfall during March to April instead of in May when the precipitation was abundant. Also, the evapotranspiration was partially influenced by the accumulated precipitation during February to April of the current year when the rainfall was less. The result illustrates that evapotranspiration and especially leaf flush in TDFs are sensitive to the timing of precipitation.

In the wet season, the average NDVI was highly affected (*r-value=0.66*) by the accumulated precipitation during January to June of the current year, and the average LST was highly influenced (*r-value=-0.69*) by the total rainfall during the previous August to the current September. This indicates that greenness is affected not only by the magnitude of precipitation but also the timing of precipitation. The evapotranspiration is more affected by the magnitude of precipitation rather than the timing of precipitation.

In the wet-to-dry season, the average NDVI did not significantly correlate with SPIs, indicating that water availability is not a factor that affects the greenness of TDFs. The average LST was strongly influenced (*r-value=-0.82*) by the accumulated precipitation during the previous November to the current December, indicating that the evapotranspiration in TDFs is only sensitive to the magnitude of precipitation for a long period.

3.4.3 Estimate of the primary response of TDFs to meteorological drought

The primary response of TDFs to water deficiency is a decline in primary productivity (Dale et al., 2001; Xiao et al., 2004). The MODIS Gross primary productivity (GPP) algorithm (Running et al., 2004) estimates the GPP as a function of the photosynthetically active radiation (PAR), NDVI, LST, air temperature, and maximum light use efficiency (ε_{max}). Among them, the NDVI, LST, and ε_{max} are relative to vegetation characteristics. The MODIS GPP algorithm estimates the ε_{max} based on the Biome Properties Look-Up Table (BPLUT), which mistakes TDFs for desert. However, the primary response of TDFs to meteorological drought can be indirectly estimated based on the temporal correlation analysis of NDVI and LST and SPIs (Figure 3.4 and Figure 3.5), based on the hypothesis that ε_{max} varies with season but not with year. The GPP of TDFs is considered to be affected by meteorological drought when both NDVI and LST have significant correlations with specific SPIs simultaneously.

In the dry season, the SPI-NDVI correlations reached a high level from a duration of 8 months to a duration of 17 months for the fixed lag of 0 month, and the SPI-LST correlations reached a low level from a duration of 11 months to a duration of 16 months for the fixed lag of 0 months (Figure 3.4). GPP was considered to respond to the precipitation with a duration of 11 months (the minimum intersection) and a lag of *0* months. The NDVI-LST correlation (*r-value=-0.85*) was highly negative (Figure 3.5), indicating that water is the predominant factor for the growth of TDFs in the dry season. We inferred that the average GPP is strongly influenced by the accumulated precipitation from the preceding February to the current March. In the dry-to-wet season, the SPI-NDVI correlations reached a high level from a duration of 2 to 3 months for the fixed lag of 1 month, and the SPI-NDVI correlations reached a low level at a duration of 3 months for the fixed lag of 1 month (Figure 3.4). GPP s responded to the precipitation with a duration of 3 months and a lag of 1 month. The NDVI-LST correlation (*r-value=-0.85*) was highly negative in the dry-to-wet season (Figure 3.5). We inferred that the average GPP was strongly affected by the total precipitation from February to April of the current year. In the wet season, the average NDVI was highly affected by the total precipitation from January to June of the current year. The average LST was highly influenced by the accumulated precipitation from the previous December to the current September. The NDVI-LST correlation was moderately negative (*r-value=-0.52*). We inferred that GPP is moderately influenced by the precipitation from January to June of the current year based on the hypothesis that the greenness is a more important parameter than evapotranspiration for calculating GPP. In the wet-to-dry season, the NDVI-LST correlation was not significant (Figure 3.5), indicating that water is not the dominant factor in the growth of TDFs. We can infer that GPP is not influenced by precipitation in the wet-to-dry season.

3.5 Conclusion

The response of the NDVI and the LST to the SPIs, is crucial to understand how TDFs respond to meteorological droughts. In this study, I conducted temporal correlations between the MODIS-derived NDVI and LST to the SPIs between March 2000 and March 2017 in the TDFs at the Santa Rosa National Park Monitoring Super Site (SRNP-EMSS) at monthly and seasonal scales.

I found that the NDVI and LST largely depend on the seasonality as well as the magnitude, duration, and timing of precipitation. In the dry season, the average NDVI and LST were sensitive to the magnitude of a long period of precipitation. In the dry-to-wet season, the average NDVI and LST were strongly and moderately sensitive to the magnitude of short-term precipitation and the timing of precipitation, respectively. In the wet season, the average NDVI was highly sensitive to half-year accumulated precipitation. The average LST was highly sensitive to the magnitude of long-term precipitation. In the wet-to-dry season, precipitation is not a key factor controlling NDVI, but average LST is highly sensitive to the magnitude of long-term precipitation.

Regarding the GPP response of the SRNP-EMSS to meteorological drought, I conclude that GPP is affected by yearly, short-term, and half-year accumulated precipitation in the dry, dry-to-wet season, and wet season respectively. In the wet-to-dry season, GPP was not influenced by precipitation.

3.6 References

Allen, C. D., Breshears, D. D., & McDowell, N. G. (2015). On underestimation of global vulnerability to tree mortality and forest die-off from hotter drought in the Anthropocene. *Ecosphere, 6*(8), 129.

Anderson, L. O., Malhi, Y., Aragão, L. E., Ladle, R., Arai, E., Barbier, N., & Phillips, O. (2010). Remote sensing detection of droughts in Amazonian forest canopies. *New Phytologist, 187*(3), 733-750.

Asner, G. P., Nepstad, D., Cardinot, G., & Ray, D. (2004). Drought stress and carbon uptake in an Amazon forest measured with spaceborne imaging spectroscopy. *Proceedings of the National Academy of Sciences, 101*(16), 6039-6044.

Balvanera, P., Castillo, A., & Martínez-Harms, M. J. (2011). Ecosystem services in seasonally dry tropical forests. *Seasonally dry tropical forests* (pp. 259-277) Springer.

Brando, P. M., Goetz, S. J., Baccini, A., Nepstad, D. C., Beck, P. S., & Christman, M. C. (2010). Seasonal and interannual variability of climate and vegetation indices across the amazon. *Proceedings of the National Academy of Sciences, 107*(33), 14685-14690.

Calvo-Alvarado, J., McLennan, B., Sánchez-Azofeifa, A., & Garvin, T. (2009). *Deforestation and forest restoration in Guanacaste, Costa Rica: Putting conservation policies in context, 285(6)*, 931-940

Calvo-Rodriguez, S., Sanchez-Azofeifa, A. G., Duran, S. M., & Espirito-Santo, M. M. (2017). Assessing ecosystem services in neotropical dry forests: A systematic review. *Environmental Conservation, 44*(1), 34-43.

Campos, F. A. (2018). A synthesis of long-term environmental change in santa rosa, costa rica. *Primate life histories, sex roles, and adaptability* (pp. 331-358) Springer.

Cao, S., Sanchez-Azofeifa, G. A., Duran, S. M., & Calvo-Rodriguez, S. (2016). Estimation of aboveground net primary productivity in secondary tropical dry forests using the Carnegie–Ames–Stanford approach (CASA) model. *Environmental Research Letters, 11*(7), 075004.

Cao, S., & Sanchez-Azofeifa, A. (2017). Modeling seasonal surface temperature variations in secondary tropical dry forests. *International Journal of Applied Earth Observation and Geoinformation, 62*, 122-134.

Castro, S. M., Sanchez-Azofeifa, G. A., & Sato, H. (2018). Effect of drought on productivity in a Costa Rican tropical dry forest. *Environmental Research Letters, 13*(4), 045001Chadwick, W. W., Paduan, J. B., Clague, D. A., Dreyer, B. M., Merle, S. G., Bobbitt, A. M., Nooner, S. L. (2016). Voluminous eruption from a zoned magma body after an increase in supply rate at Axial Seamount. *Geophysical Research Letters, 43*(23), 12,070.

Choat, B., Jansen, S., Brodribb, T. J., Cochard, H., Delzon, S., Bhaskar, R., Hacke, U. G. (2012). Global convergence in the vulnerability of forests to drought. *Nature, 491*(7426), 752.

Dale, V. H., Joyce, L. A., McNulty, S., Neilson, R. P., Ayres, M. P., Flannigan, M. D., Peterson, C. J. (2001). Climate change and forest disturbances: Climate change can affect forests by

altering the frequency, intensity, duration, and timing of fire, drought, introduced species, insect and pathogen outbreaks, hurricanes, windstorms, ice storms, or landslides. *Bioscience, 51*(9), 723-734.

Goward, S. N., Xue, Y., & Czajkowski, K. P. (2002). Evaluating land surface moisture conditions from the remotely sensed temperature/vegetation index measurements: An exploration with the simplified simple biosphere model. *Remote Sensing of Environment, 79(2-3)*, 225-242.

Guttman, N. B. (1999). Accepting the standardized precipitation index: A calculation algorithm. *Journal of the American Water Resources Association, 35*(2), 311-322.

Hoekstra, J. M., Boucher, T. M., Ricketts, T. H., & Roberts, C. (2005). Confronting a biome crisis: Global disparities of habitat loss and protection. *Ecology Letters, 8*(1), 23-29.

Janzen, D. H. (1988). Management of habitat fragments in a tropical dry forest: Growth. *Annals of the Missouri Botanical Garden,* 105-116.

Janzen, D. H. (2000). Costa Rica's area de conservacin Guanacaste: A long march to survival through non-damaging biodevelopment. *Biodiversity, 1*(2), 7-20.

Ji, L., & Peters, A. J. (2003). Assessing vegetation response to drought in the northern Great Plains using vegetation and drought indices. *Remote Sensing of Environment, 87*(1), 85-98.

Kalacska, M., Sanchez-Azofeifa, G. A., Calvo-Alvarado, J. C., Quesada, M., Rivard, B., & Janzen, D. H. (2004). Species composition, similarity and diversity in three successional stages of a seasonally dry tropical forest. *Forest Ecology and Management, 200*(1-3), 227-247.

Karnieli, A., Bayasgalan, M., Bayarjargal, Y., Agam, N., Khudulmur, S., & Tucker, C. J. (2006). Comments on the use of the vegetation health index over Mongolia. *International Journal of Remote Sensing, 27*(10), 2017-2024.

Karnieli, A., Agam, N., Pinker, R. T., Anderson, M., Imhoff, M. L., Gutman, G. G., Goldberg, A. (2010). Use of NDVI and land surface temperature for drought assessment: Merits and limitations. *Journal of Climate, 23*(3), 618-633.

Liu, J., Sun, O. J., Jin, H., Zhou, Z., & Han, X. (2011). Application of two remote sensing GPP algorithms at a semiarid grassland site of north china. *Journal of Plant Ecology, 4*(4), 302-312.

Maass, J. M., Balvanera, P., Castillo, A., Daily, G. C., Mooney, H. A., Ehrlich, P., García-Oliva, F. (2005). Ecosystem services of tropical dry forests: Insights from longterm ecological and social research on the pacific coast of mexico. *Ecology and Society: A Journal of Integrative Science for Resilience and Sustainability, 10*(1), 1-23.

McDowell, N., Pockman, W. T., Allen, C. D., Breshears, D. D., Cobb, N., Kolb, T., Yepez, E. A. (2008). Mechanisms of plant survival and mortality during drought: Why do some plants survive while others succumb to drought? *New Phytologist, 178*(4), 719-739.

McKee, T. B., Doeskin, N. J., & Kleist, J. (1993). (1993). The relationship of drought frequency and duration to time scales. Paper presented at the 179-184.

Murphy, P. G., & Lugo, A. E. (1986). Ecology of tropical dry forest. *Annual Review of Ecology and Systematics, 17*(1), 67-88.

Nichol, J. E., & Abbas, S. (2015). Integration of remote sensing datasets for local scale assessment and prediction of drought. *Science of the Total Environment, 505*, 503-507.

Olukayode Oladipo, E. (1985). A comparative performance analysis of three meteorological drought indices. *International Journal of Climatology, 5*(6), 655-664.

Palmer, W. C. (1965). Meteorological drought, US Department of Commerce, Research Paper 45, 58.

Patel, N. R., Chopra, P., & Dadhwal, V. K. (2007). Analyzing spatial patterns of meteorological drought using standardized precipitation index. *Meteorological Applications, 14*(4), 329-336.

Phillips, O. L., Arago, L. E., Lewis, S. L., Fisher, J. B., Lloyd, J., Lopez-Gonzalez, G., Quesada, C. A. (2009). Drought sensitivity of the amazon rainforest. *Science, 323*(5919), 1344-1347.

Portillo-Quintero, C. A., & Sanchez-Azofeifa, G. A. (2010). Extent and conservation of tropical dry forests in the Americas. *Biological Conservation, 143*(1), 144-155.

Prihodko, L., & Goward, S. N. (1997). Estimation of air temperature from remotely sensed surface observations. *Remote Sensing of Environment, 60(3)*, 335-346.

Quesada, M., Sanchez-Azofeifa, G. A., Alvarez-Anorve, M., Stoner, K. E., Avila-Cabadilla, L., Calvo-Alvarado, J., Fernandes, G. W. (2009). Succession and management of tropical dry forests in the americas: Review and new perspectives. *Forest Ecology and Management, 258*(6), 1014-1024.

Rhee, J., Im, J., & Carbone, G. J. (2010). Monitoring agricultural drought for arid and humid regions using multi-sensor remote sensing data. *Remote Sensing of Environment, 114*(12), 2875-2887.

Rouault, G., Candau, J., Lieutier, F., Nageleisen, L., Martin, J., & Warzée, N. (2006). Effects of drought and heat on forest insect populations in relation to the 2003 drought in Western Europe. *Annals of Forest Science, 63*(6), 613-624.

Running, S. W., Nemani, R. R., Heinsch, F. A., Zhao, M., Reeves, M., & Hashimoto, H. (2004). A continuous satellite-derived measure of global terrestrial primary production. *Bioscience, 54*(6), 547-560.

Sanchez-Azofeifa, G. A., Quesada, M., Rodríguez, J. P., Nassar, J. M., Stoner, K. E., Castillo, A., Cuevas-Reyes, P. (2005). Research priorities for neotropical dry forests. *Biotropica, 37*(4), 477-485.

Vicente-Serrano, S., Beguería, S., & López-Moreno, J. I. (2010). A multiscalar drought index sensitive to global warming: The standardized precipitation evapotranspiration index. *Journal of Climate, 23*(7), 1696-1718.

Wang, J., Rich, P. M., & Price, K. P. (2003). Temporal responses of NDVI to precipitation and temperature in the central great plains, USA. *International Journal of Remote Sensing, 24*(11), 2345-2364.

Williams, A. P., Allen, C. D., Macalady, A. K., Griffin, D., Woodhouse, C. A., Meko, D. M., Grissino-Mayer, H. D. (2013). Temperature as a potent driver of regional forest drought stress and tree mortality. *Nature Climate Change, 3*(3), 292-297.

Xiao, X., Zhang, Q., Braswell, B., Urbanski, S., Boles, S., Wofsy, S., Ojima, D. (2004). Modeling gross primary production of temperate deciduous broadleaf forest using satellite images and climate data. *Remote Sensing of Environment, 91*(2), 256-270.

Zargar, A., Sadiq, R., Naser, B., & Khan, F. I. (2011). A review of drought indices. *Environmental Reviews, 19*, 333-349.

3.7 Tables and Figures

Table 3. 1 The temporal patterns (12 time durations * 6 time lags) of correlations between the SPIs and the NDVI and LST in each month. The numbers in the cells show the time period of the SPIs. For example, zero shows the current month, one indicates the first previous month, and 0–1 shows the period from the current month to the first current month.

	Duration											
Lag	1	2	3	4	5	6	7	8	9	10	11	12
0	0	0-1	0-2	0-3	0-4	0-5	0-6	0-7	0-8	0-9	0-10	0-11
1	1	1-2	1-3	1-4	1-5	1-6	1-7	1-8	1-9	1-10	1-11	1-12
2	2	2-3	2-4	2-5	2-6	2-7	2-8	2-9	2-10	2-11	2-12	2-13
3	3	3-4	3-5	3-6	3-7	3-8	3-9	3-10	3-11	3-12	3-13	3-14
4	4	4-5	4-6	4-7	4-8	4-9	4-10	4-11	4-12	4-13	4-14	4-15
5	5	5-6	5-7	5-8	5-9	5-10	5-11	5-12	5-13	5-14	5-15	5-16

Table 3. 2 The maximum temporal correlation coefficients (*r*-value) between the NDVI and the corresponding SPIs with 12 different time durations (1–12 months) and 6 different time lags (0–5 months), and the minimum temporal correlation coefficients (*r*-value) between the LST and the corresponding SPIs with 12 different time durations (1–12 months) and 6 different time lags (0–5 months) in each month. The asterisk indicates that the *p*-value is less than *0.05*. Red, blue, green and yellow shades indicate the dry season, dry-to-wet season, wet season and wet-to-dry season, respectively. The red, blue, green, and yellow indicate the dry, dry-to-wet, wet, and the wet-to-dry season, respectively.

	The maximum SPI-NDVI correlation		The minimum SPI-LST correlation	
Period	Time	*r*-value	Time	*r*-value
January	Duration=5 Lag=0	0.55*	Duration=5 Lag=0	-0.68*
February	Duration=10 Lag=0	0.79*	Duration=10 Lag=0	-0.70*
March	Duration=12 Lag=0	0.87*	Duration=12 Lag=0	-0.64*
April	Duration=12 Lag=0	0.63*	Duration=10 Lag=0	-0.62*
May	Duration=2 Lag=1	0.76*	Duration=3 Lag=1	-0.55*
June	Duration=11 Lag=2	0.65*	Duration=12 Lag=1	-0.76*
July	Duration=2 Lag=4	0.66*	Duration=6 Lag=2	-0.77*
August	Duration=3 Lag=0	0.41	Duration=9 Lag=0	-0.70*
September	Duration=1 Lag=4	0.81*	Duration=1 Lag=4	-0.69*
October	Duration=8 Lag=5	0.34	Duration=1 Lag=0	-0.54*
November	Duration=1 Lag=2	-0.04	Duration=5 Lag=5	-0.42
December	Duration=3 Lag=0	0.38	Duration=7 Lag=0	-0.79*

Table 3. 3 The maximum temporal correlation coefficients (*r*-value) between the average NDVI and the corresponding SPIs with different time durations (the current season - 24 months) and 6 different time lags (0–5 months), and the minimum temporal correlation coefficients (*r*-value) between the average LST and the corresponding SPIs with different time durations (the current season - 24 months) and 6 different time lags (0–5 months) in each season. The asterisk indicates that the *p*-value is less than *0.05*.

	The maximum SPI-NDVI correlation			The minimum SPI-LST correlation		
Period	Time		*r*-value	Time		*r*-value
Dry season	Duration=9	Lag=0	0.78*	Duration=11	Lag=0	-0.83*
Dry-to-Wet season	Duration=2	Lag=1	0.78*	Duration=3	Lag=1	-0.55*
Wet season	Duration=6	Lag=4	0.66*	Duration=10	Lag=1	-0.69*
Wet-to-Dry season	Duration=3	Lag=0	0.27	Duration=13	Lag=0	-0.82*

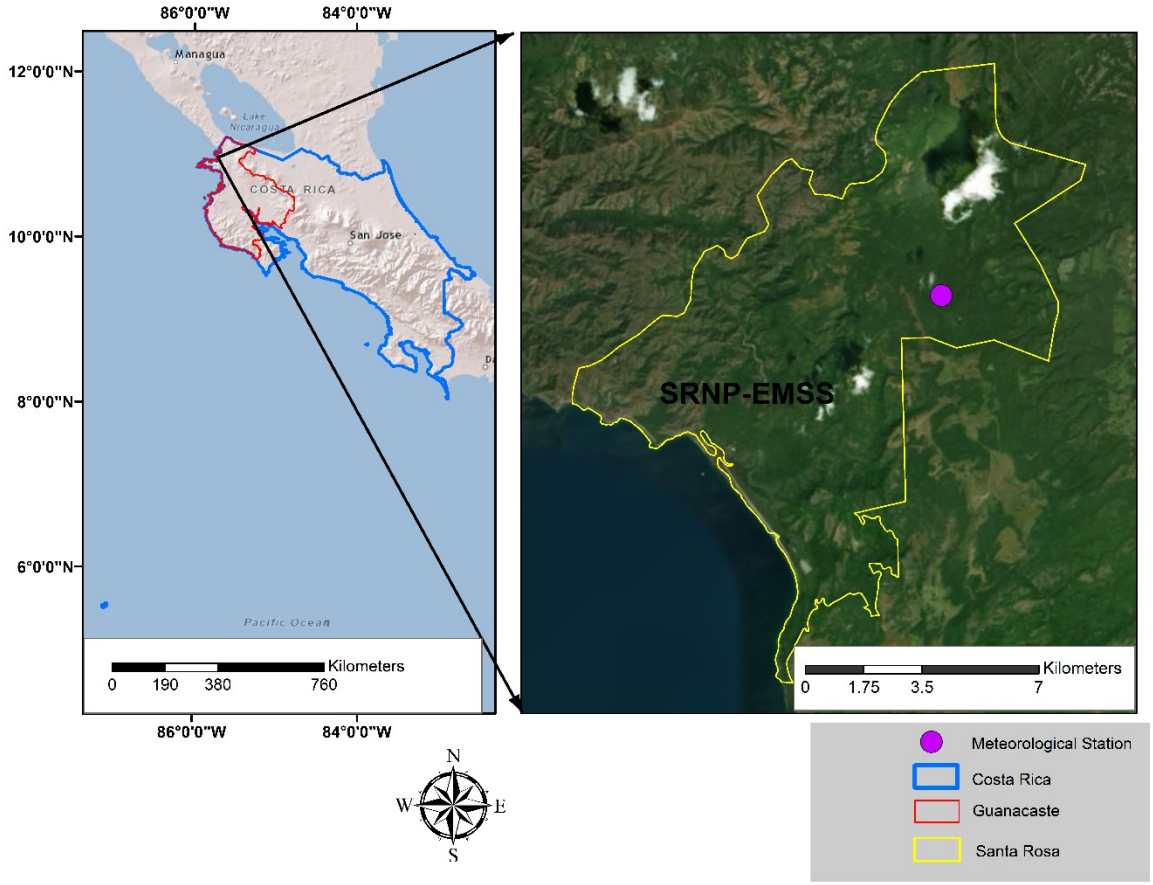

Figure 3. 1 Study area: Santa Rosa National Park Monitoring Super Site (SRNP-EMSS).

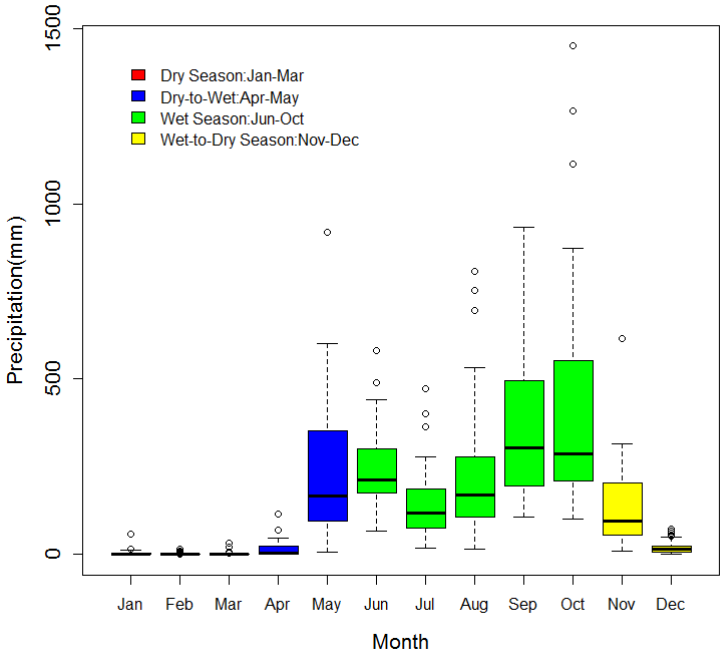

Figure 3. 2 *The monthly precipitation distribution in each month (SRNP-EMSS) from June 1976 to March 2017.*

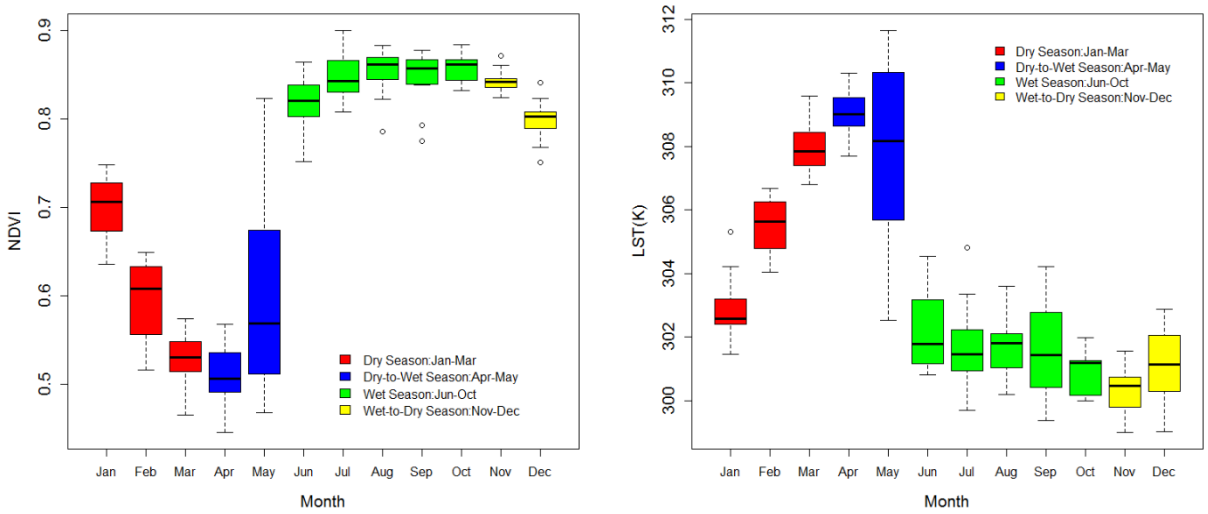

(a) NDVI distribution

(b) LST distribution

Figure. 3 The monthly distribution of the NDVI and LST in each month in Santa Rosa (SRNP-EMSS) from March 2000 to March 2017.

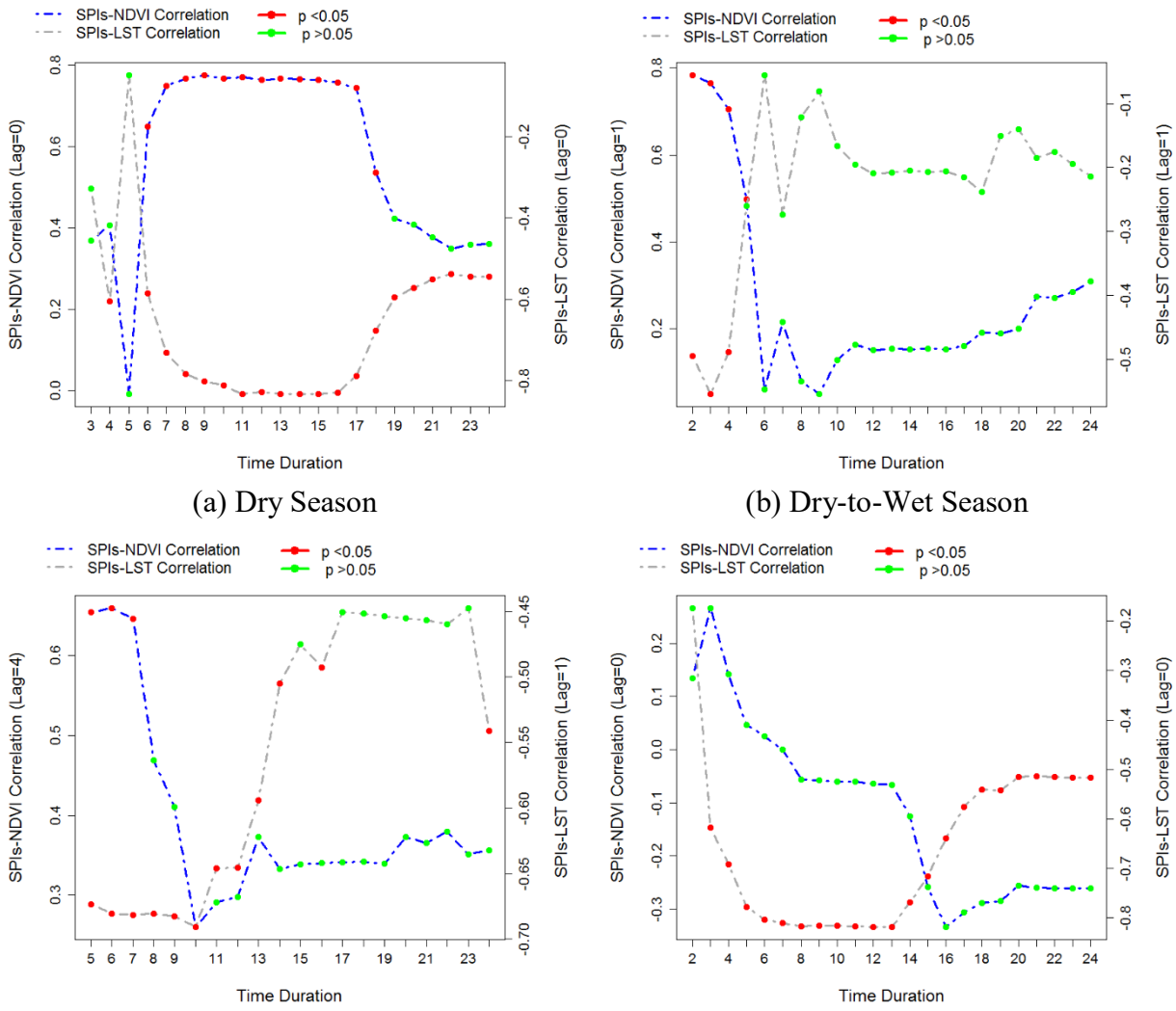

Figure. 4 Correlation coefficients as a function of time duration in the fixed time lag corresponding to the maximum SPI-NDVI correlation and the minimum SPI-LST correlation in the dry, dry-to-wet, wet and wet-to-dry season. Red dots and green dots indicate the SPI-NDVI and SPI-LST correlations with p-values less than *0.05* and no less than *0.05*, respectively.

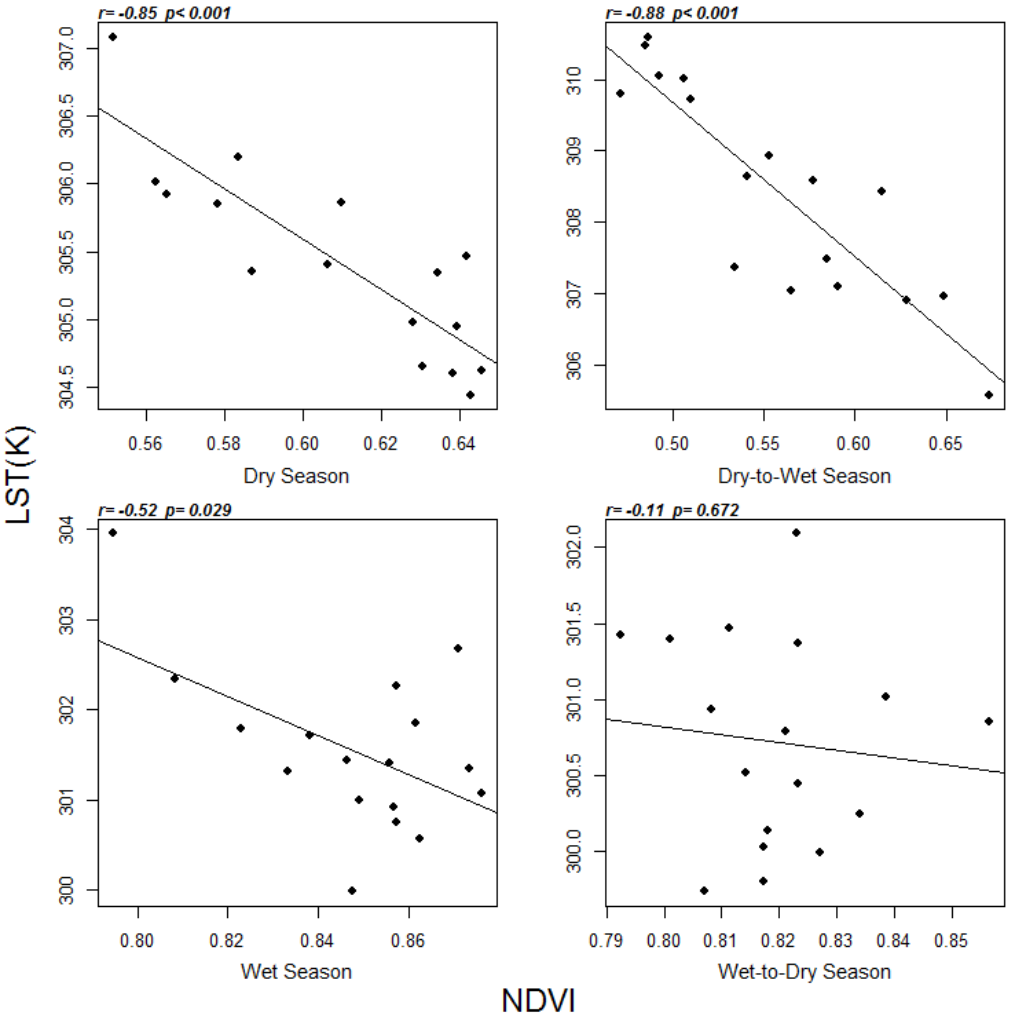

Figure 3. 5 The correlations between the average NDVI and the average LST in the dry, dry-to-wet, wet, and wet-to-dry season.

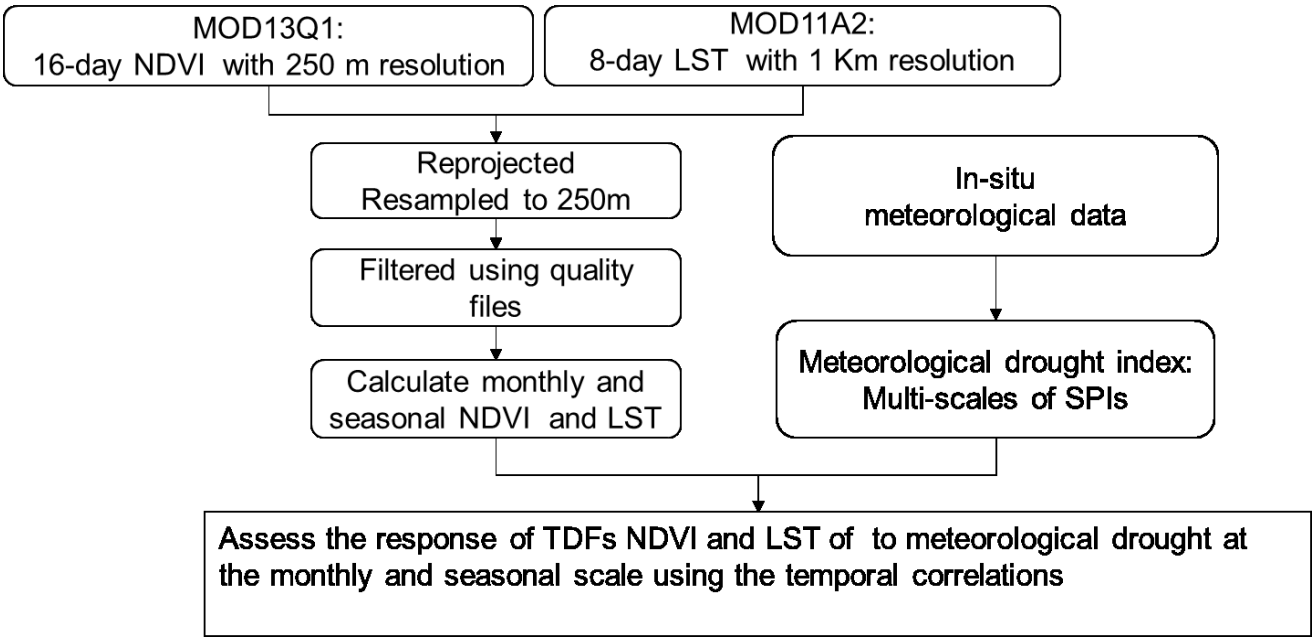

Figure 3. 6 Flowchart for assessing the temporal response of TDFs to meteorological drought

Chapter 4

Assessment of the response of Tropical Dry Forests to El Niño Southern Oscillation

4.1 Introduction

Tropical Dry Forests (TDFs) are ecosystems dominated by deciduous species, with a mean annual precipitation of 700–2000 mm, an average annual temperature greater than 25°C, and a dry season between 4 to 6 months where the precipitation is less than 100 mm (Sanchez-Azofeifa et al., 2005).

Global climate models predict more severe droughts, in terms of magnitude and duration, will occur in TDFs (Chadwick et al., 2016; Castro et al., 2018). TDFs are susceptible to droughts because the regimes of precipitation determine phenological patterns and water availability is the limiting factor for plant growth and regeneration (Lopezaraiza-Mikel et al., 2013). One important source of droughts is the El Niño Southern Oscillation (ENSO; Murphy, 2006). ENSO is defined as a coupled mechanism between large-scale oceanic and atmospheric circulation processes in the equatorial Pacific Ocean that affects global climate and weather (Propastin et al., 2010). This mechanism leads to the redistribution of precipitation and temperature patterns for certain regions of the world (IPCC, 2007). El Niño is the warm phase of ENSO resulting from a weakening of trade winds and warmer Sea Surface Temperature (SST) across the east and central tropical Pacific, while La Niña is the cold phase of ENSO associated with stronger trade winds and cooler SST (Trenberth, 1997).

El Niño-induced droughts are pronounced in the central America, north and northeast of South America, Southeast Asia, northern Australia, northern and central India, and southwest Africa (Holmgren et al., 2001) where massive TDFs are located (Miles et al., 2006). Severe El Niño-induced drought can change the structure and function of the forest ecosystem, destroy biodiversity, increase the mortality rate, and cause wildfires (Allen et al., 2010). Satellite remote sensing has been broadly used to identify terrestrial biospheric dynamics linked to El Niño due to its advantages of high temporal resolution and large and consistent coverage areas (Kogan, 1998; Brown et al., 2008; Erasmi et al., 2009; Bi et al., 2016). The satellite-derived Normalized Difference Vegetation Index (NDVI) is one of the most commonly used vegetation indices; it

reflects greenness and vigor because it is highly correlated with green leaf density and chlorophyll content in plants (Sellers et al., 1997; Heinsch et al., 2006). As a complement, Land Surface Temperature (LST) is a biophysical parameter that reflects canopy water content and evapotranspiration on the surface (Karnieli et al., 2010; Cao & Sanchez-Azofeifa, 2017). Remote sensing drought indices, such as the Vegetation Condition Index (VCI; Kogan, 1995) and the Temperature Condition Index (TCI; Kogan, 1995) have been derived using time series of remotely sensed parameters (NDVI and LST) to monitor vegetation stress and the effects of El Niño on vegetation (Kogan, 1998). These drought indices allow vegetation stress and the impacts of El Niño on vegetation to be compared in different ecosystems in various regions (Kogan et al., 1995; 1997; 2004).

A number of studies have analyzed and described the ENSO-related impacts on various ecosystems in tropical regions (Kogan, 1998; Mennis 2001; Anyamba, 2002; Boyd & Phipps, 2002; Nagai et al. 2007; Erasmi et al., 2009; Propastin et al., 2010). Some studies devoted to monitoring the short-term response of the vegetated surface to ENSO during an individual El Niño event (Kogan, 1998; Anyamba, 2002; Boyd & Phipps, 2002). Kogan (1998) recognized the vegetation stress occurring in land ecosystems in Southern Africa during the 1997–1998 El Niño using an anomaly in the vegetation and temperature index. Anyamba et al. (2002) analyzed vegetation response patterns over East and Southern Africa during El Niño in 1997 and 1998 and found that the NDVI anomaly had a positive correlation with SST anomalies for East Africa but a negative correlation for Southern Africa. Boyd & Phipps (2002) explored the impact of El Niño-induced drought stress on tropical rainforests in Sabah, Malaysia during 1997 and 1998 and concluded that middle infrared reflectance (MIR) is more sensitive to precipitation deficits caused by El Niño than NDVI in tropical rainforest ecosystems. However, such studies failed to assess the impacts of El Niño on ecosystems precisely because the El Niño-affected areas cannot be coherent between different El Niño events (Erasmi et al., 2009).

To solve this problem, a Moving Window Correlation Analysis (MWCA) is used to assess the teleconnection between El Niño and ecosystems based on multiple El Niño events (Erasmi et al., 2009; Propastin et al., 2010). Erasmi et al. (2009) investigated El Niño-related impacts on various tropical ecosystems in Indonesia during the period 1982–2006, by analyzing the relationship between monthly ENSO proxies and NDVI based on a MWCA. They found that the

resistance of vegetation to drought stress is strongly affected by land-use intensity, and degraded forest areas and croplands are more sensitive to drought conditions than natural forests. Propastin et al., (2010) analyzed the vulnerability of vegetated surfaces over Africa to El Niño using MWCA for the period 1982–2006. They concluded that the impacts of El Niño on vegetation largely depend on the vegetation type, and wooded and non-wooded vegetation types are more sensitive than tropical rainforests.

Other studies focused on the long-term response of ecosystems to ENSO (Mennis 2001; Nagai et al. 2007). Mennis (2001) explored the relationship between the SST anomaly in Pacific Niño 3.4 and NDVI in the Southeast USA for the period 1982–1992. The result indicated that El Niño events triggered a decline in vegetation vigor, and the SST anomaly had the strongest correlation with the NDVI for deciduous forests and a weak correlation with the NDVI for evergreen forests and croplands. Nagai et al. (2007) examined the relationship among time-series NDVI, climate indices (precipitation, temperature, and incoming surface solar radiation), and ENSO proxy over tropical rainforests in the Amazon basin and southeastern Asia from 1981 to 2000. The result revealed that precipitation and temperature affected by ENSO are more important factors in controlling vegetation activities over tropical rainforests than incoming surface solar radiation. The teleconnections between ENSO and climate variables (e.g. precipitation and temperature) were reported by Campos (2018) in Santa Rosa National Park, Costa Rica, where TDFs inhabit. The result revealed that the driest and wettest periods on record happened in connection with strong El Niño and La Niña, respectively. In addition, Castro et al. (2018) explored the impact of drought on the productivity of TDFs in Santa Rosa National Park, Costa Rica during the 2014–2016 El Niño event. They found that gross primary productivity declined by 13% and 42% during the 2014 and 2015 drought seasons, respectively. However, no research on the teleconnection between ENSO and vegetation variability in TDFs has been published.

The objective of this study is to quantify the response of TDFs to ENSO from long-term and short-term perspectives at multiple sites across the Americas. We use time-series VCI and TCI as the response variables, and the SST anomaly in the Niño 3.4 region as the ENSO proxy. Here I try to answer the following questions from a long and a short term response, respectively: (1) From a long term perspective, what is the temporal correlation between VCI and TCI and SST anomalies at the seasonal scale? And (2) from a short-term perspective, what are the impacts of El Niño

events on the TDFs based on the MWCA? This analysis is expected to contribute towards a deeper understanding of the vulnerability of TDFs to ENSO and the teleconnection between ENSO and climate variability across the Americas. Figure 4.7 shows the flowchart for this study.

4.2 Methods

4.2.1 Study sites

This study was conducted in four conservation areas of TDFs in the Americas: Chamela-Cuixmala Biosphere Reserve (CCBR) in Mexico, Parque Estadual da Mata Seca (PEMS) in Brazil, Tucabaca Valley Municipal Wildlife Reserve (TVMWR) in Bolivia, and Santa Rosa National Park Environmental Monitoring Super Site (SRNP-EMSS) in Costa Rica (Figure 4.1). These study areas cover different latitudes ranging from 18°15'S to 19°30'N in the Americas. Mean Annual Precipitation (MAP) in CCBR (763 mm) and PEMS (818 mm) is less, and that in SRNP-EMSS (1390 mm) and TVMWR (1234 mm) is abundant. These sites have a similar Mean Annual Temperature (MAT), around 25°C. The start time and end time of the dry season and wet season are different (Table 4.1). The study sites comprise of secondary TDFS on different levels of ecological succession. (Janzen, 1998; Maass et al., 2005; Miles et al., 2006; Madeira et al.,2009; Portillo-Quintero et al., 2015). Figure 4.2 present the different phenological phases as a function of their local NDVI and LST.

4.2.2 Remote sensing drought indices

As one of the most widely used drought indexes, the Vegetation Drought Index (VCI; Kogan 1995; 1997) was calculated using the Normalized Difference Vegetation Index (NDVI), which is highly relevant to greenness and vegetation vigor and can be viewed as a proxy of photosynthetic activity (Sellers et al. 1997). As a complement, the Temperature Drought Index (TCI) is calculated from Land Surface Temperature (LST), which is closely related to vegetation water stress, soil moisture, and evapotranspiration (Kogan 1995; 1997; Karnieli et al., 2010). The monthly VCI and TCI were obtained using the following formula:

$$VCI_{ij} = (NDVI_{ij} - NDVI_{j\,min})/(NDVI_{j\,max} - NDVI_{j\,min}) * 100 \quad (1)$$

$$TCI_{ij} = (LST_{j\,max} - LST_{j})/(LST_{j\,max} - LST_{j\,min}) * 100 \quad (2)$$

Where *i* describes the *i* th year, *j* represents the *j* th month, and $NDVI_{j\,max}$ and $NDVI_{j\,min}$ represent the maximum and minimum NDVI value in the *j* th month across all the years, respectively. $LST_{j\,max}$ and $LST_{j\,min}$ represent the maximum and minimum LST value in the *j* th month across all the years, respectively. The values of VCI and TCI between 0 and 35 represent extreme drought conditions; the values between 35 and 50 show moderate drought conditions, and values between 50 and 100 illustrate normal and humid conditions (Kogan, 1995; 1997).

I retrieved the sixteen-day and eight-day Terra Moderate Resolution Imaging Spectroradiometer (MODIS) NDVI (MOD13Q1, collection v006) and LST (MOD11A2, collection v006) products with 250-m and 1-km resolution from March 2000 to March 2017 at reverb echo (http://reverb.echo.nasa.gov/reverb/). These images were re-projected to Universal Transverse Mercator with central zone 16 N° and WGS84. The monthly NDVI and LST were aggregated on a linear weight average of sixteen-day NDVI and eight-day LST after removing the missing data based on the quality file. The weight for each sixteen-day NDVI and eight-day LST imagery is calculated by the number of days belonging to each month divided by the total number of days in the month (Rhee et al., 2010).

4.2.3 ENSO index

The intensity of a specific ENSO event can be described via various ENSO proxies. According to the definition of the National Oceanic and Atmospheric Administration (NOAA), an ENSO warm (cold) event is a phenomenon in the equatorial Pacific Ocean characterized by five consecutive three-month running mean of SST anomalies at or above +0.5°C (at or below -0.5°C) in the Niño 3.4 region (5°S–5°N, 120°W–170°W). ENSO events can be classified as neutral (|SST anomaly|<0.5), weak (0.5<|SST anomaly|<1.0), moderate (1.0<|SST anomaly|<1.5), strong (1.5<|SST anomaly|<2.0) and very strong (|SST anomaly ≥ 2.0) events. As such, El Niño events in 08/2004–03/2005 and 10/2006–02/2007 were classified as weak, those in 07/2002–03/2003and 08/2009–04/2010 were classified as moderate, and those in 12/2014–06/2016 were classified as very strong (Figure 4.3). Each El Niño event was inter-seasonal for four study sites. Therefore, I selected an SST anomaly in the Niño 3.4 region as an ENSO proxy in this study. The monthly SST anomaly can be obtained at (http://www.cpc.ncep.noaa.gov/). The teleconnection between SST anomalies in Niño 3.4 and the terrestrial biosphere has been documented for South America,

Southeast Asia, and Africa (Anyamba et al. 2001; Mennis 2001; Anyamba, 2002; Nagai et al. 2007; Propastin et al., 2010).

4.2.4 Temporal correlations between VCI and TCI and SST anomalies at the seasonal scale

To understand the teleconnection between ENSO and TDFs from a long-term perspective, the temporal correlations between time series of VCI and TCI and SST anomalies in Niño 3.4 were conducted for the dry and wet season, respectively. Time duration and time lag are two key parameters for temporal correlations. Time duration refers to the period of the mean of SST anomalies. The value of an SST anomaly in a specific duration is the mean of the monthly SST anomalies in the period. Time lag refers to the interval between the occurrence of the change in an SST anomaly and the change in drought indices. A time duration from 1 to 24 months and a time lag from 0 to 5 months were adopted in the temporal correlation analysis. As a result, there are 144 (24*6) correlation coefficients for the dry season and wet season in each study site (Table 4. 2).

4.2.5 Moving Window Correlation Analysis (MWCA)

To evaluate the impacts of different El Niño events from March 2000 to March 2017 on TDFs in our study sites, a Moving Window Correlation Analysis (MWCA) approach was used (Erasmi et al., 2009). MWCA is a powerful statistical method used to investigate variations in relationships between two variables in time. The MWCA uses a window with a defined size moving across two time-series data, and the local correlation coefficient is retrieved at each time point. The result of a MWCA is a time series of correlation coefficients with the same dimension as the input of two time-series data. In addition, the result of MWCA varies with the window size (Erasmi et al., 2009).

In this study, MWCA was conducted through two steps. In the first step, the optimal window size was selected by minimizing the four-study-site mean of one-step root mean square forecast errors (RMSFEs; Inoue et al., 2017). The one-step RMSFEs were obtained from monthly VCIs and TCIs as functions of monthly SST anomalies for the window sizes from 5 to 24 months in four sites. Then, eight one-step RMSFEs (2 response variables*4 sites) were averaged for each window size. The optimal window size was selected as the one corresponding to the minimum four-study-site mean of one-step RMSFEs. In the second step, the time-series correlation

coefficients and *p*-values were extracted, with VCI and TCI as response variables, and the SST anomaly as an independent variable using MWCA at the optimal window size, imposing different time lags from 0 to 5 months into correlation analysis.

4.3 Result

4.3.1 Monthly variation of NDVI and LST

The phenological characteristics of NDVI and LST were similar for CCBR in Mexico, and SRNP-EMSS in Costa Rica, both of which are located in the northern hemisphere (Figure 4.2 a-d). PEMS in Brazil and TVMWR in Bolivia located in the southern hemisphere have similar trends (Figure 4.2 e-h).

Overall, the median NDVIs in the dry season were lower than those in the wet season, while the median LSTs in the dry season were higher than those in the wet season in the four sites of TDFs (Figure 4.2). The NDVIs increased sharply when the wet season arrives. They grew slowly in the early stage of the wet season until to a high level (about 0.85) in the late wet season. NDVIs decreased slowly when the dry season began and then decreased gradually to a low level (under 0.6) in the late dry season. LSTs in our study sites increased mildly when the dry season started and reached high values (above 308 K) in the dry season. However, the temporal variations for the LSTs in our study sites were not consistent in the wet season, although all of them showed low values (under 302 K) in the wet season. LSTs decreased mildly when the wet season started, and sharply in the second month of the wet season at CCBR in Mexico, and SRNP-EMSS in Costa Rica. The sharp decrease occurred in the first month of the wet season at PEMS in Brazil. The decrease at TVMWR in Bolivia was gradual during the wet season. The largest variations occurred in the transitional season from dry to wet season in terms of both NDVI and LST in the four sites.

4.3.2 Temporal response of TDFs to the SST anomalies in the dry and wet season

Table 4.3 shows the teleconnection of the SST anomaly to the VCI and the TCI in the dry and wet season for each study site. At CCBR, Mexico, the VCI in the dry season (November–May) was positively affected by the 3-month average of SST anomalies without a time lag. At SRNP-EMSS, Costa Rica, the VCI and TCI in the dry season (December–April) were negatively influenced by the 2-month average of SST anomalies with a 5-month lag and 1-month SST

anomalies with a 1-month lag; the TCI in the wet season (May–November) was negatively affected by the 3-month average of SST anomalies. At PEMS, Brazil, the VCI and TCI in the dry season (May–October) were negatively affected by the 3-month average of SST anomalies without a time lag and the 2-month average of SST anomalies without a time lag; the TCI in the wet season (Nov–April) was negatively affected by the 2-month average of SST anomalies without a time lag. At TVMWR, Bolivia, VCI in the wet season (Nov–May) was positively affected by 21- month averages of SST anomalies without a 5-month lag.

Table 4.3 illustrates that both the VCI and TCI of SRNP-EMSS, Costa Rica and PEMS, Brazil were negatively affected by SST anomalies in the dry seasons. For the further analysis, Figure 4.3 shows the correlation coefficients between the VCI and TCI at SRNP-EMSS, Costa Rica and PEMS, Brazil and multiple SST anomalies (time durations from 1 to 24 months; time lag from 0 to 5 months). The results illustrate that both the VCI and TCI at SRNP-EMSS, Costa Rica and PEMS, Brazil in the dry season were negatively affected by several specific SST anomalies simultaneously. In particular, the duration of these SST anomalies was less than 13 months. The lag time of these SST anomalies ranged from 0 to 5 months in SRNP-EMSS, Costa Rica and from 0 and 3 months in PEMS, Brazil.

4.3.3 The impacts of El Niño events on TDFs

Figure 4.5 shows the average of eight one-step RMSFEs obtained from the VCIs and TCIs of four study sites as the function of SST anomalies for different window sizes (5 to 24 months). The result indicated low average one-step RMSFEs occurred at window sizes of 15 and 16 months. Lower RMSFEs can also be observed in larger window sizes, but in these cases, the window sizes exceed the total lengths of El Niño events. Thus, the optimal window size is selected as 15 months, as an odd number is more convenient for the further MWCA.

Figure 4.6 shows MWCAs based on monthly VCIs and TCIs of four study sites and the monthly SST anomaly in the Niño 3.4 region, employing a window size of 15 months and multiple time lags (0 to 5 months) from March 2000 to March 2017. The results revealed that temporal patterns in responses of VCIs and TCIs to SST anomalies were nonstationary. Time lag is a key parameter affecting the MWCA between VCIs and TCIs and SST anomalies. The temporal regions of significantly negative correlations between VCIs and TCIs and SST anomalies illustrated the

potential occurrence of El Niño-related drought. The temporal patterns of El Niño periods and the corresponding periods and time lags of El Niño-driven VCI and TCI decrease in four study sites are summarized in Table 4.4. This reveals the impacts of El Niño events on TDFs over the four study sites from March 2000 to March 2017. Five El Niño events led to 3, 2, 2, 2, and 1 times of VCI decrease, and 2, 1, 2, 1, and 4 times of TCI decrease in four study sites in turn.

4.4 Discussion

4.4.1 Teleconnection between ENSO and precipitation over TDFs

The predominant factor for the growth of TDFs is water availability (Cao et al., 2016; Castro et al., 2018). Thus, the response of TDFs to SST anomalies are largely influenced by the teleconnections between ENSO and precipitation. The VCI and TCI are complementary indicators that reflect the precipitation conditions over TDFs (Kogan 1995; 1997; Cao et al., 2016; Castro et al., 2018). As such, ENSO is considered to play a key role in precipitation over TDFs when either the VCI or TCI is significantly influenced by SST anomalies.

Table 4.3 indicates that SST anomalies across multiple ENSO phases (warm, neutral, and cold phases) can affect precipitation regimes in study sites. Precipitation patterns at CCBR, Mexico, SRNP-EMSS, Costa Rica, and PEMS, Brazil were influenced by short-duration SST anomalies. The precipitation patterns at TVMWR, Bolivia was affected by the long-duration SST anomalies. In additions, higher SST anomalies across multiple ENSO phases tend to trigger excessive precipitation at CCBR, Mexico and TVMWR, Bolivia, and less precipitation at SRNP-EMSS, Costa Rica and PEMS, Brazil.

Table 4.5 reveals that SST anomalies during the ENSO warm phase can lead to droughts in study sites. It implies that the intensity of an El Niño event plays an important role in drought conditions for a wide region instead of a specific local region. In other words, stronger El Niño events can lead to severe droughts in larger areas over the four sites, but there is no direct relationship between the intensity of an individual El Niño event and the precipitation condition in each study site. Table 4.5 also indicates that the climate conditions at SRNP-EMSS, Costa Rica, CCBR, Mexico and TVMWR, Bolivia are sensitive to El Niño events. The short-term teleconnection between SST anomalies during the ENSO warm phase and precipitation was weak for PEMS, Brazil. But long-term teleconnection between SST anomalies across multiple ENSO

phases (warm, neutral, and cold) and precipitation was significant. It revealed that the precipitation over PEMS, Brazil should be strongly influenced by the ENSO cold phase (La Niña) instead of the warm phase (El Niño).

4.4.2 Teleconnection between ENSO and productivity of TDFs

The primary response of forests to climate anomalies is a decline in productivity. The Gross Primary Productivity (GPP) is the function of the NDVI and LST (Xiao et al., 2004). Thus, the productivity of TDFs is considered to be affected by ENSO when both VCI and TCI have significant correlations with specific SST anomalies.

Table 4.3 also indicates that SST anomalies across multiple ENSO phases (warm, neutral, and cold phases) potentially affect the GPP of TDFs in the dry season rather than wet season. One of the reasons is that the abundant precipitation in the wet season (Figure 4. 2) which can mitigate the effect of climate anomalies (Rhee et al., 2010). The GPP at CCBR, Mexico and TVMWR, Bolivia in the dry season were not significantly influenced by SST anomalies. This is because the TCI at CCBR, Mexico and both the VCI and TCI at TVMWR, Bolivia in the dry season did not respond to the specific precipitation pattern related to ENSO. The GPP at SRNP-EMSS, Costa Rica and PEMS, Brazil in the dry season were significantly influenced by SST anomalies (Figure 4.4).

Table 4.6 reveals that the GPP of TDFs in SRNP-EMSS, Costa Rica are the most sensitive to El Niño events, followed by those in CCBR, Mexico. It implies that the teleconnections between SST anomalies during ENSO warm phases and climate conditions are strong, and TDFs are sensitive to El Niño-driven droughts. However, the GPP of TDFs over PEMS, Brazil and TVMWR, Bolivia are resistant to El Niño events. Although the ocean-atmosphere coupling for TVMWR, Bolivia during El Niño events is strong (Table 4.5), the TDFs are resistant to El Niño-driven droughts due to deep roots, which can be reflected indirectly by higher greenness and lower evapotranspiration (Figure 4.2). The weak ocean-atmosphere coupling during ENSO warm phase for TVMWR, Brazil is the reason for the resistance of TDFs to El Niño events (Table 4.6). It also implies that the primary response of TDFs to SST anomalies does not depend on the intensity of El Niño events for each site and the whole region. This is due to two reasons. First, the effects of

SST anomalies on precipitation in a specific site are not consistent between El Niño events. On the other hand, TDFs have some resistance to the El Niño driven drought.

4.4.3 Comparison of greenness and evapotranspiration in response to precipitation

The relationship between the VCI and TCI and SST anomalies can indirectly reflect how greenness and evapotranspiration respond to climate conditions. The capacities of greenness and evapotranspiration over TDFs reflecting climate conditions vary with season and site. Greenness is sensitive to precipitation at CCBR, Mexico in the dry season and at TVMWR, Bolivia in the wet season. On the other hand, although both greenness and evapotranspiration are good indicators to reflect the climate condition at SRNP-EMSS, Costa Rica and PEMS, Brazil in the dry and wet seasons, evapotranspiration is more sensitive to precipitation than greenness (Table 4.3). Table 4.4 reveals that greenness and evapotranspiration at TDFs are complementary biophysical properties which can reflect the intensity of El Niño-driven droughts. The shorter time lags of TCI-SST anomalies for CCBR, Mexico and SRNP-EMSS, Costa Rica (Table 4.4) hints that evapotranspiration has a stronger capacity to capture the onset of El Niño-driven droughts in CCBR, Mexico and SRNP-EMSS, Costa Rica, where El Niño tends to trigger severe impacts on the GPP of TDFs (Table 4.6).

4.5 Conclusion

The relationship between SST anomalies in the Pacific Niño 3.4 region, and remote sensing drought indices is key to understand how ENSO influences climatology, and therefore GPP over TDFs in the Americas. In this study, a temporal correlation analysis at a seasonal scale and an optimized Moving Window Correlation Analysis (MWCA) between VCI, TCI and SST anomalies were conducted to analyze the long-term and short-term responses of TDFs to ENSO.

I found that long-term SST anomalies across multiple ENSO phases (warm, neutral, and cold phases) can impact the GPP of TDFs over SRNP-EMSS (Costa Rica), and the PEMS (Brazil) in the dry season. The GPP of TDFs in the wet season were not influenced by long-term SST anomalies due to availability of enough precipitation to sustain basic ecosystem services. In the other hand, I conclude that high short-term SST anomalies during ENSO warm phases tend to trigger severe droughts at the selected study sites. GPP was sensitive to El Niño-driven droughts over CCBR (Mexico) and SRNP-EMSS (Costa Rica). GPP response at the PEMS (Brazil) was

weak to El Niño events, because the site tends to be more influenced by La Niña than El Niño. Although high SST anomalies tends to lead to drought at the TVMW (Bolivia), the GPP response is weak because the biophysical and ecological characteristics of this forest.

I also found that ecosystem level greenness and evapotranspiration are complementary indicators to better understand climatic conditions at TDFs in the Americas. The greenness at the CC-BR (Mexico) during the dry season, and at the TVMW (Bolivia) in the wet season can significantly respond to the precipitation conditions. The canopy evapotranspiration at the SRNP-EMSS (Costa Rica) and the PEMS (Brazil) is more sensitive to precipitation conditions than greenness in both the dry and wet seasons. In addition, canopy evapotranspiration is a better indicator than greenness to capture the onset of El Niño-driven droughts at the CCBR (Mexico) and SRNP-EMSS (Costa Rica), where the teleconnection between El Niño and climate parameters is significant.

4.6 References

Allen, C. D., Macalady, A. K., Chenchouni, H., Bachelet, D., McDowell, N., Vennetier, M., Hogg, E. T. (2010). A global overview of drought and heat-induced tree mortality reveals emerging climate change risks for forests. *Forest Ecology and Management, 259*(4), 660-684.

Anyamba, A., Tucker, C. J., & Mahoney, R. (2002). From El Niño to La Niña: Vegetation response patterns over east and southern Africa during the 1997–2000 period. *Journal of Climate, 15*(21), 3096-3103.

Bi, J., Myneni, R., Lyapustin, A., Wang, Y., Park, T., Chi, C., Knyazikhin, Y. (2016). Amazon forests' response to droughts: A perspective from the MAIAC product. *Remote Sensing, 8(4)*, 356.

Boyd, D. S., Phipps, P. C., Foody, G. M., & Walsh, R. (2002). Exploring the utility of NOAA AVHRR middle infrared reflectance to monitor the impacts of ENSO-induced drought stress on Sabah rainforests. *International Journal of Remote Sensing, 23(23),* 5141-5147.

Brown, J. F., Wardlow, B. D., Tadesse, T., Hayes, M. J., & Reed, B. C. (2008). The vegetation drought response index (VegDRI): A new integrated approach for monitoring drought stress in vegetation. *GIScience & Remote Sensing, 45*(1), 16-46.

Campos, F. A. (2018). A synthesis of long-term environmental change in Santa Rosa, Costa Rica. *Primate life histories, sex roles, and adaptability*, 331-358.

Cao, S., & Sanchez-Azofeifa, A. (2017). Modeling seasonal surface temperature variations in secondary tropical dry forests. *International Journal of Applied Earth Observation and Geoinformation, 62*, 122-134.

Castro, S. M., Sanchez-Azofeifa, G. A., & Sato, H. (2018). Effect of drought on productivity in a Costa Rican tropical dry forest. *Environmental Research Letters, 13*(4), 045001.

Chadwick, W. W., Paduan, J. B., Clague, D. A., Dreyer, B. M., Merle, S. G., Bobbitt, A. M., Nooner, S. L. (2016). Voluminous eruption from a zoned magma body after an increase in supply rate at axial seamount. *Geophysical Research Letters, 43(23),* 12,063-12,070.

Erasmi, S., Propastin, P., Kappas, M., & Panferov, O. (2009). Spatial patterns of NDVI variation over Indonesia and their relationship to ENSO warm events during the period 1982–2006. *Journal of Climate, 22(24)*, 6612-6623.

Heinsch, F. A., Zhao, M., Running, S. W., Kimball, J. S., Nemani, R. R., Davis, K. J., Ricciuto, D. M. (2006). Evaluation of remote sensing based terrestrial productivity from MODIS using regional tower eddy flux network observations. *IEEE Transactions on Geoscience and Remote Sensing, 44(7)*, 1908-1925.

Holmgren, M., Scheffer, M., Ezcurra, E., Gutiérrez, J. R., & Mohren, G. M. (2001). El Niño effects on the dynamics of terrestrial ecosystems. *Trends in Ecology & Evolution, 16(2*), 89-94.

Inoue, A., Jin, L., & Rossi, B. (2017). Rolling window selection for out-of-sample forecasting with time-varying parameters. *Journal of Econometrics, 196*(1), 55-67.

IPCC. (2007). IPCC WGI Fourth Assessment Report, Summary for policy makers. Paris, February.

Janzen, D. H. (1988). Management of habitat fragments in a tropical dry forest: Growth. *Annals of the Missouri Botanical Garden,* 105-116.

Karnieli, A., Agam, N., Pinker, R. T., Anderson, M., Imhoff, M. L., Gutman, G. G., Goldberg, A. (2010). Use of NDVI and land surface temperature for drought assessment: Merits and limitations. *Journal of Climate, 23*(3), 618-633.

Kogan, F. N. (1995). Application of vegetation index and brightness temperature for drought detection. *Advances in Space Research, 15*(11), 91-100.

Kogan, F. N. (1997). Global drought watch from space. *Bulletin of the American Meteorological Society, 78*(4), 621-636.

Kogan, F. N. (1998). A typical pattern of vegetation conditions in southern Africa during El Nino years detected from AVHRR data using three-channel numerical index. *International Journal of Remote Sensing, 19(18)*, 3688-3694.

Kogan, F. N. (2000). Satellite-observed sensitivity of world land ecosystems to El Nino/La Nina. *Remote Sensing of Environment, 74*(3), 445-462.

Kogan, F., Stark, R., Gitelson, A., Jargalsaikhan, L., Dugrajav, C., & Tsooj, S. (2004). Derivation of pasture biomass in Mongolia from AVHRR-based vegetation health indices. *International Journal of Remote Sensing, 25(14)*, 2889-2896.

Lopezaraiza-Mikel, M., Quesada, M., Álvarez-Añorve, M., Ávila-Cabadilla, L., Martén-Rodríguez, S., Calvo-Alvarado, J. (2013). Phenological patterns of tropical dry forests along latitudinal and successional gradients in the Neotropics. *Tropical dry forests in the Americas,* 119-146.

Madeira, B. G., Espírito-Santo, M. M., Neto, S. D., Nunes, Y. R., Azofeifa, G. A. S., Fernandes, G. W., & Quesada, M. (2009). Changes in tree and liana communities along a successional gradient in a tropical dry forest in South-Eastern Brazil. *Plant Ecology, 201*(1), 291-304.

Mennis, J. (2001). Exploring relationships between ENSO and vegetation vigour in the South-East USA using AVHRR data. *International Journal of Remote Sensing, 22*(16), 3077-3092.

Miles, L., Newton, A. C., DeFries, R. S., Ravilious, C., May, I., Blyth, S., Gordon, J. E. (2006). A global overview of the conservation status of tropical dry forests. *Journal of Biogeography, 33(3)*, 491-505.

Murphy, K. (2006). The ENSO-fire dynamic in insular Southeast Asia. *Climatic Change, 74(4),* 435-455.

Nagai, S., Ichii, K., & Morimoto, H. (2007). Interannual variations in vegetation activities and climate variability caused by ENSO in tropical rainforests. *International Journal of Remote Sensing, 28(6)*, 1285-1297.

Portillo-Quintero, C., Sanchez-Azofeifa, A., Calvo-Alvarado, J., Quesada, M., & do Espirito Santo, Mario Marcos. (2015). The role of tropical dry forests for biodiversity, carbon and

water conservation in the Neotropics: Lessons learned and opportunities for its sustainable management. *Regional Environmental Change, 15*(6), 1039-1049.

Propastin, P., Fotso, L., & Kappas, M. (2010). Assessment of vegetation vulnerability to ENSO warm events over Africa. *International Journal of Applied Earth Observation and Geoinformation, 12*, S8-S89.

Rhee, J., Im, J., & Carbone, G. J. (2010). Monitoring agricultural drought for arid and humid regions using multi-sensor remote sensing data. *Remote Sensing of Environment, 114*(12), 2875-2887.

Sanchez-Azofeifa, A., Powers, J. S., Fernandes, G. W., & Quesada, M. (2013). Tropical dry forests in the Americas: Ecology, Conservation, and Management.

Sanchez-Azofeifa, G. A., Quesada, M., Rodríguez, J. P., Nassar, J. M., Stoner, K. E., Castillo, A., Cuevas-Reyes, P. (2005). Research priorities for Neotropical dry forests. *Biotropica, 37*(4), 477-485.

Sellers, P. J., Dickinson, R. E., Randall, D. A., Betts, A. K., Hall, F. G., Berry, J. A., Nobre, C. A. (1997). Modeling the exchanges of energy, water, and carbon between continents and the atmosphere. *Science, 275(5299)*, 502-509.

Trenberth, K. E. (1997). The definition of El Niño. *Bulletin of the American Meteorological Society, 78(12)*, 2771-2777.

Xiao, X., Zhang, Q., Braswell, B., Urbanski, S., Boles, S., Wofsy, S., Ojima, D. (2004). Modeling gross primary production of temperate deciduous broadleaf forest using satellite images and climate data. *Remote Sensing of Environment, 91*(2), 256-270.

4.7 Tables and Figures

Table 4. 1 Description of the study sites.

Site	Location	Area	Mean Annual Precipitation (MAP)	Mean Annual Temperature (MAT)	Dry season	Wet season
CCBR, Mexico	19°30'N, 104°58'W	127 km^2	763 mm	24.6°	Nov-May	Jun-Oct
SRNP-EMSS, Costa Rica	10°48'N, 85°36'W	108 km^2	1390 mm	26.6°	Dec-Apr	May-Nov
PEMS, Brazil	14°51'S, 43°59'W	116 km^2	818 mm	24°	May-Oct	Nov-Apr
TVMWR, Bolivia	18°15'S, 59°15'W	1937 km^2	1234 mm	23.9°	Jun-Oct	Nov-May

Table 4. 2 Temporal patterns (24 time durations * 6 time lags) of correlations between the VCI and TCI and the corresponding multi-scale SST anomalies. The numbers in the cells show the time period for the mean of SST anomalies. Zero corresponds to the current month, one indicates the first previous month, and zero to one shows the period from the current month to the first previous month.

	Duration											
Lag	1	2	3	4	5	6	7	8	9	…	23	24
0	0	0-1	0-2	0-3	0-4	0-5	0-6	0-7	0-8	…	0-22	0-23
1	1	1-2	1-3	1-4	1-5	1-6	1-7	1-8	1-9	…	1-23	1-24
2	2	2-3	2-4	2-5	2-6	2-7	2-8	2-9	2-10	…	2-24	2-25
3	3	3-4	3-5	3-6	3-7	3-8	3-9	3-10	3-11	…	3-25	3-26
4	4	4-5	4-6	4-7	4-8	4-9	4-10	4-11	4-12	…	4-26	4-27
5	5	5-6	5-7	5-8	5-9	5-10	5-11	5-12	5-13	…	5-27	5-28

Table 4. 3 The extremums of temporal correlations between the VCI and TCI and SST anomalies in the dry and wet season across the latitudinal gradients of TDFs. The extremum (R_{max} *(duration, lag)* or R_{min} *(duration, lag)*) for the dry season and wet season in each study site was selected from 144 (24 duration*6 lag) correlation coefficients. If the maximum absolutes are obtained by the positive correlations, the extremums are chosen as the maximum values; if the maximum absolutes are obtained by negative correlations, the extremums are chosen as the minimum values. The stars indicate significant correlations with a *p*-value less than *0.05*. No stars indicate that *p*-values greater than *0.05*. Yellow shades indicate significant correlations.

	VCI-SST anomaly correlation		TCI-SST anomaly correlation	
	Dry season	Wet season	Dry season	Wet season
CCBR, Mexico	$R_{max}(3,0)=0.34^*$	$R_{min}(3,5)=-0.13$	$R_{min}(24,5)=-0.14$	$R_{min}(5,3)=-0.17$
SRNP-EMSS, Costa Rica	$R_{min}(2,5)=-0.42^*$	$R_{max}(24,5)=0.14$	$R_{min}(1,1)=-0.58^*$	$R_{min}(3,0)=-0.32^*$
PEMS, Brazil	$R_{min}(3,0)=-0.38^*$	$R_{min}(14,0)=-0.27$	$R_{min}(2,0)=-0.45^*$	$R_{min}(2,0)=-0.36^*$
TVMWR, Bolivia	$R_{max}(1,0)=0.20$	$R_{max}(21,5)=0.35^*$	$R_{max}(24,5)=0.12$	$R_{max}(16,5)=0.27$

Table 4. 4 El Niño periods and corresponding periods and time lags of El Niño-driven VCI and TCI decrease. The periods of El Niño-driven VCI and TCI decrease are the intersections of three periods: (1) the periods between El Niño outbreaks and El Niño ending plus the maximum lag time (5 months), (2) the periods in which the results of MWCA based-VCIs and TCIs and SST anomaly were negatively significant, and (3) the periods in which VCIs and TCIs are less than 50 (threshold for drought).

El Niño episode	El Niño-driven VCI decrease (CCBR, Mexico)	El Niño-driven TCI decrease (CCBR, Mexico)	El Niño-driven VCI decrease (SRNP-EMSS, Costa Rica)	El Niño-driven TCI decrease (SRNP-EMSS, Costa Rica)	El Niño-driven VCI decrease (PEMS, Brazil)	El Niño-driven TCI decrease (PEMS, Brazil)	El Niño-driven VCI decrease (TVMWR, Bolivia)	El Niño-driven TCI decrease (TVMWR, Bolivia)
07/2002-03/2003 (9 month) Moderate	02/2003-06/2003 Time lag=4	02/2003-05/2003 Time lag=3	01/2003-03/2003 Time lag=2	02/2003-04/2003 Time lag=1	None	None	07/2002-12/2002 Time lag=0	None
08/2004-03/2005 (8 month) Weak	10/2004-05/2005 Time lag=5	09/2004-04/2005 Time lag=4	12/2004-07/2005 Time lag=5	None	None	None	None	None
10/2006-02/2007 (5 month) Weak	01/2007-07/2007 Time lag=5	01/2007-06/2007 Time lag=4	01/2007-03/2007 Time lag=3	10/2006, 01/2007/-02/2007 Time lag=2	None	None	None	None
08/2009-04/2010 (9 month) Moderate	None	None	08/2009 Time lag=2	09/2009-04/2010 Time lag=0	None	None	09/2015 Time lag=5	None
12/2014-06/2016 (19 month) Very strong	None	08/2015-09/2015 Time lag=2 11/2015 Time lag=5	03/2015 Time lag=5 01/2016-04/2016 Time lag=2	03/2015-08/2015, 12/2015-04/2016 Time lag=0 06/2016-10/2016 Time lag=2	None	01/2015-06/2015 Time lag=2 12/2015-08/2016 Time lag=1	None	04/2016-05/2016 Time lag=2 07/2016 08/2016 Time lag =1

Table 4. 5 Five El Niño events and corresponding El Niño-driven droughts in each study site. One indicates that the El Niño event trigger drought. Zero indicates the El Niño event does not trigger drought. Total El Niño percentage is the total times of occurrence of droughts in each site divided by the total times of El Niño events. Total sites percentage is the total times of occurrence of droughts in El Niño event divided by the total number of study sites.

El Niño episode	El Niño-driven drought (CCBR, Mexico)	El Niño-driven drought (SRNP-EMSS, Costa Rica)	El Niño-driven drought (PEMS, Brazil)	El Niño-driven drought (TVMWR, Bolivia)	Total sites percentage
07/2002-03/2003 (9 month) Moderate	1	1	0	1	75%
08/2004-03/2005 (8 month) Weak	1	1	0	0	50%
10/2006-02/2007 (5 month) Weak	1	1	0	0	50%
08/2009-04/2010 (9 month) Moderate	0	1	0	1	50%
12/2014-06/2016 (19 month) Very strong	1	1	1	1	100%
Total El Niño percentage	80%	100%	20%	60%	65%

Table 4. 6 Five El Niño events and corresponding El Niño-driven productivity declines in each study site. One indicates that the El Niño event trigger drought. Zero indicates the El Niño event does not trigger productivity decline. Total El Niño percentage is the total times of occurrence of productivity declines in each site divided by the total times of El Niño events. Total sites percentage is the total times of occurrence of productivity declines in El Niño event divided by the total number of study sites.

El Niño episode	El Niño-driven productivity decline (CCBR, Mexico)	El Niño-driven productivity decline (SRNP-EMSS, Costa Rica)	El Niño-driven productivity decline (PEMS, Brazil)	El Niño-driven productivity decline (TVMWR, Bolivia)	Total percentage
07/2002-03/2003 (9 month) Moderate	1	1	0	0	50%
08/2004-03/2005 (8 month) Weak	1	0	0	0	25%
10/2006-02/2007 (5 month) Weak	1	1	0	0	50%
08/2009-04/2010 (9 month) Moderate	0	1	0	0	25%
12/2014-06/2016 (19 month) Very strong	0	1	0	0	25%
Total percentage	60%	80%	0%	0%	35%

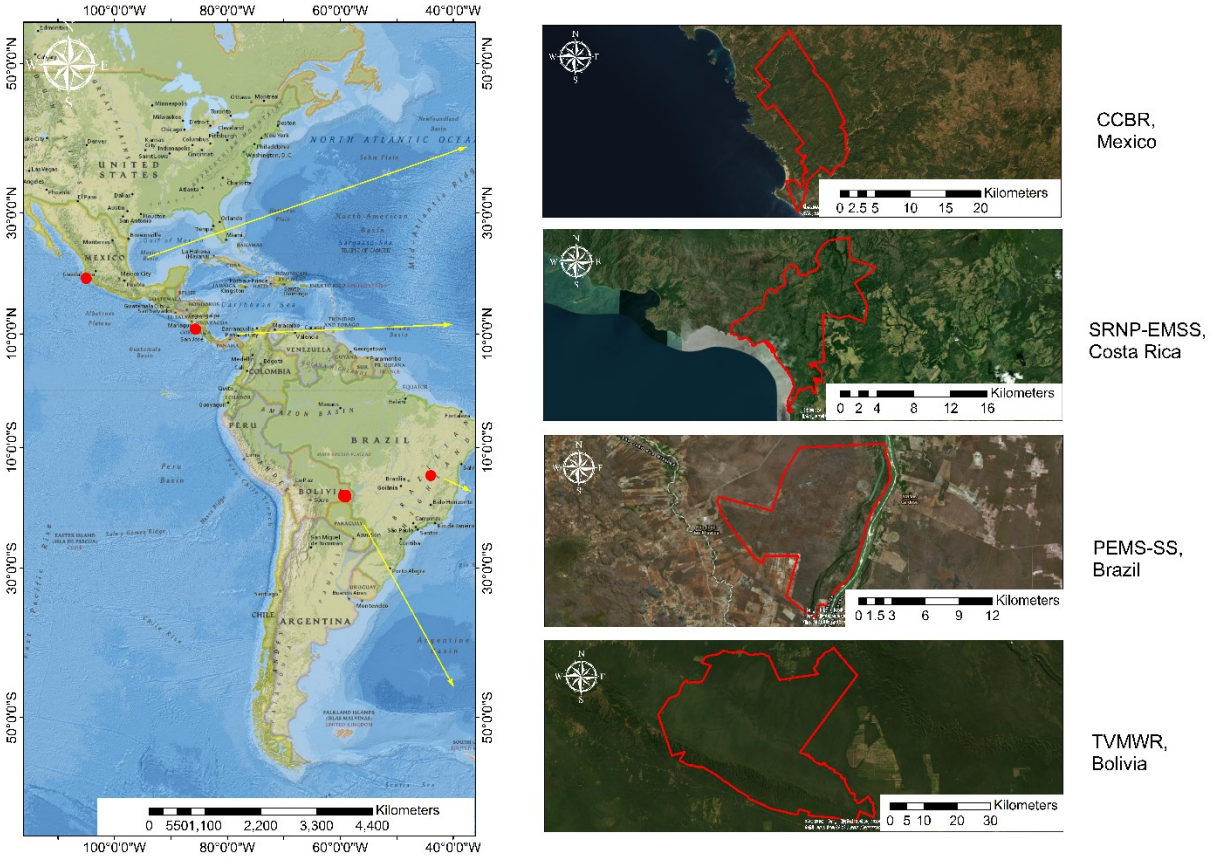

Figure 4. 1 Study sites.

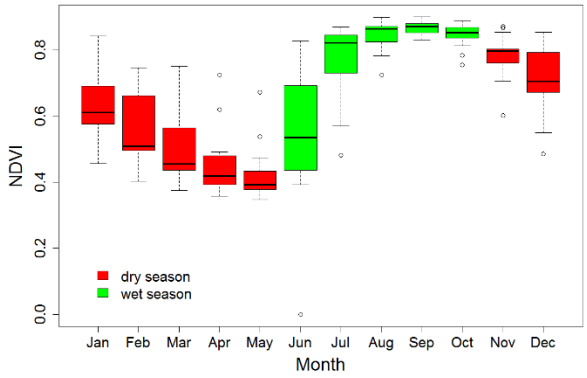

(a) NDVI in CCBR, Mexico

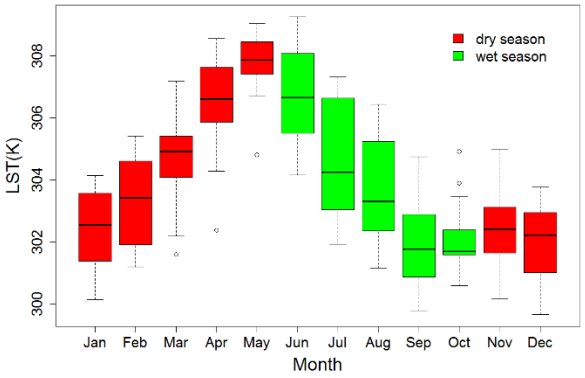

(b) LST in CCBR, Mexico

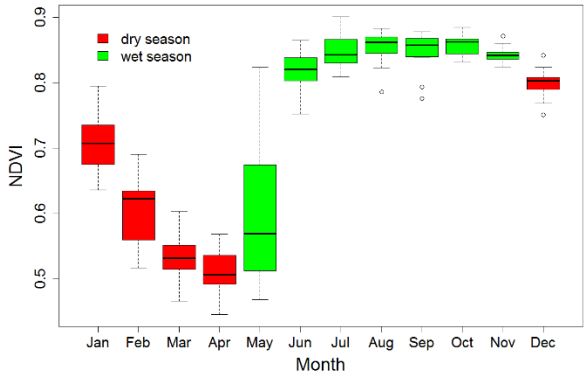

(c) NDVI in SRNP-EMSS, Costa Rica

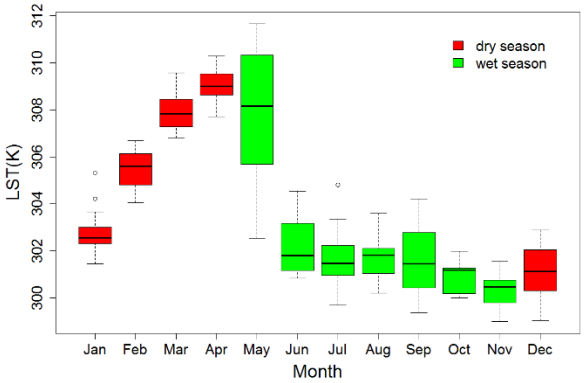

(d) LST in SRNP-EMSS Costa Rica

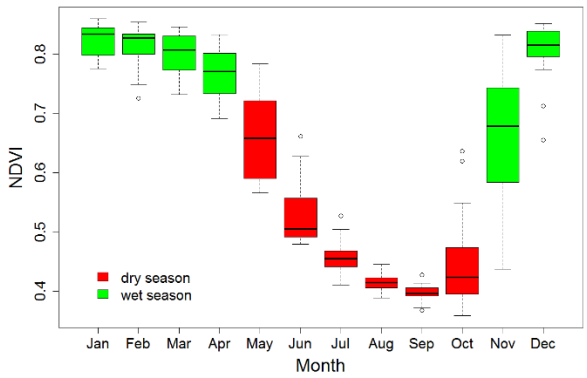

(e) NDVI in PEMS, Brazil

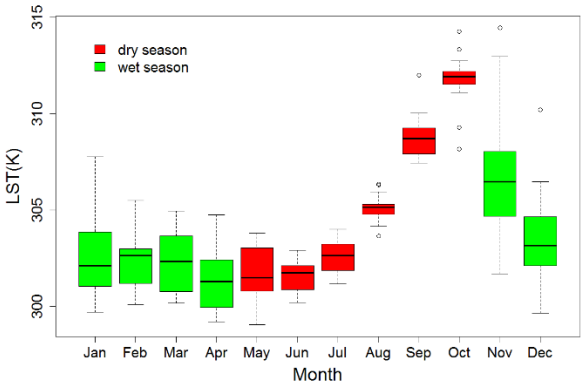

(f) LST in PEMS, Brazil

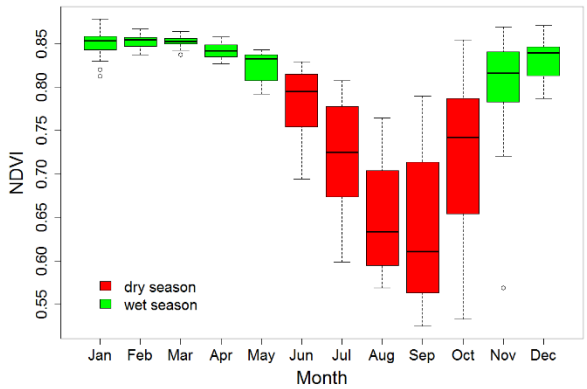

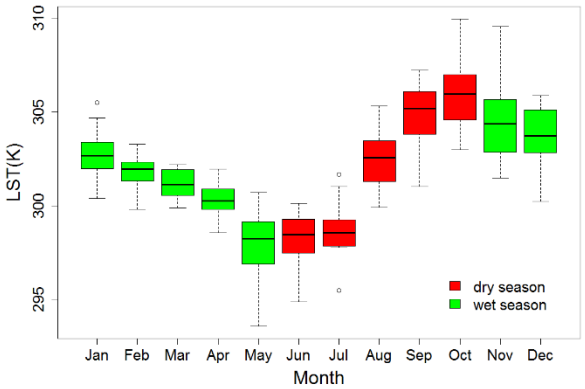

(g) NDVI in TVMWR, Bolivia (h) LST in TVMWR, Bolivia

Figure 4. 2 Monthly NDVI and LST distributions across the latitudinal gradient of TDFs in the Americas from March 2000 to March 2017

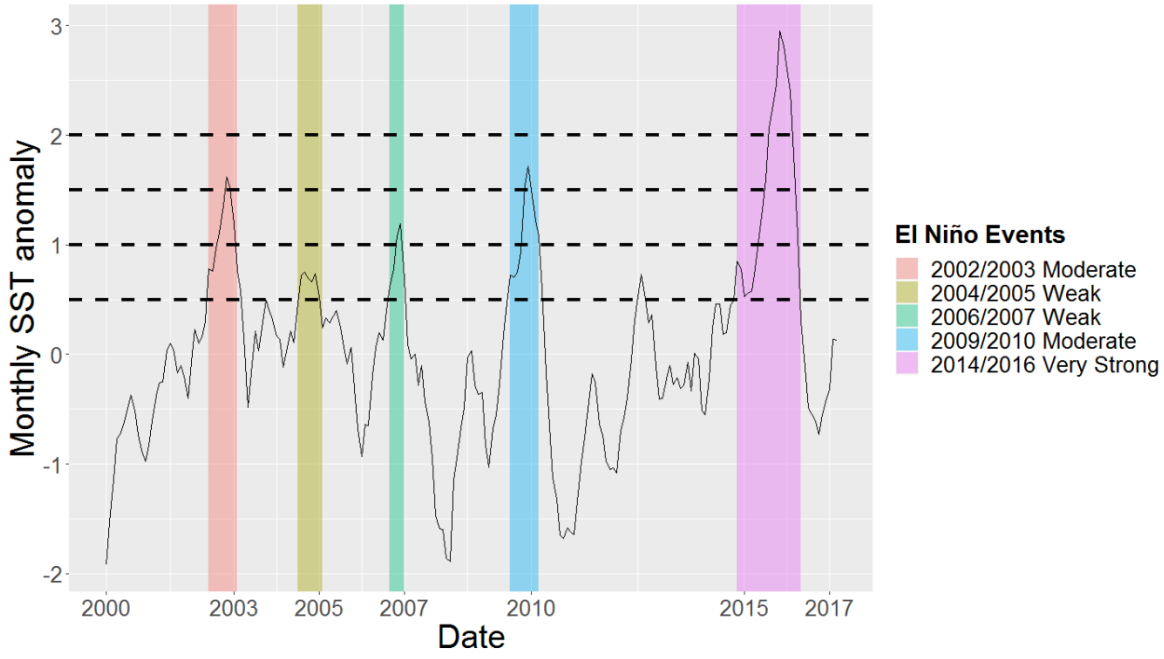

Figure 4. 3 The monthly SST anomaly in the Niño 3.4 region. The five El Niño events from March 2000 to March 2017 have been highlighted.

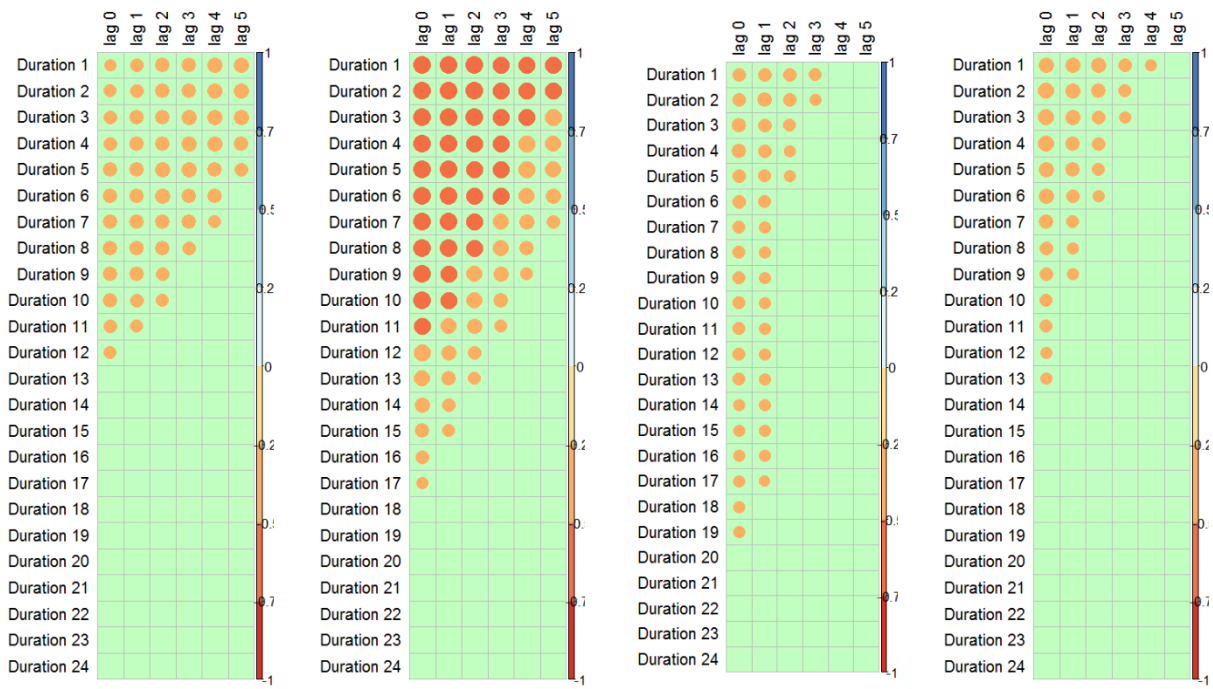

VCI-SST anomaly TCI-SST anomaly VCI-SST anomaly TCI-SST anomaly

(a) Dry season in SRNP-EMSS, Costa Rica (b) Dry season in PEMS, Brazil

Figure 4. 4 The response of TDFs to SST anomalies from a long-term perspective in SRNP-ENSS and PEMS in the dry season. Orange circles represents negative correlations (significance level=*0.05*).The blank gaps showed no significant correlations. The circle sizes are corresponding to the absolute values of correlation coefficients.

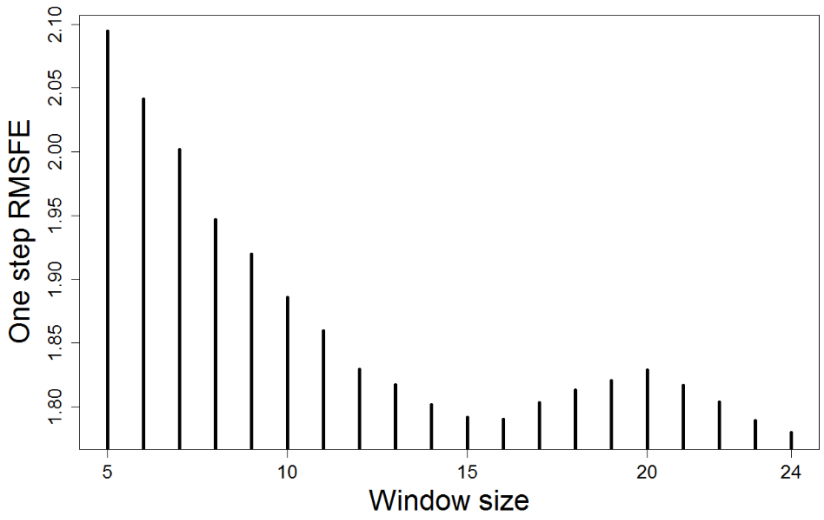

Figure 4. 5 The mean of 8 one-step RMSFEs derived from VCIs and TCIs of four study sites as the function of the SST anomalies, using different window sizes (5 to 24 months).

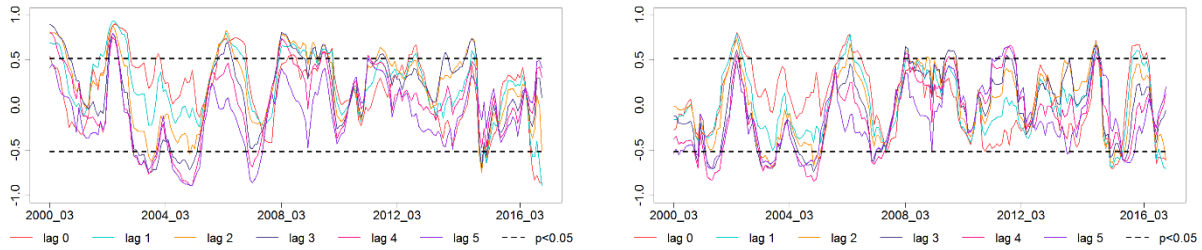

(a) CCBR, Mexica

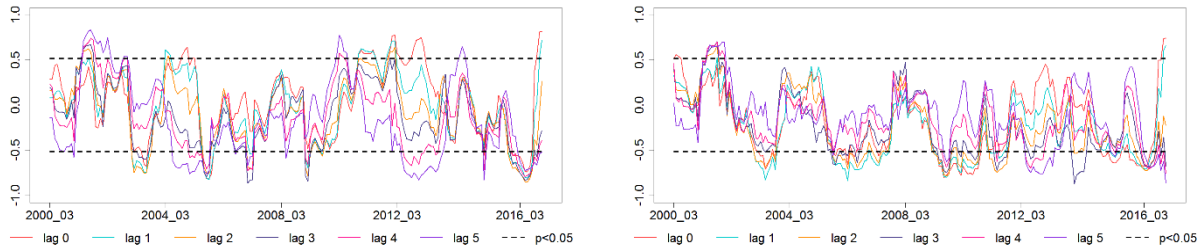

(b) SRNP-EMSS, Costa Rica

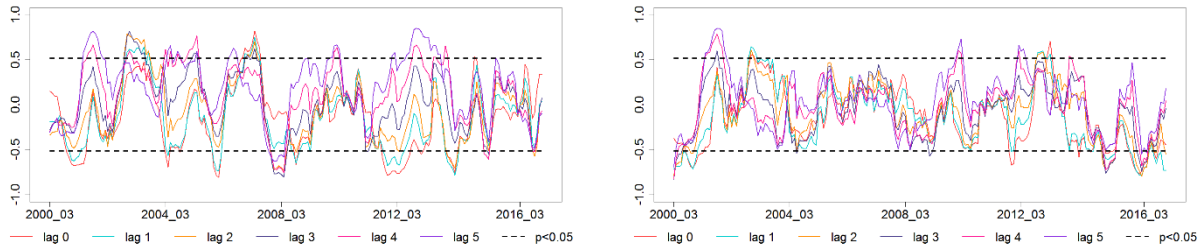

(c) PEMS, Brazil

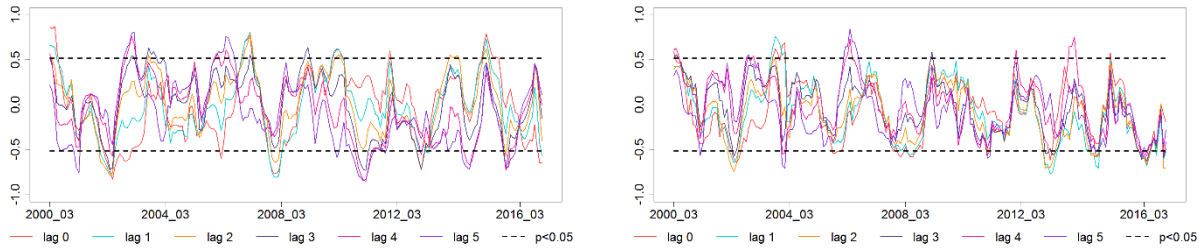

(d) TVMWR, Bolivia

MWCAs based on VCIs and SST anomaly MWCAs based on TCIs and SST anomaly

Figure 4. 6 Moving window correlation analyses of monthly VCIs and TCIs of the four sites and the monthly SST anomaly in the Niño 3.4 region from March 2000 to March 2017, calculated with a 15-month moving window and multiple time lags from 0 to 5 months. Two dashed lines are corresponding to the positive and negative thresholds with statistical significance ($p<0.05$).

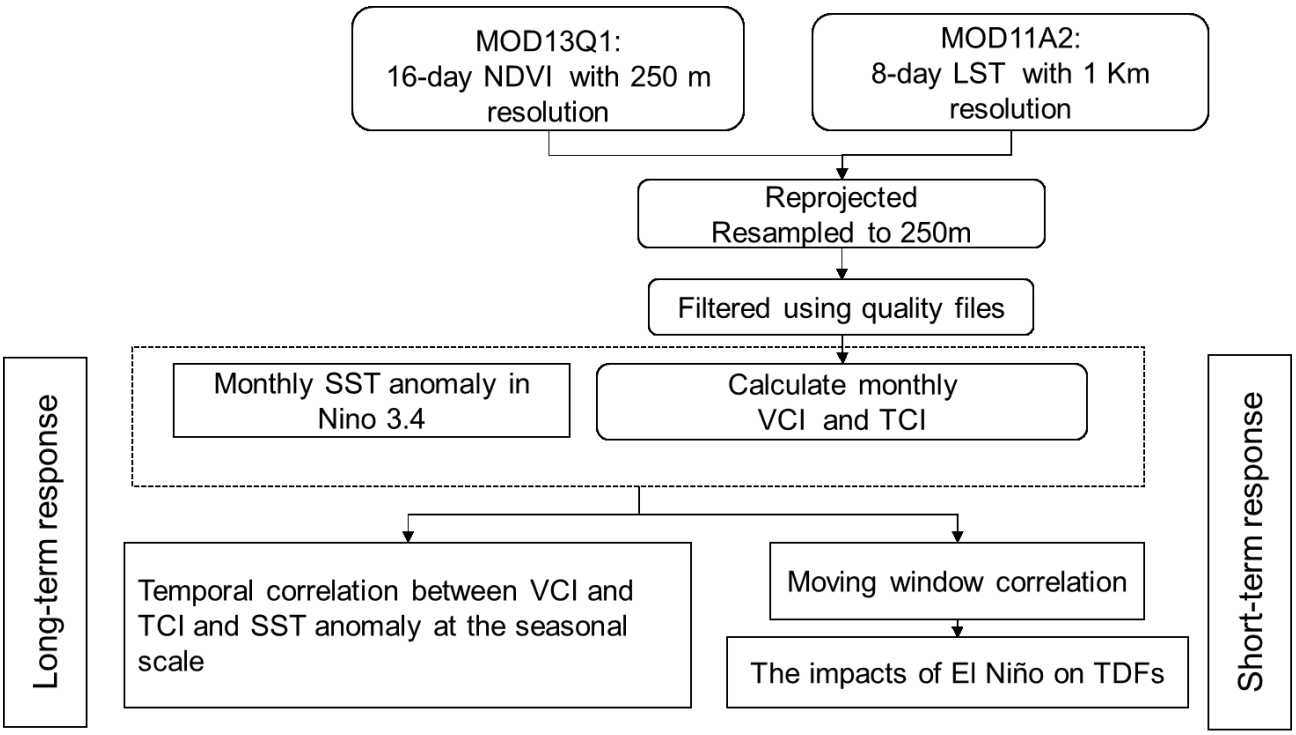

Figure 4. 7 Flowchart for assessing the response of TDFs to ENSO

Chapter 5

Synthesis

5.1 Conclusions and contributions

The main objective of my Ph.D. dissertation was to evaluate remote-sensing drought indices and to assess the response of Tropical Dry Forests (TDFs) to meteorological drought and El Niño Southern Oscillation (ENSO). In this context, my research focused on the evaluation of the utility of three commonly used remote sensing indices, Vegetation Condition Index (VCI), Temperature Condition Index (TCI), and Vegetation Health Index (VHI), to monitor meteorological drought in TDFs. In addition, the response of TDFs to meteorological drought was assessed by conducting the temporal correlations between biophysical parameters, Normalized Difference Vegetation Index (NDVI) and Land Surface Temperature (LST), and a meteorological index, the Standardized Precipitation Index (SPI), at the monthly and seasonal scale. Furthermore, the response of TDFs to meteorological drought was evaluated by exploring the relationship between time-series remote sensing drought indices, VCI and TCI, and an ENSO proxy, SST anomaly, from long-term and short-term perspectives.

The main conclusions and contributions for each chapter in the present thesis are summarized as follows:

Chapter 2. Evaluating the utility of various drought indices to monitor meteorological drought in Tropical Dry Forests.

The study in Chapter 2 is the first to assess the utility of remote sensing parameters to monitor the meteorological drought in TDFs. To date, such studies were conducted in the Tropical Moist Forests instead of TDFs (Phillips et al., 2009; Anderson et al., 2010; Williams et al., 2013). To my knowledge, no studies of drought monitoring based on remote sensing indices in TDFs have been reported. In the study, I assessed the ability of three remote sensing indices, the Vegetation Condition Index (VCI), the Temperature Condition Index (TCI), and the Vegetation Health Index (VHI) to monitor the meteorological drought for the monthly, seasonal, and yearly scales in the TDFs. The result shows that the ability of these indices for meteorological drought

monitoring varies with timing. Overall, the TCI outperforms the VCI and VHI in terms of seasonal and annual scale. These indices performed well in monitoring meteorological drought in the dry season, poorly in the in the dry-to-wet season, and moderately in the wet season. The TCI performed best in monitoring meteorological drought in the wet-to-dry period, followed by VHI, whereas the VCI performed worst. All of these remote sensing-based drought indices failed to detect drought in May during the green-up period and in September, October and November when the water content in the root regions was abundant. Our results indicate that the evapotranspiration of TDFs is more sensitive than canopy greenness to detect meteorological drought.

The remote sensing indices used in this study can increase the ability to provide a real-time meteorological drought monitoring and an early warning of drought events in TDFs.

Chapter 3. Assessing the temporal response of Tropical Dry Forests to the meteorological drought.

Research related to the assessment of the response of TDFs to climate anomalies is very limited. The study in Chapter 3, using the temporal correlations analysis of NDVI, LST and Standard Precipitation Indexes (SPIs) is the first one to assess the response of TDFs to a meteorological drought from a long-term perspective. Our results indicate that the NDVI and LST are largely influenced by seasonality as well as the magnitude, duration, and timing of precipitation. The responses of the NDVI and LST to meteorological drought mainly reflect how greenness and evapotranspiration in the TDFs respond to precipitation. We find that greenness and evapotranspiration are highly sensitive to precipitation when TDFs suffer from long-term water deficiency, and they tend to be slightly resistant to meteorological drought when precipitation is abundant. Greenness is more resistant to short-term rainfall deficiency than evapotranspiration, but greenness is more sensitive to precipitation after a period of rainfall deficiency. Precipitation can still strongly influence evapotranspiration on the canopy surface, but greenness is not controlled by the water availability but rather phenological timing when the leaves begins to fall in the dry-to-wet season. In addition, the primary response of TDFs to meteorological drought was also estimated. In the dry season, the average Gross Primary Productivity (GPP) was strongly influenced by the accumulated precipitation from the preceding February to the current March. In the dry-to-wet season, the average GPP was strongly affected by the total precipitation from February to April of the current year. In the wet season, the GPP was moderately influenced by

precipitation from January to June of the current year. In the wet-to-dry season, the GPP was not influenced by precipitation. In general, these results can be used to increase our understanding of how TDFs respond to water deficiency, and of its sensitivity and resilience to climate disturbance in the face of climate change in the future.

Chapter 4. Assessing the response of Tropical Dry Forests across the Americas to El Niño Southern Oscillation.

The study in *Chapter 4* is the first to assess the response of TDFs across the Americas to ENSO. The study is based on the assumption these forests along a latitudinal gradient in the Americas are significantly affected by drought related to El Niño Southern Oscillation (ENSO). The analysis builds upon two drought indices: the Vegetation Condition Index (VCI) and Temperature Condition Index (TCI) calculated from Moderate Resolution Imaging Spectroradiometer (MODIS) products and an ENSO proxy, the Sea Surface Temperature (SST) anomaly in the Niño 3.4 region. The long-term and short-term responses of TDFs at multiple sites (Chamela-Cuixmala Biosphere Reserve (CCBR) in Mexico, the Parque Estatual da Mata Seca (PEMS) in Brazil, the Tucabaca Valley Municipal Wildlife Reserve (TVMWR) in Bolivia, and the SRNP-EMSS in Costa Rica) from March 2000 to March 2017 were analyzed. Temporal correlation analysis for seasonal scale and Moving Window Correlation Analysis (MWCA) at an optimal window size were used to explore the long-term and short-term responses of TDFs to ENSO. Our results indicate that both long-term and short-term responses depend on the teleconnections between ENSO and climate parameters and the biophysical characteristics of TDFs at multiple sites. My results suggest that the GPP of TDFs at SRNP-EMSS and the PEMS in the dry season were significantly influenced by ENSO signals because of strong long-term Ocean-Atmosphere coupling and their sensitivity to climate conditions at these sites. TDFs at the CCBR and the SRNP-EMSS were sensitive to El Niño events because higher SST anomalies during ENSO warm phase are likely to induce severe drought, and these forests are sensitive to precipitation deficiencies over these sites. TDFs at the PEMS were resistant to El Niño events due to weak short-term Ocean-Atmosphere coupling. Even though El Niño events tended to cause drought at TVMWR, TDFs were resistant to El Niño drought due to its deeper roots. In addition, the variations in VCI and TCI reflect the response of greenness and evapotranspiration to precipitation. They are complementary drought indicators. Greenness of TDFs at the CCBR in the dry season, and TVMWR in the wet season can reflect rainfall precipitation. Canopy

evapotranspiration in the dry and wet season was sensitive to water deficiency at the SRNP-EMSS and the PEMS. Besides, it also had a stronger capacity than greenness to capture the onset of El Niño-induced droughts in CCBR and SRNP-EMSS.

My results conclude that the assessment of the response of TDFs to SST anomalies can increase our knowledge of how TDFs in central and South America respond to ENSO, and of the sensitivity and resilience of TDFs to drought driven by El Niño events.

5.2 Limitations to Research Projects

Several factors are limiting the accuracy and generalization of the results and conclusions, including the Study Area, Data Sources, Temporal Resolution, Remote-sensing Indices, and Vegetation Types.

Study Area: The assessment of the utility of various drought indices and the temporal correlation analysis of NDVI and LST and SPIs in Chapter 2 and 3 were conducted on a single TDFs (the SRNP-EMSS), therefore it is difficult to extrapolate these findings to other TDFS across the Americas. Thus, further analysis should be conducted in multiple TDFs regions like Chapter 4.

Data Sources: In Chapter 2 and 3, I focused on the relationship between the abiotic factors, mainly the meteorological parameters, and remote-sensing indices reflecting vegetation condition in Santa Rosa National Park. The biotic factors such as the biodiversity influenced the vegetation condition significantly during the growth of TDFs. I considered the biotic factors did not change much a the SRNP-EMSS during March 2000 and March 2017, which is not very precise. To make the result more reliable, the biotic factors should be added in the model in future work.

Temporal Resolution: In Chapter 3, the 16-day NDVI and 8-day LST MODIS products were aggregated to 1-month temporal resolution. The response of TDFs to the meteorological drought is very sensitive to the time lags. The TDFs in the transitional dry-to wet season are very sensitive to sporadic rainfall in the dry season, the time lag between TDFs and precipitation in this period tends to be less than 1 month. The similar situation also occurred in the short-term rainfall deficiency period in late July. As such, future work should be conducted on higher temporal-resolution MODIS products.

Remote-sensing Indices: In Chapter 2, I assessed the utility of commonly used remote-sensing indices, VCI, TCI, and VHI, to monitor the meteorological drought. These indices are constructed on the visible, near-infrared, and thermal bands. Besides,the short-wave bands are sensitive to the water content in the canopy and microwave bands are sensitive to soil moisture content. Thus, the remote-sensing indices derived on short-wave bands, such as Normalized Difference Water Index (NDWI), and microwave bands, such as the Tropical Rainfall Measuring Mission(TRMM) should be added in future studies.

Vegetation types: In Chapter 2,3 and 4, I used the spatial averages of drought indices to evaluate the performance of remote sensing indicesand to assess the response to meteorological drought and SST anomalies. Different vegetation types and locations may have different performances and responses. Therefore, an extra analysis should be added based on different vegetation types in future work.

5.3 Future research

In the future, I will focus on increasing the accuracy of the models and improving the ability of its generalization via adopting extra data resource. In addition, I will expand my research to some new fields.

5.3.1 Improve previous work:

1. *Multiple TDFs sites:* I will adopt multiple TDFs sites across the America, including Chamela, Mexico; Santa Rosa, Costa Rica; Mata Seca, Brazil; and Santa Cruz, Bolivia, to assess the utilities of remote sensing indices and the temporal response of TDFs to meteorological drought.
2. *High temporal remote-sensing indices: 16*-day NDVI and *8*-day LST MODIS products will be used. The Eight-day LST products will be aggregated to *16*-day instead of one month. The temporal resolution, therefore, for the temporal correlation analysis will be *16*-day.
3. *More remote-sensing indices:* The NDWI and TRMM as complementary indices will be added to assess their utilities to monitor the meteorological drought.
4. *Vegetation types:* The GIS data classifying the TDFs into three successions (Early, Intermediate, and Late) will be integrated to analyze the response of TDFs to the

meteorological drought. ANOVA could be used to analyze how different successional TDFs respond to the meteorological drought.

5.3.2 New research avenues:

1. *Phenological changes in TDFs due to climate change*

Climate change has changed the overall magnitude of rainfall, the timing and inter-annual variability worldwide (Zeng et al., 1999). Changes in the rainfall patterns will occur in TDFs regions in America (Castro et al., 2018) where rainfall amount and timing are key factors controlling primary productivity and phenology of growth (Feng et al., 2013). The primary response of tropical forests to climate anomalies is the decline in primary productivity (Xiao et al., 2004). In Chapter *3*, I have analyzed how TDFs respond to the meteorological drought. But the impact of climate change on the phenology is understudied. In the future, I will learn and conclude how the phenology shifts with climate change.

2. *Analysis of the relationship between remote sensing indices and meteorological indices based on the wavelet analysis*

Remote sensing indices, such as NDVI and LST, are key indicators to reflect the biophysical processes. As such, the relationship between these remote-sensing indices and meteorological indices is key to understand the impact of climate anomalies on vegetation, including TDFs ecosystems. The correlation analysis of remote-sensing indices and meteorological indices is based on the assumption that the time-series remote-sensing indices are stationary (Ji & Peters, 2003; Rhee et al., 2010; Zhang et al., 2017), including the *Chapter 2*, *3* and *4*. However, these indices are not always stationary. In further studies, a multi-resolution analysis (MRA) based on the wavelet transform (WT) will be implemented to study NDVI and LST time series in the TDFs. These non-stationary NDVI and LST time series can be decomposed using this MRA as a sum of series associated with different temporal scales. The MRA can help build the relationship between remote-sensing indices and meteorological indices by taking the biotic factors into consideration, which will increase the ability of the proposed procedure to monitor vegetation dynamics in the TDFs.

3. The differences in the response of Tropical Moist Forests and Tropical Dry Forests to the meteorological drought and El Niño Southern Oscillation

Tropical moist forests (TMFs) are characterized by low variability in annual temperature and high levels of rainfall (>200 cm). TMFs are dominated by semi-evergreen and evergreen deciduous tree species (Bierregaard et al., 1992). Many studies investigated the response of TMFs to meteorological drought and the ENSO (Phillips et al., 2009; Propastin et al., 2010; Williams et al. 2013; Brum et al., 2018). Besides, in *Chapter* 3 and Chapter *4*, the response TDFs to the meteorological drought and ENSO are also analyzed. The limiting factor for the growth is irradiance and temperature for TMFs but is precipitation for TDFs. Therefore, the growth period for TMFs and TDFs are dry and wet season respectively. The different phenology and biotic characteristics may lead to the differences in the response to climate anomalies. In my future, the comparison of the responses of TMFs and TDFs will be conducted. I will focus on the impacts in terms of productivity, phenology, and water use. Additionally, I am also interested in the sensitivity and resilience of TMFs and TDFs to climate anomalies.

5.4 References

Anderson, L. O., Malhi, Y., Aragao, L. E., Ladle, R., Arai, E., Barbier, N., & Phillips, O. (2010). Remote sensing detection of droughts in Amazonian forest canopies. *New Phytologist, 187*(3), 733-750.

Bierregaard Jr, R. O., Lovejoy, T. E., Kapos, V., dos Santos, A. A., & Hutchings, R. W. (1992). The biological dynamics of tropical rainforest fragments. *Bioscience,* 859-866.

Brum, M., Gutiérrez López, J., Asbjornsen, H., Licata, J., Pypker, T., Sanchez, G., & Oiveira, R. S. (2018). ENSO effects on the transpiration of eastern amazon trees. *Philosophical Transactions of the Royal Society B: Biological Sciences, 373*(1760), 20180085.

Castro, S. M., Sanchez-Azofeifa, G. A., & Sato, H. (2018). Effect of drought on productivity in a Costa Rican tropical dry forest. *Environmental Research Letters, 13*(4), 045001.

Feng, X., Porporato, A., & Rodriguez-Iturbe, I. (2013). Changes in rainfall seasonality in the tropics. *Nature Climate Change, 3*(9), 811.

Ji, L., & Peters, A. J. (2003). Assessing vegetation response to drought in the northern Great Plains using vegetation and drought indices. *Remote Sensing of Environment, 87*(1), 85-98.

Phillips, O. L., Aragão, L. E., Lewis, S. L., Fisher, J. B., Lloyd, J., López-González, G., Quesada, C. A. (2009). Drought sensitivity of the amazon rainforest. *Science, 323*(5919), 1344-1347.

Propastin, P., Fotso, L., & Kappas, M. (2010). Assessment of vegetation vulnerability to ENSO warm events over africa. *International Journal of Applied Earth Observation and Geoinformation, 12*, S83-S89.

Rhee, J., Im, J., & Carbone, G. J. (2010). Monitoring agricultural drought for arid and humid regions using multi-sensor remote sensing data. *Remote Sensing of Environment, 114*(12), 2875-2887.

Williams, A. P., Allen, C. D., Macalady, A. K., Griffin, D., Woodhouse, C. A., Meko, D. M., Grissino-Mayer, H. D. (2013). Temperature as a potent driver of regional forest drought stress and tree mortality. *Nature Climate Change, 3*(3), 292-297.

Xiao, X., Zhang, Q., Braswell, B., Urbanski, S., Boles, S., Wofsy, S., Ojima, D. (2004). Modeling gross primary production of temperate deciduous broadleaf forest using satellite images and climate data. *Remote Sensing of Environment, 91*(2), 256-270.

Zeng, N. (1999). Seasonal cycle and interannual variability in the amazon hydrologic cycle. *Journal of Geophysical Research: Atmospheres, 104*(D8), 9097-9106.

Zhang, L., Jiao, W., Zhang, H., Huang, C., & Tong, Q. (2017). Studying drought phenomena in the continental United States in 2011 and 2012 using various drought indices. *Remote Sensing of Environment, 190*, 96-106.

Bibliography

Allen, C. D., Breshears, D. D., & McDowell, N. G. (2015). On underestimation of global vulnerability to tree mortality and forest die-off from hotter drought in the Anthropocene. *Ecosphere, 6*(8), 129.

Allen, C. D., Macalady, A. K., Chenchouni, H., Bachelet, D., McDowell, N., Vennetier, M.,Hogg, E. T. (2010). A global overview of drought and heat-induced tree mortality reveals emerging climate change risks for forests. *Forest Ecology and Management, 259*(4), 660-684.

Amalo, L. F., & Hidayat, R. (2017). Comparison between remote-sensing-based drought indices in east Java. *Earth and Environmental Science*, *54(1)*, 012009.

Anderson, L. O., Malhi, Y., Aragão, L. E., Ladle, R., Arai, E., Barbier, N., & Phillips, O. (2010). Remote sensing detection of droughts in Amazonian forest canopies. *New Phytologist, 187*(3), 733-750.

Anyamba, A., Tucker, C. J., & Mahoney, R. (2002). From El Niño to La Niña: Vegetation response patterns over east and southern Africa during the 1997–2000 period. *Journal of Climate, 15*(21), 3096-3103.

Asner, G. P., Nepstad, D., Cardinot, G., & Ray, D. (2004). Drought stress and carbon uptake in an amazon forest measured with Spaceborne imaging spectroscopy. *Proceedings of the National Academy of Sciences, 101*(16), 6039-6044.

Asner, G. P. (1998). Biophysical and biochemical sources of variability in canopy reflectance. *Remote Sensing of Environment, 64(3)*, 234-253.

Balvanera, P., Castillo, A., & Martínez-Harms, M. J. (2011). Ecosystem services in seasonally dry tropical forests. *Seasonally dry tropical forests.* 259-277.

Bayarjargal, Y., Karnieli, A., Bayasgalan, M., Khudulmur, S., Gandush, C., & Tucker, C. J. (2006). A comparative study of NOAA–AVHRR derived drought indices using change vector analysis. *Remote Sensing of Environment, 105*(1), 9-22

Bhuiyan, C., Singh, R. P., & Kogan, F. N. (2006). Monitoring drought dynamics in the Aravalli region (India) using different indices based on ground and remote sensing data. *International Journal of Applied Earth Observation and Geoinformation, 8(4),* 289-302.

Bi, J., Myneni, R., Lyapustin, A., Wang, Y., Park, T., Chi, C., Knyazikhin, Y. (2016). Amazon forests' response to droughts: A perspective from the MAIAC product. *Remote Sensing, 8(4)*, 356.

Bierregaard Jr, R. O., Lovejoy, T. E., Kapos, V., dos Santos, A. A., & Hutchings, R. W. (1992). The biological dynamics of tropical rainforest fragments. *Bioscience,* 859-866.

Boyd, D. S., Phipps, P. C., Foody, G. M., & Walsh, R. (2002). Exploring the utility of NOAA AVHRR middle infrared reflectance to monitor the impacts of ENSO-induced drought stress on Sabah rainforests. *International Journal of Remote Sensing, 23(23),* 5141-5147.

Brando, P. M., Goetz, S. J., Baccini, A., Nepstad, D. C., Beck, P. S., & Christman, M. C. (2010). Seasonal and interannual variability of climate and vegetation indices across the amazon. *Proceedings of the National Academy of Sciences, 107*(33), 14685-14690.

Brown, J. F., Wardlow, B. D., Tadesse, T., Hayes, M. J., & Reed, B. C. (2008). The vegetation drought response index (VegDRI): A new integrated approach for monitoring drought stress in vegetation. *GIScience & Remote Sensing, 45*(1), 16-46.

Brum, M., Gutiérrez López, J., Asbjornsen, H., Licata, J., Pypker, T., Sanchez, G., & Oiveira, R. S. (2018). ENSO effects on the transpiration of eastern amazon trees. *Philosophical Transactions of the Royal Society B: Biological Sciences, 373*(1760), 20180085.

Calvo-Alvarado, J., McLennan, B., Sánchez-Azofeifa, A., & Garvin, T. (2009). *Deforestation and forest restoration in Guanacaste, Costa Rica: Putting conservation policies in context, 258(6),* 931-940

Calvo-Rodriguez, S., Sanchez-Azofeifa, A. G., Duran, S. M., & Espirito-Santo, M. M. (2017). Assessing ecosystem services in Neotropical dry forests: A systematic review. *Environmental Conservation, 44*(1), 34-43.

Campos, F. A. (2018). A synthesis of long-term environmental change in Santa Rosa, Costa Rica. *Primate life histories, sex roles, and adaptability*, 331-358.

Cao, S., Sanchez-Azofeifa, G. A., Duran, S. M., & Calvo-Rodriguez, S. (2016). Estimation of aboveground net primary productivity in secondary tropical dry forests using the Carnegie–Ames–Stanford approach (CASA) model. *Environmental Research Letters, 11(7)*, 075004.

Cao, S., & Sanchez-Azofeifa, A. (2017). Modeling seasonal surface temperature variations in secondary tropical dry forests. *International Journal of Applied Earth Observation and Geoinformation, 62, 122-134.*

Carter, G. A. (1991). Primary and secondary effects of water content on the spectral reflectance of leaves. *American Journal of Botany,* 916-924.

Carter, G. A., Cibula, W. G., & Miller, R. L. (1996). Narrow-band reflectance imagery compared with thermal imagery for early detection of plant stress. *Journal of Plant Physiology, 148(5),* 515-522.

Castro, S. M., Sanchez-Azofeifa, G. A., & Sato, H. (2018). Effect of drought on productivity in a Costa Rican tropical dry forest. *Environmental Research Letters, 13*(4), 045001.

Castillo, M., Rivard, B., Snchez-Azofeifa, A., Calvo-Alvarado, J., & Dubayah, R. (2012). LIDAR remote sensing for secondary tropical dry forest identification. *Remote Sensing of Environment, 121*, 132-143.

Chadwick, W. W., Paduan, J. B., Clague, D. A., Dreyer, B. M., Merle, S. G., Bobbitt, A. M., Nooner, S. L. (2016). Voluminous eruption from a zoned magma body after an increase in supply rate at axial seamount. *Geophysical Research Letters, 43*(23), 1206-12070.

Choat, B., Jansen, S., Brodribb, T. J., Cochard, H., Delzon, S., Bhaskar, R., Hacke, U. G. (2012). Global convergence in the vulnerability of forests to drought. *Nature, 491*(7426), 752.

Dabrowska-Zielinska, K., Kogan, F., Ciolkosz, A., Gruszczynska, M., & Kowalik, W. (2002). Modelling of crop growth conditions and crop yield in poland using AVHRR-based indices. *International Journal of Remote Sensing, 23*(6), 1109-1123.

Dale, V. H., Joyce, L. A., McNulty, S., Neilson, R. P., Ayres, M. P., Flannigan, M. D., Peterson, C. J. (2001). Climate change and forest disturbances: Climate change can affect forests by altering the frequency, intensity, duration, and timing of fire, drought, introduced species, insect and pathogen outbreaks, hurricanes, windstorms, ice storms, or landslides. *Bioscience, 51*(9), 723-734.

Du, L., Tian, Q., Yu, T., Meng, Q., Jancso, T., Udvardy, P., & Huang, Y. (2013). A comprehensive drought monitoring method integrating MODIS and TRMM data. *International Journal of Applied Earth Observation and Geoinformation, 23*, 245-253.

Dutta, D., Kundu, A., Patel, N. R., Saha, S. K., & Siddiqui, A. R. (2015). Assessment of agricultural drought in Rajasthan (India) using remote sensing derived vegetation condition index (VCI) and standardized precipitation index (SPI). *The Egyptian Journal of Remote Sensing and Space Science*, *18(1),* 53-63.

Engelbrecht, B. M., Comita, L. S., Condit, R., Kursar, T. A., Tyree, M. T., Turner, B. L., & Hubbell, S. P. (2007). Drought sensitivity shapes species distribution patterns in tropical forests. *Nature, 447*(7140), 80.

Erasmi, S., Propastin, P., Kappas, M., & Panferov, O. (2009). Spatial patterns of NDVI variation over indonesia and their relationship to ENSO warm events during the period 1982–2006. *Journal of Climate, 22*(24), 6612-6623.

Feng, X., Porporato, A., & Rodriguez-Iturbe, I. (2013). Changes in rainfall seasonality in the tropics. *Nature Climate Change, 3*(9), 811.

Goward, S. N., Xue, Y., & Czajkowski, K. P. (2002). Evaluating land surface moisture conditions from the remotely sensed temperature/vegetation index measurements: An exploration with the simplified simple biosphere model. *Remote Sensing of Environment, 79(2-3)*, 225-242.

Guttman, N. B. (1999). Accepting the standardized precipitation index: A calculation algorithm. *Journal of the American Water Resources Association, 35*(2), 311-322.

Hoekstra, J. M., Boucher, T. M., Ricketts, T. H., & Roberts, C. (2005). Confronting a biome crisis: Global disparities of habitat loss and protection. *Ecology Letters, 8*(1), 23-29.

Holmgren, M., Scheffer, M., Ezcurra, E., Gutiérrez, J. R., & Mohren, G. M. (2001). El Niño effects on the dynamics of terrestrial ecosystems. *Trends in Ecology & Evolution, 16(2*), 89-94.

IPCC. (2007). IPCC WGI Fourth Assessment Report, Summary for policy makers. Paris, February.

Janzen, D. H. (1988). Management of habitat fragments in a tropical dry forest: Growth. Annals of the Missouri Botanical Garden, 105-116.

Janzen, D. H. (2000). Costa Rica's area de Conservacion Guanacaste: A long march to survival through non-damaging biodevelopment. *Biodiversity, 1*(2), 7-20.

Ji, L., & Peters, A. J. (2003). Assessing vegetation response to drought in the northern Great Plains using vegetation and drought indices. *Remote Sensing of Environment, 87*(1), 85-98.

Kalacska, M., Sanchez-Azofeifa, G. A., Calvo-Alvarado, J. C., Quesada, M., Rivard, B., & Janzen, D. H. (2004). Species composition, similarity and diversity in three successional stages of a seasonally dry tropical forest. *Forest Ecology and Management, 200*(1-3), 227-247.

Karnieli, A., Bayasgalan, M., Bayarjargal, Y., Agam, N., Khudulmur, S., & Tucker, C. J. (2006). Comments on the use of the vegetation health index over Mongolia. *International Journal of Remote Sensing, 27(10)*, 2017-2024.

Karnieli, A., Agam, N., Pinker, R. T., Anderson, M., Imhoff, M. L., Gutman, G. G., Goldberg, A. (2010). Use of NDVI and land surface temperature for drought assessment: Merits and limitations. *Journal of Climate, 23(3)*, 618-633.

Kassas, M. (1998). Currents of change: El Niño‘s impact on climate and society. *The Environmentalist, 19*(2), 177-178.

Kogan, F. N. (1995). Application of vegetation index and brightness temperature for drought detection. *Advances in Space Research, 15*(11), 91-100.

Kogan, F. N. (1997). Global drought watch from space. *Bulletin of the American Meteorological Society, 78*(4), 621-636.

Kogan, F. N. (1998). A typical pattern of vegetation conditions in southern Africa during El Nino years detected from AVHRR data using three-channel numerical index. *International Journal of Remote Sensing, 19(18)*, 3688-3694.

Kogan, F. N. (2000). Satellite-observed sensitivity of world land ecosystems to El Nino/La Nina. *Remote Sensing of Environment, 74*(3), 445-462.

Kogan, F. (2002). World droughts in the new millennium from AVHRR-based vegetation health indices. *Eos, Transactions American Geophysical Union, 83(48)*, 557-563.

Kogan, F., Stark, R., Gitelson, A., Jargalsaikhan, L., Dugrajav, C., & Tsooj, S. (2004). Derivation of pasture biomass in Mongolia from AVHRR-based vegetation health indices. *International Journal of Remote Sensing, 25(14)*, 2889-2896.

Li, W., Cao, S., Campos-Vargas, C., & Sanchez-Azofeifa, A. (2017). Identifying tropical dry forests extent and succession via the use of machine learning techniques. *International Journal of Applied Earth Observation and Geoinformation, 63*, 196-205.

Liu, J., Sun, O. J., Jin, H., Zhou, Z., & Han, X. (2011). Application of two remote sensing GPP algorithms at a semiarid grassland site of north china. *Journal of Plant Ecology, 4*(4), 302-312.

Lopezaraiza-Mikel, M., Quesada, M., Álvarez-Añorve, M., Ávila-Cabadilla, L., Martén-Rodríguez, S., Calvo-Alvarado, J. (2013). Phenological patterns of tropical dry forests along latitudinal and successional gradients in the Neotropics. Tropical dry forests in the Americas, 119-146.

Maass, J. M., Balvanera, P., Castillo, A., Daily, G. C., Mooney, H. A., Ehrlich, P., García-Oliva, F. (2005). Ecosystem services of tropical dry forests: Insights from longterm ecological and social research on the pacific coast of mexico. *Ecology and Society: A Journal of Integrative Science for Resilience and Sustainability, 10*(1), 1-23.

Madeira, B. G., Espírito-Santo, M. M., Neto, S. D., Nunes, Y. R., Azofeifa, G. A. S., Fernandes, G. W., & Quesada, M. (2009). Changes in tree and liana communities along a successional gradient in a tropical dry forest in South-Eastern Brazil. *Plant Ecology, 201*(1), 291-304.

McDowell, N., Pockman, W. T., Allen, C. D., Breshears, D. D., Cobb, N., Kolb, T., Yepez, E. A. (2008). Mechanisms of plant survival and mortality during drought: Why do some plants survive while others succumb to drought? *New Phytologist, 178*(4), 719-739.

McKee, T. B., Doeskin, N. J., & Kleist, J. (1993). The relationship of drought frequency and duration to time scales. *Eighth Conference on Applied Climatology, Anaheim, California*, 179–184.

Mennis, J. (2001). Exploring relationships between ENSO and vegetation vigour in the south-east USA using AVHRR data. *International Journal of Remote Sensing, 22*(16), 3077-3092.

Miles, L., Newton, A. C., DeFries, R. S., Ravilious, C., May, I., Blyth, S., Gordon, J. E. (2006). A global overview of the conservation status of tropical dry forests. *Journal of Biogeography, 33(3)*, 491-505.

Murphy, K. (2006). The ENSO-fire dynamic in insular Southeast Asia. *Climatic Change, 74*(4), 435-455.

Murphy, P. G., & Lugo, A. E. (1986). Ecology of tropical dry forest. *Annual Review of Ecology and Systematics, 17*(1), 67-88.

Nagai, S., Ichii, K., & Morimoto, H. (2007). Interannual variations in vegetation activities and climate variability caused by ENSO in tropical rainforests. *International Journal of Remote Sensing, 28(6)*, 1285-1297.

Nichol, J. E., & Abbas, S. (2015). Integration of remote sensing datasets for local scale assessment and prediction of drought. *Science of the Total Environment, 505*, 503-507.

Olukayode Oladipo, E. (1985). A comparative performance analysis of three meteorological drought indices. *International Journal of Climatology, 5*(6), 655-664.

Palmer, W. C. (1965). Meteorological drought, US Department of Commerce, *Research Paper 45*, 58.

Parry, M. L., Canziani, O. F., Palutikof, J. P., Van Der Linden, Paul J, & Hanson, C. E. (2007). IPCC, 2007: Climate change 2007: Impacts, adaptation and vulnerability. *Cambridge University Press, Cambridge, UK,*

Patel, N. R., Chopra, P., & Dadhwal, V. K. (2007). Analyzing spatial patterns of meteorological drought using standardized precipitation index. *Meteorological Applications, 14*(4), 329-336.

Phillips, O. L., Aragão, L. E., Lewis, S. L., Fisher, J. B., Lloyd, J., López-González, G., Quesada, C. A. (2009). Drought sensitivity of the amazon rainforest. *Science*, 323(5919), 1344-1347.

Phillips, O. L., Van Der Heijden, G., Lewis, S. L., López-González, G., Aragão, L. E., Lloyd, J., Dávila, E. A. (2010). Drought–mortality relationships for tropical forests. *New Phytologist, 187*(3), 631-646.

Portillo-Quintero, C. A., & Sanchez-Azofeifa, G. A. (2010). Extent and conservation of tropical dry forests in the Americas. *Biological Conservation, 143*(1), 144-155.

Portillo-Quintero, C., Sanchez-Azofeifa, A., Calvo-Alvarado, J., Quesada, M., & do Espirito Santo, Mario Marcos. (2015). The role of tropical dry forests for biodiversity, carbon and water conservation in the Neotropics: Lessons learned and opportunities for its sustainable management. *Regional Environmental Change, 15*(6), 1039-1049.

Prihodko, L., & Goward, S. N. (1997). Estimation of air temperature from remotely sensed surface observations. *Remote Sensing of Environment, 60(3)*, 335-346.

Propastin, P., Fotso, L., & Kappas, M. (2010). Assessment of vegetation vulnerability to ENSO warm events over Africa. *International Journal of Applied Earth Observation and Geoinformation, 12*, S83-S89.

Quesada, M., Sanchez-Azofeifa, G. A., Alvarez-Anorve, M., Stoner, K. E., Avila-Cabadilla, L., Calvo-Alvarado, J., Fernandes, G. W. (2009). Succession and management of tropical dry forests in the americas: Review and new perspectives. *Forest Ecology and Management, 258*(6), 1014-1024.

Quiring, S. M., & Ganesh, S. (2010). Evaluating the utility of the vegetation condition index (VCI) for monitoring meteorological drought in Texas. *Agricultural and Forest Meteorology, 150*(3), 330-339.

Rhee, J., Im, J., & Carbone, G. J. (2010). Monitoring agricultural drought for arid and humid regions using multi-sensor remote sensing data. *Remote Sensing of Environment, 114*(12), 2875-2887.

Rodriguez, S. C., Alvarado, J. C. C., Santo, M. M. E., & Nunes, Y. R. (2017). Changes in forest structure and composition in a successional tropical dry forest. *Revista Forestal Mesoamericana Kurú, 14*(35), 12-23.

Rouault, G., Candau, J., Lieutier, F., Nageleisen, L., Martin, J., & Warzée, N. (2006). Effects of drought and heat on forest insect populations in relation to the 2003 drought in Western Europe. *Annals of Forest Science, 63*(6), 613-624.

Running, S. W., Nemani, R. R., Heinsch, F. A., Zhao, M., Reeves, M., & Hashimoto, H. (2004). A continuous satellite-derived measure of global terrestrial primary production. *Bioscience, 54*(6), 547-560.

Sanchez-Azofeifa, A., Powers, J. S., Fernandes, G. W., & Quesada, M. (2013). Tropical dry forests in the Americas: Ecology, Conservation, and Management.

Sanchez-Azofeifa, G. A., Quesada, M., Rodríguez, J. P., Nassar, J. M., Stoner, K. E., Castillo, A., Cuevas-Reyes, P. (2005). Research priorities for Neotropical dry forests. *Biotropica, 37*(4), 477-485.

Sellers, P. J., Dickinson, R. E., Randall, D. A., Betts, A. K., Hall, F. G., Berry, J. A., Nobre, C. A. (1997). Modeling the exchanges of energy, water, and carbon between continents and the atmosphere. *Science, 275(5299)*, 502-509.

Shamsipour, A. A., Zawar-Reza, P., Alavi Panah, S. K., & Azizi, G. (2011). Analysis of drought events for the semi-arid central plains of Iran with satellite and meteorological based indicators. *International Journal of Remote Sensing, 32(24)*, 9559-9569.

Singh, R. P., Roy, S., & Kogan, F. (2003). Vegetation and temperature condition indices from NOAA AVHRR data for drought monitoring over India. *International Journal of Remote Sensing, 24*(*22*), 4393-4402.

Trenberth, K. E. (1997). The definition of El Niño. *Bulletin of the American Meteorological Society, 78(12)*, 2771-2777.

Trejo, I., & Dirzo, R. (2002). Floristic diversity of Mexican seasonally dry tropical forests. *Biodiversity & Conservation, 11*(11), 2063-2084.

Vicente-Serrano, S., Beguería, S., & López-Moreno, J. I. (2010). A multiscalar drought index sensitive to global warming: The standardized precipitation evapotranspiration index. *Journal of Climate, 23*(7), 1696-1718.

Wang, J., Rich, P. M., & Price, K. P. (2003). Temporal responses of NDVI to precipitation and temperature in the central great plains, USA. *International Journal of Remote Sensing, 24*(11), 2345-2364.

Williams, A. P., Allen, C. D., Macalady, A. K., Griffin, D., Woodhouse, C. A., Meko, D. M., Grissino-Mayer, H. D. (2013). Temperature as a potent driver of regional forest drought stress and tree mortality. *Nature Climate Change, 3*(3), 292-297.

Xiao, X., Zhang, Q., Braswell, B., Urbanski, S., Boles, S., Wofsy, S., Ojima, D. (2004). Modeling gross primary production of temperate deciduous broadleaf forest using satellite images and climate data. *Remote Sensing of Environment, 91*(2), 256-270.

Zargar, A., Sadiq, R., Naser, B., & Khan, F. I. (2011). A review of drought indices. *Environmental Reviews, 19*, 333-349.

Zeng, N. (1999). Seasonal cycle and interannual variability in the amazon hydrologic cycle. *Journal of Geophysical Research: Atmospheres, 104*(D8), 9097-9106.

Zhang, L., Jiao, W., Zhang, H., Huang, C., & Tong, Q. (2017). Studying drought phenomena in the continental United States in 2011 and 2012 using various drought indices. *Remote Sensing of Environment, 190*, 96-106.

Zhang, Y., Peng, C., Li, W., Fang, X., Zhang, T., Zhu, Q., Zhao, P. (2013). Monitoring and estimating drought-induced impacts on forest structure, growth, function, and ecosystem services using remote-sensing data: Recent progress and future challenges. *Environmental Reviews, 21*(2), 103-115.